PONTIFÍCIA UNIVERSIDADE CATÓLICA DO RIO GRANDE DO SUL
FACULDADE DE BIOCIÊNCIAS
PROGRAMA DE PÓS-GRADUAÇÃO EM BIOLOGIA CELULAR E MOLECULAR

DAIANA RENCK

A ENZIMA URIDINA FOSFORILASE 1 HUMANA: ALVO MOLECULAR PARA O DESENVOLVIMENTO DE NOVOS INIBIDORES PARA A QUIMIOTERAPIA DO CÂNCER

Porto Alegre
2013

DAIANA RENCK

A ENZIMA URIDINA FOSFORILASE 1 HUMANA: ALVO MOLECULAR PARA O DESENVOLVIMENTO DE NOVOS INIBIDORES PARA A QUIMIOTERAPIA DO CÂNCER

Tese apresentada como requisito para a obtenção do grau de Doutor pelo Programa de Pós-Graduação em Biologia Celular e Molecular da Faculdade de Biociências da Pontifícia Universidade Católica do Rio Grande do Sul

Orientador:
Prof. Dr. Luiz Augusto Basso

Co-orientador:
Prof. Dr. Diógenes Santiago Santos

Porto Alegre
2013

DAIANA RENCK

Tese apresentada como requisito para a obtenção do grau de Doutor pelo Programa de Pós-Graduação em Biologia Celular e Molecular da Faculdade de Biociências da Pontifícia Universidade Católica do Rio Grande do Sul

Aprovada em: _____ de _____ de _____.

BANCA EXAMINADORA:

_____
Prof. Dr. Juliano Ferreira - UFSC

_____
Prof. Dr. Gustavo Franco Carvalhal – PUCRS

_____
Prof. Dra. Fernanda Bueno Morrone - PUCRS

Porto Alegre
2013

AGRADECIMENTOS

Ao Prof. Diógenes Santiago Santos, agradeço pela oportunidade de integrar seu grupo de pesquisas por todos esses anos. Ao Prof. Luiz Augusto Basso, agradeço pela orientação ao longo desses 6 anos, pelas correções e sugestões que fizeram com que este trabalho fosse concluído, além de todo o conhecimento compartilhado.

Agradeço aos colaboradores desse trabalho, Pablo Machado, André Souto, Rafael Roesler, Caroline Farias, Osmar Norberto de Souza, Luiz Timmers e Guilherme Petersen. Em especial, agradeço a Maria Martha Campos, André Avelino Jr e Thaís Erig por todos os ensinamentos e conselhos que foram passados com muita paciência e carinho, que com certeza foram muito importantes para a realização desse trabalho, mas acima de tudo pela amizade cultivada ao longo desses anos.

Aos queridos amigos, Thiago Milech, Natasha Kuniechick, Rafael Munareto, Ardala Breda, Christiano Neves, José Eduardo Sacconi, Valnês Rodrigues Jr, Candida Deves, Priscila Wink, Leonardo Martinelli, Paulo Patta, Bruno Abbadi, Zilpa Sánchez, Mariane Rotta, Natalia Nicoletti, Diana Rostirolla, Gaby Renard, Claudia Paiva, Anne Villela, Juleane Lunardi e Maria Gleci Ferreira agradeço por toda a ajuda, troca de experiências e compreensão que foram essenciais para a execução desse trabalho; por estarem presentes em todos os momentos, não só como colegas de profissão e trabalho, mas como amigos de tanto tempo, faço-lhes esse agradecimento mais que especial.

Ao meu namorado, Leonardo Rosado, agradeço pela troca de experiências e ensinamentos, carinho, compreensão, dedicação, companheirismo e amor do início ao fim dessa etapa.

Aos demais colegas e amigos do CPBMF e da Quatro G pela ajuda, amizade, companheirismo e pelos momentos de descontração, pois de alguma forma todos contribuíram para a realização desse trabalho.

Aos meus pais, Ary Renck e Thereza Laux, agradeço pelo amor, carinho e dedicação que recebi, estando presente ou não, durante todos esses anos; pelos momentos em que a saudade teve que ser guardada e pelo exemplo de caráter e valores que levarei para o resto da vida.

“We are a formidable mixture of nucleic acids and memory, of desire and proteins.”

François Jacob

RESUMO

O impacto do câncer no mundo vem crescendo ao longo dos anos e há algumas décadas foi classificado como um problema de saúde pública mundial. A busca por novos fármacos para o tratamento e para a melhora da qualidade de vida dos pacientes visa o desenho de fármacos com alvos moleculares definidos, a fim de atingir rotas metabólicas do tumor. Dentre as rotas celulares, a via de salvamento de pirimidinas apresenta alvos moleculares interessantes para o desenho de possíveis novos fármacos quimioterápicos. A enzima humana uridina fosforilase 1 (hUP1) é uma das enzimas-chave dessa via, sendo responsável pelo controle da concentração homeostática da uridina, através da fosforólise reversível de uridina à uracil e ribose-1-fosfato na presença de fosfato inorgânico. A uridina tem sido proposta como um modulador para auxiliar na diminuição dos efeitos adversos gerados durante o tratamento com 5-fluorouracil (5-FU). Os dados da caracterização cinética foram utilizados como ponto de partida para o planejamento de novos inibidores da hUP1. Este trabalho descreve a síntese desses novos compostos, assim como a caracterização cinética e termodinâmica; análise em cultura de células eucarióticas e experimentos em roedores também auxiliaram na seleção de um composto promissor. A partir do composto líder, com valores de inibição na faixa de nanomolar, derivatizações químicas foram realizadas em locais específicos da molécula e a obtenção de compostos com afinidades aprimoradas foi confirmada. A partir da caracterização cinética e termodinâmica, determinamos que os melhores inibidores atuam como inibidores competitivos e incompetitivos em relação aos substratos naturais da hUP1, uridina e fosfato inorgânico, respectivamente, revelando a capacidade desses em formar um complexo ternário não catalítico. O ensaio em cultura de células com a molécula líder revelou que o composto é capaz de elevar a sensibilidade de células tumorais ao 5-FU, não exercendo, entretanto, nenhuma influência sobre células normais. Do mesmo modo, no modelo de mucosite intestinal em ratos, o composto apresentou resultados promissores, revelando uma possível proteção da mucosa intestinal, que pode se dar através da elevação da concentração de uridina no plasma. Assim, os resultados aqui apresentados reforçam o interesse na busca de inibidores da enzima hUP1 e na estratégia do uso da uridina como um modulador bioquímico dos efeitos adversos gerados durante a quimioterapia com fluoropirimidinas.

ABSTRACT

The world impact of cancer is increasing through the years and only a few decades ago it was classified as a worldwide public health problem. Cancer cells display many biochemical and biological peculiarities and the research for new drugs to treat or improve the quality of patient life justify the design of compounds with defined molecular targets to affect biochemical pathways of the tumor. The pyrimidine salvage pathway is one of the cellular pathways that have interesting molecular targets for drug design. The human uridine phosphorylase 1 (hUP1) is a key enzyme of pyrimidine salvage and is responsible for the reversible phosphorolysis of uridine to uracil and ribose-1-phosphate in presence of inorganic phosphate. Uridine is proposed to be a biochemical modulator to counteract the host toxicity caused by chemotherapy with 5-fluorouracil (5-FU). Kinetic characterization data were the starting point for hUP1 inhibitors planning. This work describes synthesis, kinetic and thermodynamic characterization of new compounds; also, results from eukaryotic cell cultured analysis and animal models supported the selection of the most promising compound. From the lead molecule, presenting inhibition values in nanomolar range, chemical replacement experiments were performed in specific spots of the molecule, leading to derived compounds with improved affinity profile. By kinetic characterization and thermodynamic discrimination profile the most potent inhibitors were characterized as competitive and uncompetitve inhibitors towards hUP1 natural substrates uridine and inorganic phosphate, respectively, showing its abilities to form a noncatalytic ternary complex. The cell cultured assessment with our lead compound showed the improved capacity of the compound to boost the sensibility of tumor cells to 5-FU treatment, with no significant influence on normal cells. Likewise, in murine model of mucositis, our data suggest that the lead compound maybe efficient to intestinal mucosa protection and to inhibit the hUP1 enzyme-mediated increase in the uridine plasma levels. Thus, the results presented here strengthen the interest for hUP1 inhibitors and for the uridine use as a biochemical modulator of side effects observed during fluoropyrimidines chemotherapy.

LISTA DE ILUSTRAÇÕES

LISTA DE SIGLAS

5-FU: 5-fluorouracil

a.C.: antes de Cristo

AMP: adenosina 5’-monofosfato

Arg: arginina

ATP: adenosina 5’-trifosfato

BAU: 5-benzilaciclouridina

DNA: ácido desoxirribonucleico

*Ec*UP: uridina fosforilase de *Escherichia coli*

FdUMP: fluorodesoxiuridina monofosfato

FUTP: fluorouridina 5’-trifosfato

hDPD: dihidropirimidina desidrogenase humana

hTP: timidina fosforilase humana

hTS: timidilato sintase humana

hUP: uridina fosforilase humana

hUP1: uridina fosforilase 1 humana

hUP2: uridina fosforilase 2 humana

INCA: Instituto Nacional de Câncer

K_i: constante de inibição

OMS: Organização Mundial da Saúde

P_i: fosfato inorgânico

PNP: purina nucleosídeo fosforilase

PSAU: 5-(fenilselenenil)aciclouridina

PTAU: 5-(feniltio)aciclouridina

PyNP: pirimidina nucleosídeo fosforilase

R1P: ribose-1-fosfato

RNA: ácido ribonucleico

S_N1: substituição nucleofílica de 1ª ordem

S_N2: substituição nucleofílica de 2ª ordem

*Tc*UP: uridina fosforilase de *Trypanossoma cruzi*

UDG: uracil DNA glicosilase

UMP: uridina 5'-monofosfato

UTP: uridina 5'-trifosfato

SUMÁRIO

Capítulo 1

Capítulo 2

Capítulo 3

Capítulo 4

Capítulo 1

1 INTRODUÇÃO

1.1 Uma visão geral do câncer: sua breve história, estimativas e tratamento

Os seres humanos e outros animais têm apresentado casos de câncer ao longo de toda a história. As primeiras evidências foram encontradas em ossos fossilizados, em múmias egípcias e em relatos de manuscritos antigos, apesar de não terem sido denominadas como câncer. O Papiro de Edwin Smith, uma cópia de um livro egípcio sobre cirurgia, é o achado mais antigo já catalogado, datando 3.000 anos a.C.. Nele consta o relato de oito casos de tumores de mama, tratados com cauterização; porém, o manuscrito classifica a doença como “sem tratamento”. A terminologia *câncer* teve início com o filósofo grego Hipócrates ao introduzir o termo carcinoma (caranguejo em grego) e, anos depois, o filósofo romano Celsus traduziu o termo grego para o latim, câncer (1).

Diversas hipóteses sobre a origem do câncer surgiram durante o percurso da sua história. Hipócrates acreditava que a doença surgia do balanço errado dos quatro fluídos corporais (sangue, fleuma, bile amarela e bile preta), e como nessa época as autópsias eram proibidas por influência da religião, a hipótese perpetuou por muitos anos. Para substituir a teoria do balanço de fluídos corporais, outro fluído surgiu: a linfa. Por volta do ano de 1700, acreditava-se que o câncer era formado por linfa fermentada variando apenas sua densidade, acidez e alcalinidade. Apenas no ano de 1838, o patologista alemão Johannes Müller demonstrou que o câncer era composto de células e não de linfa; porém ele acreditava que as células cancerosas eram provenientes de elementos que surgiam entre os tecidos normais. Na mesma época, outro patologista alemão, Rudolph Virchow, determinou que todas as células, incluindo as cancerosas, eram provenientes de outras células, e sugeriu a irritação crônica como causa da doença. Ainda no século XIX, surgiu a hipótese de que o câncer fosse uma doença infecciosa. Esta suposição tomou grandes proporções, levando o primeiro hospital de câncer da França a ser realocad, pois a população temia que a doença se espalhasse por toda a cidade (1,2).

Atualmente, segundo a Organização Mundial da Saúde (OMS), o câncer é uma denominação geral para um grupo de mais de cem doenças, e embora haja diversos tipos de cânceres, todos eles começam devido ao crescimento descontrolado e desordenado de células que podem afetar quase todas as partes do

corpo (3). Além do crescimento desordenado e descontrolado, características como autossuficiência para sinais de crescimento, insensibilidade à sinais anti-proliferativos, invasão tecidual e metástase e mecanismo de fuga da apoptose estão presentes na maioria das células cancerosas (4). O crescimento de células cancerosas é diferente do crescimento de células normais, pois, ao invés de sofrerem apoptose, as células tumorais continuam a se multiplicar, podendo desenvolver a característica de invadir tecidos vizinhos ou distantes, processo esse conhecido como metástase. O surgimento de células cancerosas ocorre através de danos no ácido desoxirribonucleico (DNA), o qual não é corrigido por nenhum sistema de reparo e também não leva a célula à morte. Desse modo, através da divisão celular descontrolada, a(s) mutação(ões) são passadas para as células-filha, as quais por sua vez podem acumular novas mutações ao longo desse processo. Esses danos podem ocorrer através de fatores ambientais, como tabagismo e infecções, ou através de fatores hereditários, como condições imunológicas e mutações, podendo esses fatores agir juntos ou em sequência para iniciar ou promover a carcinogênese. Os fatores hereditários ainda não são passíveis de modificações, porém os fatores externos são potencialmente modificáveis, e esses, são responsáveis por aproximadamente 70 % dos casos de cânceres (5).

Até a década de 70, o câncer era tido como uma doença de países desenvolvidos; porém, esse panorama vem mudando nas últimas décadas, transformando o câncer em um problema mundial de saúde pública, principalmente em países com poucos recursos. Em relação ao cenário mundial, a OMS estimou que, para o ano de 2030, ocorrerão 27 milhões de casos novos, 17 milhões de mortes e 75 milhões de pessoas vivas, porém portadoras da doença. Segundo o último relatório da OMS para o ano de 2008 (3), verificamos que o Brasil encontra-se em uma faixa preocupante para o sexo masculino em relação às taxas de mortes para cada 100 mil habitantes (**Figura 1A**). Porém, quando verificamos os mesmos dados para o sexo feminino, visualizamos que o Brasil está na segunda menor zona de classificação (**Figura 1B**), melhor do que países desenvolvidos, como Estados Unidos e Canadá.

Figura 1 - Taxa de mortes a cada 100 mil habitantes para o ano de 2008

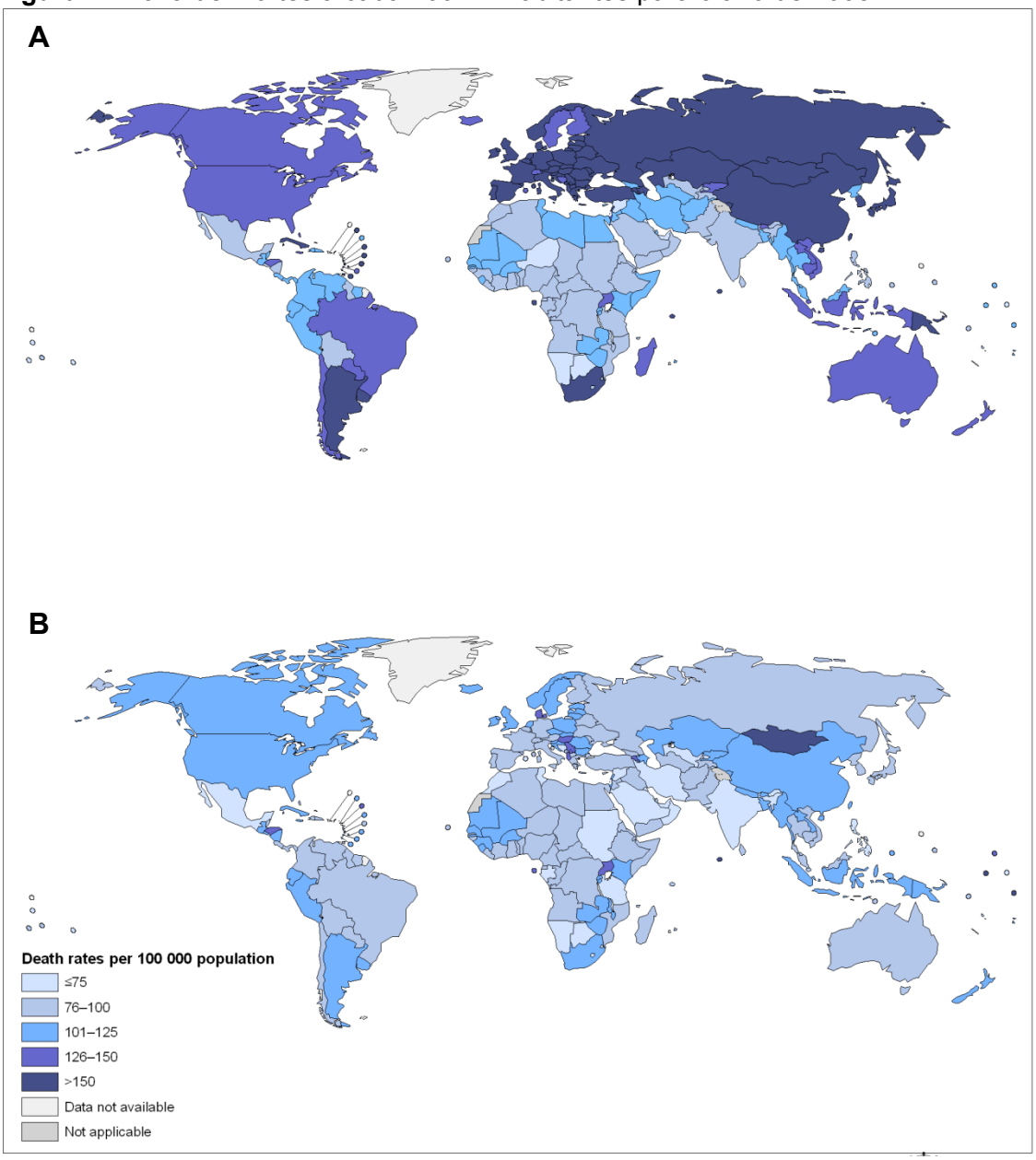

Fonte: Organização Mundial da Saúde (3).
Nota: (**A**), distribuição mundial das taxas de mortes para 100 mil habitantes para o sexo masculino. (**B**), distribuição mundial das taxas de mortes para 100 mil habitantes para o sexo feminino.

Seguindo o mesmo perfil mundial, a transição epidemiológica começou a ocorrer no Brasil a partir da década de 60, quando as doenças infecciosas e parasitárias deixaram de ser a principal causa de morte na população e deram lugar às doenças do sistema circulatório e às neoplasias. O Instituto Nacional de Câncer (INCA) estimou em seu último relatório, que para o período de 2012 a 2013, serão esperados aproximadamente 518 mil novos casos em todo território nacional. Desses, espera-se uma divisão homogênea entre os sexos: de 258 mil casos novos em homens e 260 mil casos novos em mulheres (6). A **Figura 2** ilustra os tipos de

tumores e suas incidências para homens e mulheres, salientando o câncer de próstata e o câncer de mama como os mais incidentes, respectivamente. Ao analisar as taxas brutas de incidência por região do país (**Figura 3A** e **3B**), notamos que o Rio Grande do Sul encontra-se entre os estados com as maiores taxas, mais uma vez não havendo diferenças entre homens e mulheres, com 395 e 338 casos estimados para cada 100 mil habitantes, respectivamente (6).

Figura 2 - Distribuição proporcional dos dez tipos de câncer mais incidentes estimados para 2012 por sexo, exceto pele não melanoma

Localização primária	casos novos	percentual
Próstata	60.180	30,8%
Traqueia, Brônquio e Pulmão	17.210	8,8%
Cólon e Reto	14.180	7,3%
Estômago	12.670	6,5%
Cavidade Oral	9.990	5,1%
Esôfago	7.770	4,0%
Bexiga	6.210	3,2%
Laringe	6.110	3,1%
Linfoma não Hodgkin	5.190	2,7%
Sistema Nervoso Central	4.820	2,5%

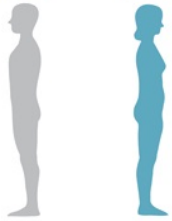

Localização primária	casos novos	percentual
Mama Feminina	52.680	27,9%
Colo do Útero	17.540	9,3%
Cólon e Reto	15.960	8,4%
Glândula Tireoide	10.590	5,6%
Traqueia, Brônquio e Pulmão	10.110	5,3%
Estômago	7.420	3,9%
Ovário	6.190	3,3%
Corpo do Útero	4.520	2,4%
Sistema Nervoso Central	4.450	2,4%
Linfoma não Hodgkin	4.450	2,4%

Fonte: Instituto Nacional de Câncer (6).

Figura 3 - Representação das taxas brutas de incidência por 100 mil habitantes estimadas para o ano de 2012

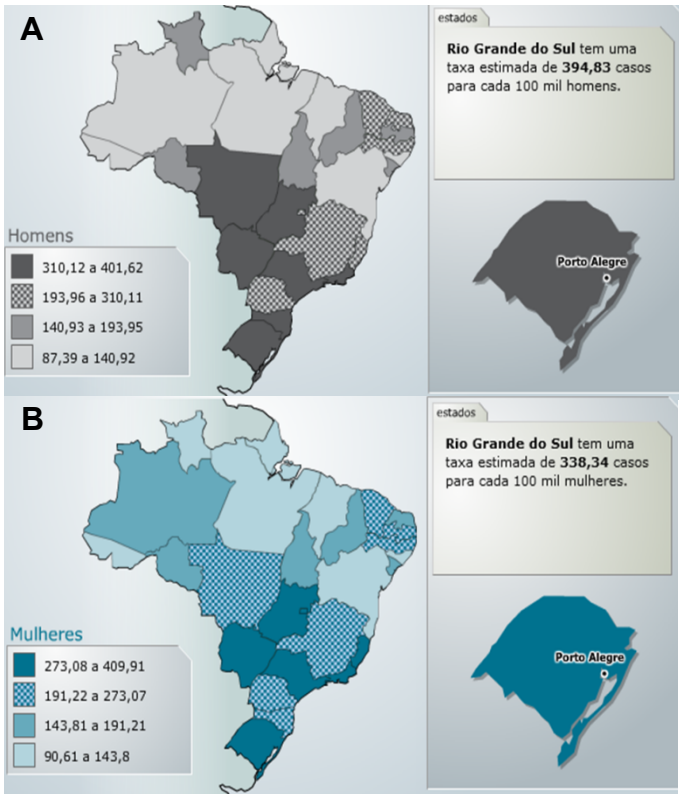

Fonte: Instituto Nacional de Câncer (6).
Nota: Em (**A**), distribuição nacional das taxas brutas de incidência para o sexo masculino. Em (**B**), distribuição nacional das taxas brutas de incidência para o sexo feminino.

Juntamente com a evolução do conhecimento sobre o câncer, veio o desenvolvimento dos diferentes tipos de tratamento. Os primeiros relatos do período de Hipócrates e Celsus são exclusivamente de cirurgias, processo esse precário e com diversas complicações. Em 1846, com a introdução da anestesia, o procedimento evoluiu drasticamente e, até hoje, a cirurgia é uma dos tratamentos de primeira linha para certos tipos de tumores. Houve o aperfeiçoamento em relação à remoção do tumor, retirando-se cada vez menos tecido sadio durante a operação (1,2). O uso da radioterapia teve seu início com a descoberta dos raios-x, mas seu uso só foi implementado com a descoberta do elemento químico radio em 1898 por Pierre e Marie Curie. Porém, a era moderna da radioterapia começou em 1950, com a introdução da terapia por cobalto e, até hoje, ela tem evoluído com técnicas mais precisas, as quais geram menos dano ao tecido normal, assim como a cirurgia (2).

A quimioterapia teve seu começo no início do ano de 1900, quando o químico alemão Paul Ehrlich desenvolveu drogas para o tratamento de doenças infecciosas e introduziu o termo *quimioterapia*, definindo-o como o uso de agentes químicos para o tratamento de uma doença. As primeiras quatro décadas do século XX foram marcadas praticamente pelo desenvolvimento de modelos animais, tendo como seu grande evento o desenvolvimento do modelo de transplante de tumores em roedores, por Georges Clowes (2,7). Mas foi no período da Segunda Guerra Mundial e no período que a sucedeu, onde a quimioterapia mais evoluiu. O gás mostarda começou a ser estudado devido de hipoplasia medular e linfoide, o que levou seu uso no tratamento de linfomas malignos (1,7). Logo após, houve o desenvolvimento de agentes anti-folato, como o metotrexato, e no mesmo ano dois pesquisadores isolaram uma substância que inibia o metabolismo da adenina que, em 1951, gerou dois compostos que tiveram um papel importante no tratamento de leucemias agudas, as tiopurinas. Em 1957, Charles Heidelberger identificou que hepatomas de ratos incorporavam mais uracil que células normais e adicionou uma molécula de flúor à posição 5 da base pirimídica desenvolvendo, desse modo, um dos quimioterápicos mais utilizados na clínica até hoje e um dos focos desse trabalho: o 5-fluorouracil (5-FU). Já no início da década de 60, houve a descoberta da atividade de alcalóides da planta *Vinca rosea* (vincristina) e a introdução de um esquema de administração combinado denominado *VAMP* (vincristina, ametopterin, 6-mercaptopurina e prednisona) (2). Esse foi o primeiro ciclo de tratamento que elevou em 60 % a taxa de remissão, introduzindo a ideia de cura do câncer. No final dessa

década, foi incorporada de forma definitiva a ideia de quimioterapia combinada, podendo-se classificar, desde 1976, o câncer de testículo como curável, através da terapia combinada com cisplatina, vimblastina e bleomicina (1,7). Em 1990, o sistema de triagem de compostos mudou para um método mais sofisticado de crescimento de células tumorais utilizando um sistema de cultura de células; já no meio da década, houve a introdução dos anticorpos monoclonais no esquema de administração combinada. A partir desse período, com o sequenciamento do genoma humano, a quimioterapia entrou em uma era de transição, denominada terapia direcionada a um alvo específico. Esse foco levou à identificação de novos alvos terapêuticos, que são utilizados atualmente para o desenvolvimento de drogas. O primeiro exemplo, aprovado em 2001 pelo FDA, dessa geração de drogas focadas em alvos específicos é o inibidor da Bcr-Abl tirosina quinase (Imatinib). Desde então a quimioterapia tem se focado em descobrir novas moléculas que tenham um único alvo específico (2,7), e inibidores da tirosina quinase já foram introduzidos como o Genifitinib (aprovado em 2003) e o Sunitinib (aprovado em 2006), assim como um inibidor de proteossomo, o Bortezomib (aprovado em 2003). A partir de 2008, uma nova técnica denominada hipertermia tem sido avaliada para auxiliar no tratamento de radioterapia e quimioterapia. Essa técnica é desenvolvida por poucas clínicas e consiste no aquecimento de todo o tumor (hipertermia local) ou um aquecimento de todo um órgão ou até mesmo de todo o corpo (hipertermia regional), através de ondas de ultrassom, ondas de rádio ou outras fontes de energia (8). A **Figura 4** resume de forma breve a história do desenvolvimento da quimioterapia no mundo.

Vislumbrando esse cenário, o progresso do tratamento contra o câncer não dependeu apenas do melhor entendimento sobre a doença e da possibilidade de melhores instrumentos cirúrgicos, mas também da combinação entre os tratamentos, como cirurgia, radioterapia e quimioterapia. Desse modo, desde o ano de 2005 verificamos um declínio nas taxas de incidência e mortalidade da doença, apesar de esforços ainda serem necessários para o desenvolvimento de novos fármacos para o tratamento da doença, assim como para a melhora da qualidade de vida dos pacientes.

Figura 4 - Linha do tempo dos eventos relacionados ao desenvolvimento da quimioterapia do câncer

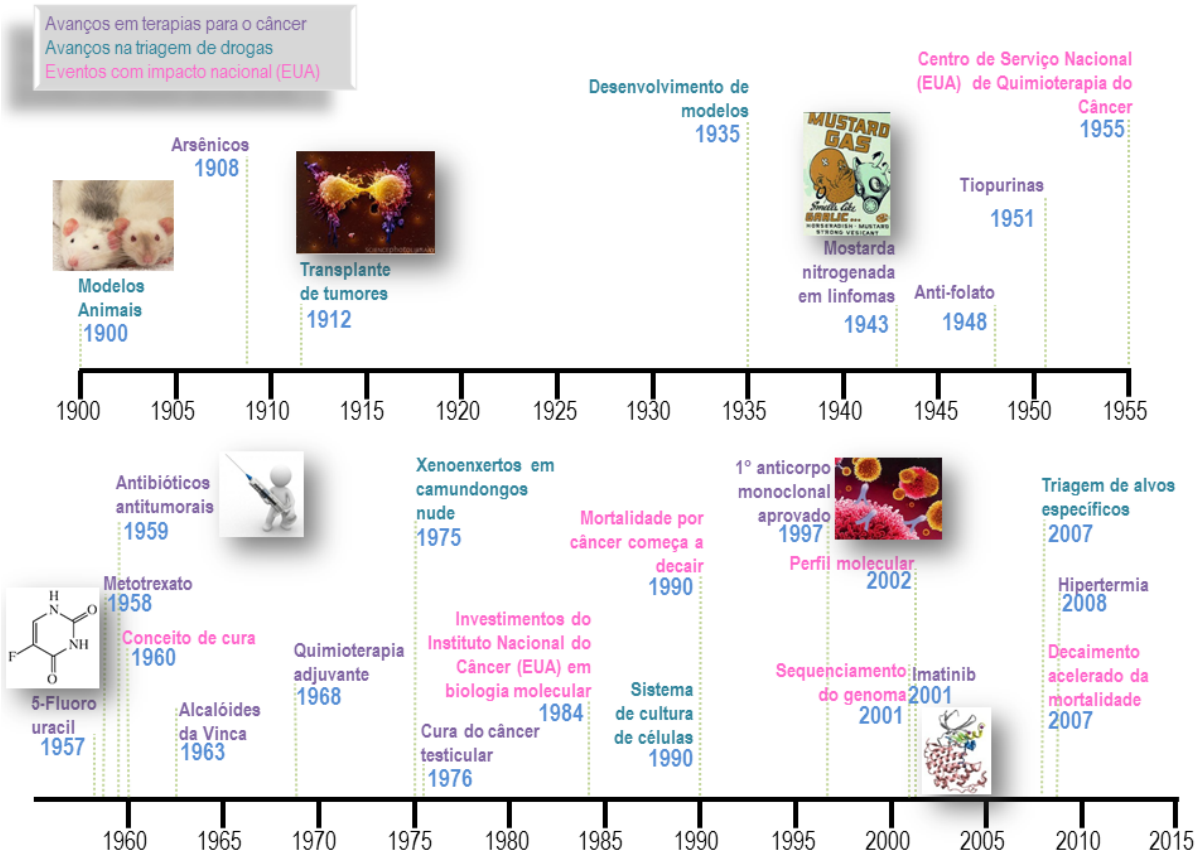

Fonte: Adaptado de DeVita et al. (7).

1.2 Biossíntese de Nucleotídeos

Dentre as rotas celulares que possuem alvos interessantes para o desenvolvimento de novos possíveis fármacos para o tratamento do câncer, tem-se o metabolismo de nucleotídeos. Os nucleotídeos são onipresentes e participam de quase todos os processos bioquímicos: constituem as unidades monoméricas do DNA e do ácido ribonucleico (RNA); fornecem energia por meio da hidrólise da adenosina 5'-trifosfato (ATP) e da guanosina 5'-trifosfato; regulam rotas metabólicas através dos níveis de ATP, adenosina 5'-difosfato e adenosina 5'-monofosfato (AMP); atuam como mediadores de sinais hormonais (AMP cíclico e guanosina monofosfato cíclico) e de reações enzimáticas. Os nucleotídeos são formados por ésteres de fosfato de um monossacarídeo de cinco átomos de carbono (pentose), nos quais a base nitrogenada está ligada covalentemente ao carbono do resíduo de monossacarídeo (**Figura 5**). Os ribonucleotídeos constituem as unidades

monoméricas do RNA, no qual a pentose é a D-ribose, enquanto que os desoxirribonucleotídeos possuem a desoxi-D-ribose como pentose e constituem as unidades monoméricas do DNA (9). Os nucleotídeos são divididos em nucleotídeos de purina e de pirimidinas, e sua importância no metabolismo celular se dá pelo fato de que quase todas as células sintetizam esses compostos. A biossíntese ocorre através de duas vias: pela via *de novo*, onde os nucleotídeos são formados a partir de precursores simples; e pela via de salvamento, onde os nucleotídeos são formados a partir da reciclagem de bases livres e nucleosídeos (9).

Figura 5 - Estrutura representativa do nucleotídeo uridina 5'-monofosfato (UMP)

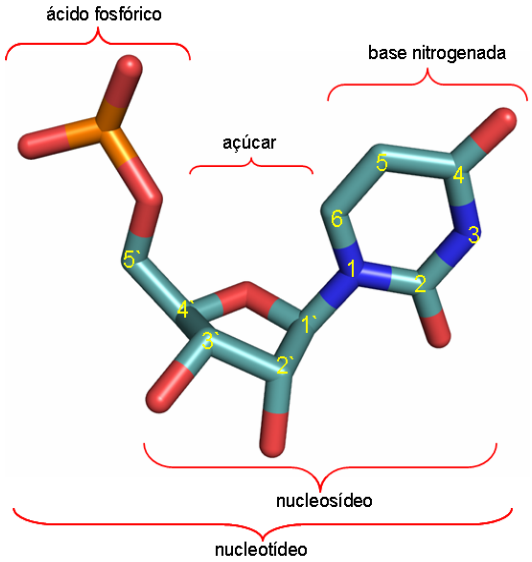

Fonte: Adaptada de Voet & Voet (9).

1.2.1 A biossíntese de nucleotídeos de pirimidinas

A biossíntese de pirimidinas é um processo mais simples do que a dos nucleotídeos de purinas (devido à etapa de formação do anel) e, como mencionado anteriormente, os nucleotídeos podem ser sintetizados através de duas rotas enzimáticas distintas. O UMP (**Figura 5**) é o nucleotídeo comum formado entre as duas vias, e é a partir dele que são formados todos os outros nucleotídeos de pirimidinas (10,11). A via *de novo* (**Figura 6**) consiste em uma rota de seis etapas enzimáticas para a formação do UMP, partindo de ATP, glutamina e dióxido de carbono. Porém, esse mesmo produto pode ser formado a partir da via de salvamento (**Figura 6**), por meio do processo de reciclagem de bases livres (uracil) e nucleosídeos (uridina e citidina) e um gasto menor de energia.

A via de salvamento de pirimidinas consiste também em um importante alvo para o tratamento de neoplasias, doenças virais e parasitárias, visto que as enzimas que constituem esta via são responsáveis pela ativação de alguns fármacos utilizados no tratamento dessas patologias (12). Do mesmo modo, as enzimas pirimidina nucleosídeo fosforilases (PyNP) são consideradas alvos moleculares importantes para o desenvolvimento de fármacos para o tratamento do câncer, visto que as células cancerosas utilizam preferencialmente a via de salvamento para a proliferação celular por seu menor gasto energético (13), revelando o crescente interesse por esses alvos enzimáticos.

Figura 6 - Via *de novo* e de salvamento de nucleotídeos de pirimidinas

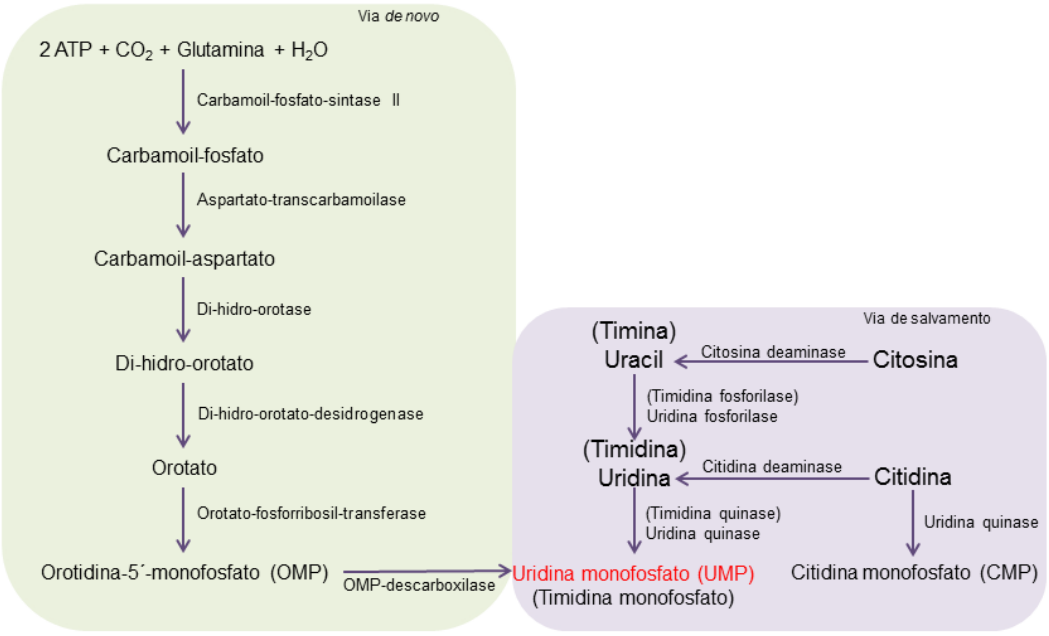

Fonte: Adaptado de Voet & Voet (9).
Nota: Em vermelho está destacado o produto comum entre as duas vias. ATP, adenosina 5'-trifosfato; CO_2, dióxido de carbono; H_2O, molécula de água.

1.3 O 5-fluorouracil (5-FU) e o papel protetor da uridina

Drogas antimetabólicas agem através da inibição de processos biossintéticos essenciais ou pela sua incorporação no DNA e no RNA, inibindo as funções normais dessas moléculas. Os fármacos baseados em pirimidinas são uma classe de quimioterápicos que começou a ser desenvolvidas em 1950, e seus principais representantes são o 5-FU, a gencitabina e a citarabina (14). O 5-FU foi sintetizado

por Charles Heidelberger em 1957 (15) e consiste em um análogo da base pirimídica uracil com um átomo de flúor na posição 5, substituindo um hidrogênio. Os fármacos baseados em pirimidinas são considerados pró-drogas e são, portanto, convertidos em metabólitos citotóxicos de nucleosídeos ou nucleotídeos a fim de terem a sua ação esperada (14). Desse modo, as enzimas que compõem o metabolismo de pirimidinas utilizam essas drogas do mesmo modo que seus substratos naturais (16,17). Por ser um análogo do uracil, o 5-FU entra rapidamente na célula utilizando o mesmo mecanismo de transporte facilitado e é metabolizado pelas mesmas enzimas que a base livre. Dentro da célula, o 5-FU é convertido aos seus metabólitos ativos, sendo os principais o fluorodesoxiuridina monofosfato (FdUMP) e o fluorouridina 5'-trifosfato (FUTP) que causam danos ao DNA e RNA, respectivamente. Os nucleotídeos citotóxicos podem ser gerados através de três vias, como ilustrado na **Figura 7**: 1) a conversão sequencial do 5-FU a FdUMP pela timidina fosforilase humana (hTP) e pela timidina quinase; 2) a conversão de 5-FU a FUMP pela orotato fosforibosiltransferase; 3) pela conversão sequencial de 5-FU em FUMP pela uridina fosforilase humana (hUP) e pela uridina quinase.

Figura 7 - Metabolismo do 5-FU

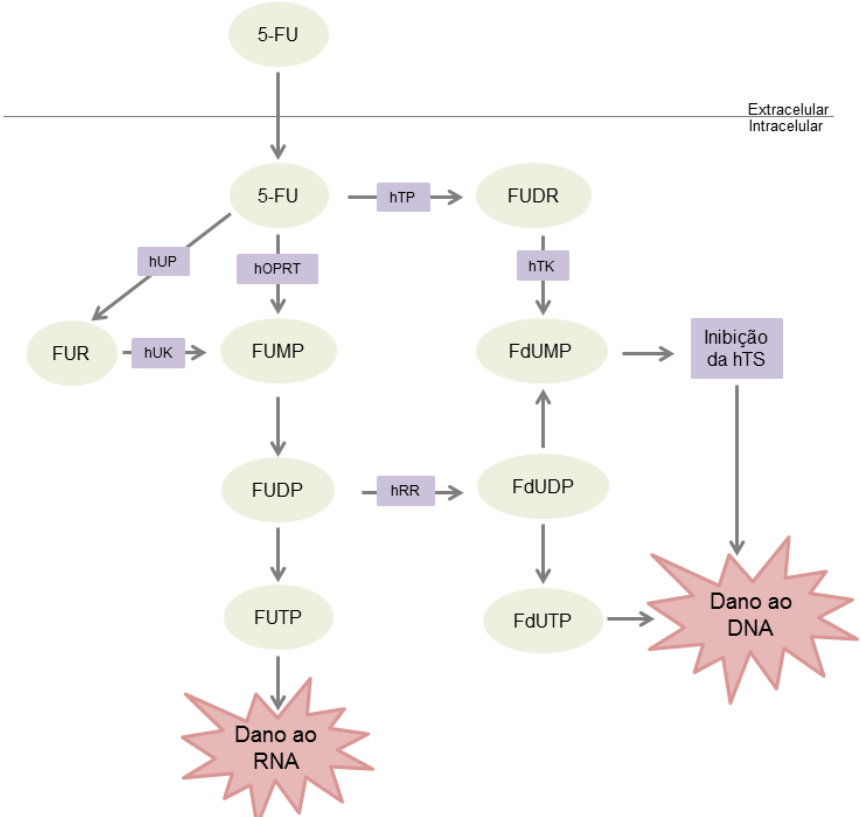

Fonte: Adaptada de Longley et al. (18).

Nota: hTP, timidina fosforilase; FUDR, fluorodesoxiuridina; hUP, uridina fosforilase; hOPRT, orotato fosforibosiltransferase; hTK, timidina quinase; FUR, fluorouridina; hUK, uridina quinase; FUMP, fluorouridina monofosfato; FdUMP, fluorodesoxiuridina monofosfato; hTS, timidilato sintase; FUDP, fluorouridina difosfato; hRR, ribonucleotideo redutase; FdUDP, fluorodesoxiuridina difosfato; FUTP, fluorouridina trifosfato; FdUTP, fluorodesoxiuridina trifosfato.

Porém, apenas uma pequena parcela do 5-FU é ativada por essas vias, visto que de 80-90 % do quimioterápico administrado é degradado a 5,6 dihidrofluorouracil pela enzima dihidropirimidina desidrogenase humana (hDPD) (14,18). O dano ao DNA é gerado através da principal via de ação do medicamento: a inibição da enzima timidilato sintase humana (hTS) pelo FdUMP. O FdUMP se liga de forma irreversível no sítio de ligação ao nucleotídeo da enzima, formando um complexo estável e inibindo a formação de desoxitimidina 5'-monofosfato, que é a única fonte de grupos timidilato que são necessários para a replicação e reparo do DNA. Já o dano ao RNA é gerado pela incorporação do FUTP, comprometendo o processamento e as funções normais dos diferentes tipos de RNA (18).

O 5-FU foi introduzido no uso clínico há mais de 50 anos e até hoje é utilizado para o tratamento de tumores sólidos, principalmente câncer de cólon e reto, câncer de mama e câncer de cabeça e pescoço (19,20). Esse fármaco é administrado por via intravenosa, em dois esquemas principais: via *bolus* ou infusão contínua. Os esquemas de tratamento e os números de ciclos necessários dependem de cada paciente, assim como do tipo de tumor e da sua localização no corpo, mas os esquemas padrões de ciclos incluem a administração uma vez por semana durante seis semanas ou cinco dias consecutivos de quatro a cinco semanas (repetições de ciclos a cada oito semanas) na dose de 400-600 mg/m^2 (19,20). Devido à meia vida curta (de apenas 20 minutos) (21), as células tumorais são expostas por um breve período de tempo ao quimioterápico, fazendo com que as infusões contínuas tenham um melhor resultado em relação ao *bolus* (19). Atualmente existem duas pró-drogas do 5-FU que são administradas por via oral: a capecitabina que é ativada por enzimas do citocromo P450, e o tegafur, que é combinado com a base livre uracil e comercializado com o nome de UFT (19,20). O uracil é um substrato competitivo da hDPD e o seu papel na combinação farmacêutica é diminuir a degradação do 5-FU pela enzima (14). As monoterapias, no entanto, dificilmente produzem bons resultados, e o 5-FU normalmente é administrado em esquemas de terapias combinadas (19), com drogas que diminuam sua degradação, aumentem sua ativação ou melhorem a ligação do FdUMP à hTS.

Assim como diversos outros quimioterápicos, o 5-FU apresenta efeitos adversos ao paciente. Dentre os mais comuns estão: a alopecia, a perda de peso, náuseas, vômitos e mucosite, tanto intestinal quanto bucal (19). A mucosite consiste em um dos principais e mais graves efeitos adversos relacionados ao 5-FU e ainda não existe tratamento de prevenção ou cura dessas ulcerações, fazendo-se uso apenas de tratamentos preventivos, como a higiene bucal e o uso de medicamentos que aliviem a dor (21,22). A mucosite é caracterizada por quatro fases, cada uma independente da outra: uma inflamatória (liberação de citocinas), uma fase epitelial (redução da renovação epitelial), uma ulcerativa (falha na barreira da mucosa e neutropenia) e, por fim, uma fase de renovação (retorno da proliferação e diferenciação celular) (23). A frequência da mucosite varia e é influenciada pelo diagnóstico do paciente, idade, estado de saúde, tipo, dose e esquema de tratamento da droga. Em média, a mucosite acomete de 40-80 % dos pacientes, aparecendo de cinco a dez dias após o tratamento e costuma desaparecer dentro de três a quatro semanas após o término da quimioterapia (23). Esse efeito tóxico compromete de forma significativa a qualidade de vida dos pacientes em tratamento, visto que gera diarreia e dores severas, além de modificar o esquema de alimentação e muitas vezes o esquema de tratamento, levando à sua interrupção. A interrupção na quimioterapia afeta as células tumorais de maneira positiva, fazendo com que aquelas células que estavam apresentando resistência ao 5-FU possam se multiplicar, tornando o tumor mais agressivo (24). Além disso, essas ulcerações são portas de entrada para bactérias, facilitando o desenvolvimento de uma infecção generalizada (sepse) que, muitas vezes, leva o paciente a óbito devido à infecção e não ao câncer (25).

Consta na literatura a hipótese de que os efeitos adversos gerados pelo uso do 5-FU são devido ao dano ao RNA, enquanto que o efeito citotóxico do medicamente se dá pelo dano ao DNA (26,27). O nucleosídeo uridina é relatado como um agente promissor para a diminuição desses efeitos colaterais, sugerindo a sua atuação como um modulador bioquímico. Um modulador bioquímico é um agente farmacológico que eleva o efeito biológico da quimioterapia pelo aumento da seletividade de ação do quimioterápico ou pela proteção seletiva do hospedeiro (19). As células tumorais estão em constante divisão celular, se multiplicando mais rapidamente que as células normais; por esse motivo, as enzimas que compõem as vias *de novo* e de salvamento de nucleotídeos estão mais ativas e/ou são mais

expressas nesse tipo de tecido. Desse modo, ao ocorrer um aumento de uridina, ocorre também uma elevação da concentração de uridina 5'-trifosfato (UTP), que irá competir com o FUTP pela incorporação ao RNA (28,29,30,31). A concentração homeostática da uridina no plasma varia numa pequena faixa de 1-5 μM, sendo essa mantida de forma rígida pela hUP. Além disso, a concentração de uridina e a atividade da hUP são controladas pelo ciclo circadiano, apresentando as maiores concentrações de uridina pelo período da manhã (11).

A estratégia do uso farmacológico da uridina teve início com a tentativa de administração do nucleosídeo por via oral e intravenosa ou através de suas pró-drogas, porém, foi necessária a utilização de doses muito elevadas da uridina para que ocorresse algum tipo de efeito, devido à rápida metabolização pela enzima hUP (32). A partir dessa constatação, surgiu a estratégia do desenvolvimento de inibidores da hUP para elevar de maneira endógena a concentração de uridina. Além disso, ao ocorrer a inibição da enzima, uma concentração maior de 5-FU estaria disponível para ser convertido ao metabólito FdUMP e, consequentemente, inibir a hTS (33). Portanto, a enzima hUP é um alvo promissor para o desenvolvimento de inibidores específicos com a finalidade de proteger os tecidos normais contra a ação do 5-FU, assim como melhorar a sensibilidade de células tumorais a esse quimioterápico.

1.4 A enzima uridina fosforilase humana

Em mamíferos existem duas PyNP, a UP e a TP que, na presença de fosfato inorgânico (P_i), catalisam a conversão reversível de uridina, timidina ou desoxiuridina para suas bases livres e ribose-1-fosfato (R1P) ou 2-desoxirribose-1-fosfato, respectivamente (34). Além de seus substratos naturais, essas enzimas participam da ativação de quimioterápicos baseados em nucleotídeos de pirimidinas, como o 5-FU. A enzima UP está presente em procariotos, leveduras e organismos superiores e a sua sequência de aminoácidos é altamente conservada entre as enzimas bacterianas, humana e de camundongo (35). A atividade de fosforólise é conservada de bactérias a humanos, embora a sequência gênica e a estrutura proteica, bem como o tamanho da proteína, variem, se apresentando, por exemplo, como um hexâmero em *Escherichia coli (E. coli; Ec*UP*)* (36) e *Salmonella typhimurium* (37),

enquanto que a proteína bovina (38) e a humana (hUP1) apresentam suas estruturas arranjadas como homodímero (**Figura 8**) (39).

Figura 8 - Estrutura tridimensional da enzima hUP1 complexada com o inibidor 5-benzilaciclouridina

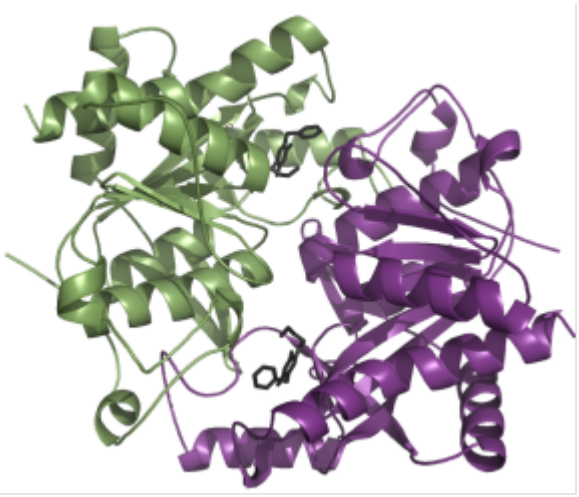

Fonte: Código de acesso PDB: 3EUE.

A enzima hUP encontra-se em duas isoformas em humanos, a isoforma 1 (hUP1) que é expressa em todos os tecidos (16), e a isoforma 2 (hUP2) que é expressa apenas em tecido renal (40). As duas isoformas estão localizadas em cromossomos diferentes e ainda não existem trabalhos na literatura que possuam algum tipo de estudo em relação à expressão tecido-específica das hUPs (41). A enzima hUP1 catalisa a fosforólise reversível de uridina a uracil e foi recentemente caracterizada bioquimicamente (42 – Anexo A). Através de experimentos de cinética enzimática em estado estacionário a enzima teve seu mecanismo cinético caracterizado como bi bi ordenado, onde o P_i se liga primeiro à enzima livre, permitindo a ligação da uridina e a formação do complexo ternário. A liberação dos produtos também ocorre de forma ordenada, com a base livre uracil sendo o primeiro produto a ser liberado seguido pela liberação da R1P (**Figura 9**) (42). Esses dados corroboram o mecanismo cinético da UP de fígado de rato (43,44), porém a *Ec*UP (45,46) e a UP de *Lactobacillus casei* (47) apresentam uma ordem de adição dos substratos aleatória, assim como a UP de *Cavia porcellus* (popularmente conhecido como porquinho-da-índia) (48), que apresenta um mecanismo ordenado porém com o substrato uridina se ligando antes do P_i. A influência do pH na catálise e na ligação dos substratos também foi determinada para a hUP1 (42). Através dos valores de pK_a e pK_b gerados por esses estudos, sugeriu-se que a cadeia lateral do

resíduo de aminoácido histidina (His) 36 e a cadeia lateral da tirosina 35 devem estar desprotonada e protonada, respectivamente, para que a catálise ocorra de forma eficiente. Em relação à ligação dos substratos, existem três resíduos de arginina (Arg) que compõe o sítio de ligação do P_i (Arg64, Arg94 e Arg138); porém, a Arg64 está em uma conformação oposta, não participando do evento de ligação, e fazendo com que a Arg94 ou a Arg138 (uma de cada subunidade do homodímero) influenciem a ligação do substrato ao sítio ativo (39). A influência do pH para o substrato uridina sugere que a His36 deve estar desprotonada, corroborando a influência do pH na catálise, onde esse resíduo também é essencial, e que a protonação da cadeia lateral do resíduo de aminoácido Arg219 é necessária para a ligação da uridina, devido a conservação desse resíduo na *Ec*UP, onde foi visto seu papel fundamental na ligação da base livre uracil (36,42).

Todos esses dados são de extrema importância quando temos em vista o desenho racional de drogas com alvos moleculares estabelecidos, uma vez que as enzimas catalisam reações químicas de várias etapas e atingem uma aceleração fenomenal da velocidade da reação a partir da associação dos grupamentos funcionais das cadeias laterais dos aminoácidos no sítio ativo da enzima e no estado de transição. Os inibidores enzimáticos que exploram estas interações químicas estão entre as drogas mais potentes e eficazes, sendo uma das grandes apostas da indústria farmacêutica (49). Portanto, a análise do mecanismo cinético é essencial para programas de desenvolvimento de fármacos cujos modos de ação são a inibição enzimática.

Figura 9 - Mecanismo cinético proposto para a hUP1

$$E \rightleftharpoons E\text{-}P_i \rightleftharpoons E\text{-}P_i\text{-}Urd \rightleftharpoons E\text{-}Uracil\text{-}R1P \rightleftharpoons E\text{-}R1P \rightleftharpoons E$$

Fonte: Renck et al. (42).

1.4.1 Inibidores da hUP1

Os primeiros compostos específicos para a hUP surgiram em 1981 através dos derivados de aciclonucleosídeos de pirimidinas (aciclotimidina, aciclouridina, aciclofluorouridina, aciclobromouridina e acicloiodouridina). Esses compostos foram testados contra a enzima extraída diretamente do citosol de células do tipo Sarcoma 180, demonstrando uma constante de inibição (K_i) na faixa de 3-30 μM e com um

perfil inibitório competitivo em relação ao substrato uridina (50). Logo após a constatação de que os aciclonucleosídeos de pirimidinas eram mais potentes do que os conjugados de açúcar, que haviam sido descritos anteriormente, compostos que combinavam a estratégia dos aciclonucleosídeos e as bases 5-benziluracil e 5-benziloxibenziluracil foram sintetizados, gerando compostos com K_i de 1,6 μM e 270 μM, respectivamente (51). O composto com a melhor atividade inibitória *in vitro* descrito na literatura até este presente trabalho, e que até hoje vem sendo extensivamente estudado, foi derivado do 5-benziluracil: o 5-benzilaciclouridina (BAU) com um K_i de 98 nM contra o substrato uridina, apresentando um perfil de inibição competitivo (52). Após, foi sintetizada uma série de 15 estruturas novas derivadas desse, onde a relação estrutura-atividade das aciclouridinas foi determinada (53). Para todos os compostos, assim como para o BAU, a atividade inibitória foi específica para a hUP, não demonstrando nenhuma ação sobre a outra PyNP (hTP). Em 1985, os pesquisadores Darnowski e Handschumacher determinaram a capacidade do BAU de elevar a concentração plasmática de uridina em camundongos, revelando que o composto aumenta em torno de 10 vezes a concentração do nucleosídeo, chegando à concentração de 50 μM mantida por 4 horas. Eles determinaram também que a administração do BAU juntamente com o 5-FU elevou em torno de 50 % a concentração necessária do quimioterápico para matar 50 % células normais, revelando seu potencial papel protetor (54). Por ser um potente inibidor da hUP, diversos estudos com o BAU foram realizados ao longo dos anos. Em 1998, foram realizados testes pré-clínicos utilizando cachorros e porcos para verificar as características farmacocinéticas e farmacodinâmicas do composto. Esse estudo revelou que o BAU foi capaz de manter a concentração de uridina elevada no plasma nas duas espécies e apresentou uma meia-vida média de 2 horas. No mesmo estudo, foi realizado um teste clínico de fase I com pacientes diagnosticados com câncer avançado, no qual o BAU foi administrado por via oral em diferentes concentrações, elevando a concentração de uridina em até 175 % quando a maior dose do composto foi administrada (55). Desde então, o composto não avançou para nenhuma outra fase dos testes clínicos, sendo relatados na literatura apenas trabalhos *in vitro* e com animais.

No início da década de 90 surgiu outra importante classe de inibidores da hUP, também muito estudados até hoje, entre os quais os que apresentaram melhores resultados em testes com animais, as pirimidinas fenilselenenil- e feniltio-

substituídas (56), sendo sintetizados inicialmente para serem agentes antivirais. O primeiro composto com promissora atividade inibitória contra a hUP foi o 5-(fenilselenenil)aciclouridina (PSAU), com um K_i de 3,8 μM. Nos anos seguintes, diversos estudos foram realizados com o PSAU e com outro derivado de grande sucesso (K_i de 353 nM), o 5-(feniltio)aciclouridina (PTAU), demonstrando a habilidade desses compostos *in vivo*, apesar de sua capacidade inibitória *in vitro* não ser superior ao BAU. Esses compostos são muito mais lipofílicos que o BAU e apresentam a vantagem de serem totalmente biodisponíveis por via oral. Apesar de ser um composto promissor, o PTAU ainda encontra-se em testes pré-clínicos até o presente momento (27,31,32,35,57,58,59). A **Figura 10** ilustra as estruturas do BAU, PSAU e PTAU.

Figura 10 - Estrutura química dos inibidores da hUP.

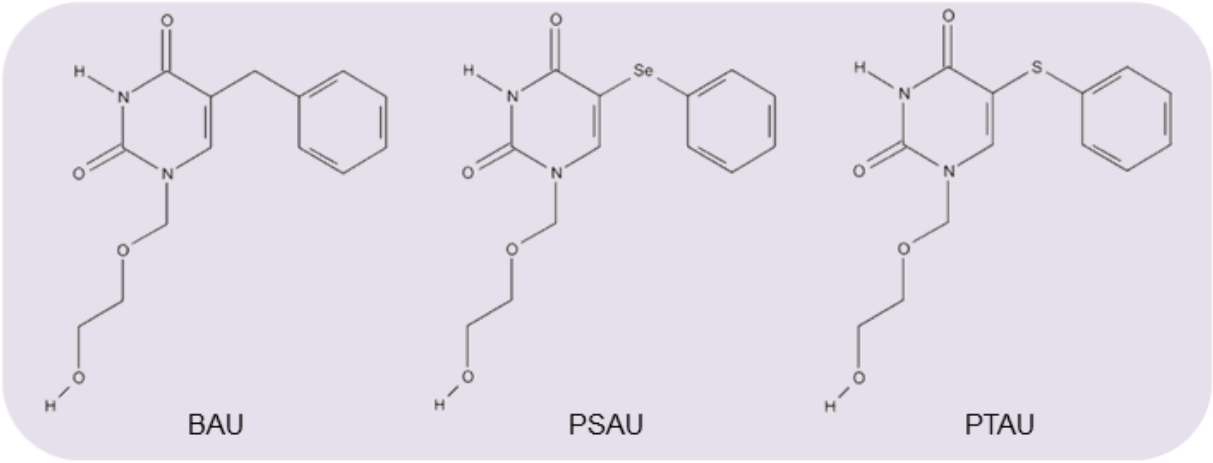

Fonte: Adaptado de Niedzwicki et al. (52), Goudgaon et al. (56).
Nota: BAU, 5-benzilaciclouridina; PSAU, 5-(fenilselenenil)aciclouridina; PTAU, 5-(feniltio)aciclouridina.

Compostos químicos com atividade inibitória podem ser obtidos a partir de análogos estruturais aos substratos, aos produtos ou ao estado de transição da reação enzimática. O estado de transição de uma enzima é o momento em que ocorre a formação do complexo ternário onde ligações químicas estão sendo formadas e quebradas. A busca por inibidores que mimetizem o estado de transição é a melhor escolha, pois é nesse estado em que a enzima possui a maior afinidade pelos substratos (60). A estratégia de obtenção de novos compostos com a capacidade inibitória sobre a hUP1 passa pela síntese de análogos ao possível estado de transição do complexo ativado produzido na catálise enzimática. Compostos análogos aos estados de transição de reações catalisadas enzimaticamente estão entre os inibidores mais potentes que se conhece (61).

A reação catalisada pela hUP1 é considerada, de um ponto de vista químico, uma reação de substituição nucleofílica que pode ser de 1ª ou 2ª ordem (S_N1 ou S_N2, respectivamente). A reação de 1ª ordem ocorre em duas etapas, com a formação de um intermediário do tipo carbocátion e o conseguinte ataque do nucleófilo ao carbocátion. A reação de 2ª ordem ocorre de maneira simultânea, com o nucleófilo aproximando-se ao mesmo tempo em que o grupamento abandonador é eliminado pela face oposta. A UP é classificada como um membro da família das fosforilases de nucleosídeos do tipo I e dentro dessa família, tem sido estudados os estados de transição da purina nucleosídeo fosforilase (PNP) (62,63), uracil DNA glicosilase (UDG) (64), hTP (65), da *Ec*UP (66) e da UP de *Trypanossoma cruzi* (*Tc*UP) (67). O mecanismo S_N1 foi observado para a PNP bovina, assim como para a UDG de *E. coli* e a *Ec*UP (36). Por outro lado, o mecanismo S_N2 tem sido relatado para a hTP, *Tc*UP e também para a *Ec*UP. Até o momento, não há um estudo detalhado sobre o estado de transição da hUP1, embora tenha sido descrito que o mecanismo S_N1 seja preferido para esta conversão enzimática (**Figura 11**) (39). Assim, a estratégia proposta pelo nosso grupo foi sintetizar compostos análogos ao estado de transição tipo S_N1.

Figura 11 - Estado de transição S_N1 e S_N2 para a reação catalisada pela hUP1 e os análogos propostos

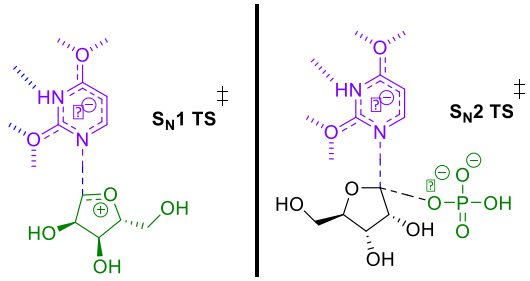

Fonte: Adaptado de Jain et al. (70)
Nota: S_N1, substituição nucleofílica de 1ª ordem; S_N2, substituição nucleofílica de 2ª ordem; TS, estado de transição,

Baseado no que já foi descrito na literatura (68,69), este trabalho se propôs também a sintetizar estruturas capazes de mimetizar a R1P pelo uso de derivados de amino álcoois acíclicos ligados como cadeias laterais de anéis piridínicos. Essa estratégia de simplificação molecular já se mostrou eficiente, mantendo a capacidade inibitória e facilitando a síntese química. O pK_a elevado da cadeia lateral dos amino álcoois produzirão um centro com carga positiva em pH fisiológico semelhante ao ribooxocarbônio formado em um possível estado de transição S_N1

para hUP1. Outra estratégia foi substituir o anel pirimidínico da uridina por um anel piridínico. Essa estratégia visa à introdução de ligações carbono-carbono substituindo a ligação *N*-ribosídica presentes no substrato. Essa modificação conduzirá a compostos mais estáveis às reações de substituição nucleofílicas no sítio ativo da hUP1. Além disso, a utilização de grupamentos químicos com a característica de retirar elétrons na posição-5 do anel piridínico tende a aumentar a acidez dos átomos de hidrogênios do anel heterocíclico, uma vez que estabilizam a base conjugada, aumentando assim a eficiência das ligações de hidrogênio formadas no sítio ativo da hUP1. Genericamente, as estruturas químicas propostas podem ser sumarizadas pelas estruturas abaixo (**Figura 12**).

Figura 12 - Esquema dos possíveis análogos de estado de transição S_N1

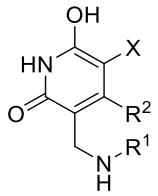

S_N1 Análogos

Fonte: O Autor (2013).
Nota: S_N1, substituição nucleofílica de 1ª ordem; R^1 = alquil álcoois; R^2 =H, alquila, arila; X = grupos retiradores de elétrons.

2 JUSTIFICATIVA

O desenho racional de drogas a partir de alvos moleculares já estabelecidos é baseado no conhecimento do modo de ação e da estrutura molecular do sítio ativo de uma determinada molécula-alvo ao qual uma determinada droga, o inibidor, liga-se. Inibidores enzimáticos correspondem a aproximadamente 25 % do mercado de fármacos dos Estados Unidos (71).

A importância da hUP na quimioterapia do câncer advém do fato dela ser uma das enzimas responsáveis pela ativação ou degradação de alguns quimioterápicos, como as 5-fluoropirimidinas. A efetividade clínica do 5-FU é limitada devido aos seus severos efeitos adversos, como mielossupressão, trombocitopenia e lesões gastrointestinais e nas mucosas, que levam à diminuição da qualidade de vida do paciente, a graves infecções, e podendo resultar em óbito. A uridina tem sido utilizada para reduzir esses efeitos adversos severos (17), sendo que sua disponibilidade e concentração são reguladas pela hUP. Porém, o uso clínico desse *"*resgate da uridina*"* é dificultado pela sua rápida degradação, iniciada pela enzima no fígado e, pela toxicidade dose-limitante, resultando na necessidade do uso de altas concentrações para obter a dose desejada à proteção dos tecidos.

Um inibidor da hUP denominado BAU, o qual é um derivado do uracil, tem sido capaz de aumentar a concentração endógena de uridina levando a uma proteção dos tecidos normais, porém esse compostos não passou as etapas de testes pré-clínicos (17). A importância da hUP na quimioterapia do câncer tem gerado um grande interesse no desenvolvimento de inibidores para essa enzima há mais de 30 anos. Desse modo, os inibidores da hUP podem aumentar a efetividade quimioterápica de drogas pela prevenção de sua degradação e/ou toxicidade ao hospedeiro (35), assim como podem atuar separadamente inibindo parcialmente a via de salvamento de pirimidinas através da não reciclagem da base uracil. Portanto, a enzima hUP representa um alvo molecular atrativo, cuja inibição pode resultar no acúmulo de uridina e consequente proteção dos tecidos normais frente aos efeitos tóxicos do 5-FU, o qual é extensivamente utilizado no tratamento quimioterápico do câncer.

3 OBJETIVOS

3.1 Objetivo Geral

Este projeto de pesquisa faz parte de um projeto maior que visa à caracterização de enzimas da via de salvamento e da síntese *de novo* de purinas e pirimidinas para o desenvolvimento racional de possíveis inibidores. Este trabalho teve por objetivo geral desenvolver a síntese e a caracterização cinética e termodinâmica de possíveis novos inibidores para a enzima hUP1 assim como analisar os efeitos protetores da uridina em modelo animal. Esses experimentos foram realizados no Centro de Pesquisas em Biologia Molecular e Funcional da PUCRS (CPBMF) e no Laboratório de Farmacologia Aplicada I da PUCRS.

3.2 Objetivos Específicos

1. Sintetizar inibidores análogos ao possível estado de transição da hUP1;
2. Avaliar o efeito dos inibidores sobre a enzima hUP1 e selecionar os melhores compostos;
3. Determinar a constante de inibição para os compostos selecionados;
4. Determinar os parâmetros termodinâmicos em diferentes condições de ligação;
5. Avaliar os possíveis efeitos citotóxicos dos inibidores em linhagens celulares normais e tumorais;
6. Avaliar os possíveis efeitos dos compostos no crescimento celular de linhagens normais e tumorais na presença de 5-FU;
7. Avaliar os efeitos dos compostos selecionados sobre alterações da mucosa intestinal associadas ao tratamento com 5-FU em ratos;
8. Avaliar os efeitos dos compostos selecionados sobre a concentração de uridina no plasma de ratos tratados ou não com 5-FU;
9. Avaliar os efeitos dos compostos selecionados sobre alterações histopatológicas no intestino de ratos tratados ou não com 5-FU;
10. Verificar os efeitos dos compostos líderes sobre a atividade de mieloperoxidase no intestino de ratos tratados com 5-FU.

Os próximos capítulos estão organizados da seguinte forma:

No **Capítulo 2** consta o artigo científico publicado no periódico internacional *Journal of Medicinal Chemistry* e é composto pelos resultados obtidos dos objetivos específicos 1-4.

No **Capítulo 3** consta o artigo científico submetido no periódico internacional *Cancer Chemotherapy and Pharmacology* e é composto pelos resultados obtidos dos objetivos específicos 5-10.

No **Capítulo 4** são apresentadas as considerações finais.

Capítulo 2

"Design of novel potent inhibitors of human uridine phosphorylase-1: synthesis, inhibition studies, thermodynamics and *in vitro* influence on 5-fluorouracil cytotoxicity"

Manuscrito publicado no periódico *Journal of Medicinal Chemistry*, 2013.

Journal of Medicinal Chemistry

Article

pubs.acs.org/jmc

Design of Novel Potent Inhibitors of Human Uridine Phosphorylase-1: Synthesis, Inhibition Studies, Thermodynamics, and in Vitro Influence on 5-Fluorouracil Cytotoxicity

Daiana Renck,[†,‡] Pablo Machado,[†,‡] Andre A. Souto,[‡,§] Leonardo A. Rosado,[†,‡] Thais Erig,[∥,⊥] Maria M. Campos,[‡,∥,⊥] Caroline B. Farias,[#] Rafael Roesler,[#,▽] Luis F. S. M. Timmers,[‡,○] Osmar N. de Souza,[‡,○] Diogenes S. Santos,*[,†,‡] and Luiz A. Basso*[,†,‡]

[†]Centro de Pesquisas em Biologia Molecular e Funcional (CPBMF), Pontifícia Universidade Católica do Rio Grande do Sul (PUCRS), 6681/92-A, TecnoPuc, Av. Ipiranga, 90619-900 Porto Alegre, Rio Grande do Sul, Brazil

[‡]Programa de Pós-Graduação em Biologia Celular e Molecular, Pontifícia Universidade Católica do Rio Grande do Sul (PUCRS), 90619-900 Porto Alegre, Rio Grande do Sul, Brazil

[§]Faculdade de Química, Pontifícia Universidade Católica do Rio Grande do Sul (PUCRS), 6681/P12 Av. Ipiranga, 90619-900 Porto Alegre, Rio Grande do Sul, Brazil

[∥]Instituto de Toxicologia e Farmacologia, Pontifícia Universidade Católica do Rio Grande do Sul (PUCRS), 6681/P12 Av. Ipiranga, 90619-900 Porto Alegre, Rio Grande do Sul, Brazil

[⊥]Faculdade de Odontologia, Pontifícia Universidade Católica do Rio Grande do Sul (PUCRS), 6681/P6 Av. Ipiranga, 90619-900 Porto Alegre, Rio Grande do Sul, Brazil

[#]Laboratório de Pesquisa em Câncer, CPE-HCPA, Universidade Federal do Rio Grande do Sul (UFRGS), 90040-060 Porto Alegre, Rio Grande do Sul, Brazil

[▽]Laboratório de Neurofarmacologia e Biologia de Tumor Neuronal, Departamento de Farmaciologia, Instituto de Ciências Básicas da Saúde, Universidade Federal do Rio Grande do Sul (UFRGS), 90040-060 Porto Alegre, Rio Grande do Sul, Brazil

[○]Laboratório de Bioinformática, Modelagem e Simulação de Biossistemas (LABIO), Faculdade de Informática, Pontifícia Universidade Católica do Rio Grande do Sul (PUCRS), 6681/P32 Av. Ipiranga, 90619-900 Porto Alegre, Rio Grande do Sul, Brazil

Supporting Information

ABSTRACT: Uridine (Urd) is a promising biochemical modulator to reduce host toxicity caused by 5-fluorouracil (5-FU) without impairing its antitumor activity. Elevated doses of Urd are required to achieve a protective effect against 5-FU toxicity, but exogenous administration of Urd is not well-tolerated. Selective inhibitors of human uridine phosphorylase (hUP) have been proposed as a strategy to increase Urd levels. We describe synthesis and characterization of a new class of ligands that inhibit hUP type 1 (hUP1). The design of ligands was based on a possible S_N1 catalytic mechanism and as mimics of the carbocation in the transition state of hUP1. The kinetic and thermodynamic profiles showed that the ligands here presented are the most potent in vitro hUP1 inhibitors developed to date. In addition, a lead compound improved the antiproliferative effects of 5-FU on colon cancer cells, accompanied by a reduction of in vitro 5-FU cytotoxicity in aggressive SW-620 cancer cells.

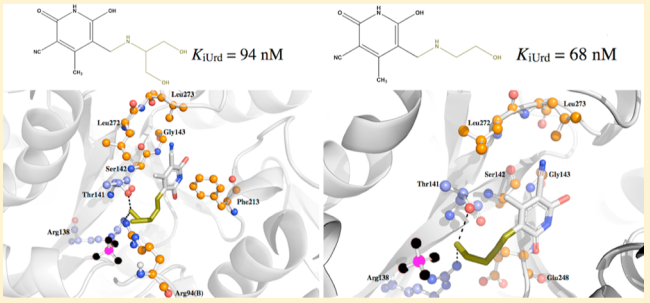

INTRODUCTION

Uridine (Urd) is a natural pyrimidine nucleoside that is involved, directly or indirectly, in many cellular processes including RNA and biomembrane synthesis,[1] galactose metabolism,[2,3] modulation of reproduction,[4] regulation of body temperature,[5] and peripheral and central nervous systems activities.[6,7] Furthermore, Urd has been described for decades as a promising biochemical modulator of 5-fluorouracil (5-FU) metabolism.[8−10] 5-FU was synthesized in 1957 by Charles Heidelberger,[11] and since then it has been broadly used in the clinical setting to treat solid tumors such as breast, colorectal, and head and neck cancers.[12,13] 5-FU requires metabolic activation and, as a uracil analogue, it is processed by the same enzymes involved in pyrimidine salvage pathway.[13,14] The active metabolites act through two main pathways: by forming a ternary complex with thymidylate synthase (TS) leading to inhibition of DNA synthesis and interference with DNA repair

Received: September 9, 2013

   dx.doi.org/10.1021/jm401389u | J. Med. Chem. XXXX, XXX, XXX−XXX

and by incorporating fluorouridine 5′-triphosphate (FUTP) into RNA.[13−16] It has been hypothesized that the therapeutic activity of 5-FU is due to DNA damage, whereas the toxic side effects are related to RNA damage by FUTP incorporation.[17−19] In this context, there has been interest in the use of Urd as a biochemical modulator to counteract the host toxicity caused by chemotherapy with fluoropyrimidines, as 5-FU, thereby enabling the increase in doses of these drugs. High levels of Urd leads to an increase in UTP levels, which will compete with FUTP for RNA incorporation.[15,18,20] However, sustainable high plasma concentration is required for Urd to exert a protective effect against 5-FU toxicity. Unfortunately, this approach is precluded by dose-limiting toxic side effects and the rapidly restored levels when either oral or intravenous infusions are administrated.[15,21] Two pro-drugs of Urd were synthesized to surmount this barrier, but the strategy failed due to the low potency and unfavorable pharmacokinetic profile.[22] The half-life of Urd in plasma is only 2 min, with more than 80% metabolized in liver by uridine phosphorylase (hUP, EC 2.4.2.3) to maintain its homeostasis concentration (1−5 μM) in plasma and tissues.[22,23] The hUP enzyme catalyzes the reversible phosphorolysis of Urd to yield uracil and ribose-1-phosphate (R1P) in the presence of inorganic phosphate (P_i).[24] The enzyme is present in two isoforms: hUP1[25] that is widely distributed in tissues and hUP2[26] that is expressed only in kidney. The hUP1 is the most studied isoform, and we have recently reported its mode of action.[27] The kinetic mechanism of recombinant hUP1 was determined as steady-state ordered bi−bi with P_i substrate binding first followed by Urd binding. In addition, measurements of pH rate profiles for hUP1 prompted us to propose the amino acids that are likely to play a role in substrate binding and catalysis.[27] These proposals were also based on reported structural data for hUP1.[28] A number hUP inhibitors have been developed, including pyrimidine acyclonucleoside analogues. This class of compounds can be represented by 5-benzyl/5-benzylbarbituric acid derivatives[29,30] and phenylselenyl/phenylthio-substitute,[29,31] the most potent of which being 5-benzyl-1-(2′-hydroxyethoxymethyl)uracil (BAU or 5-benzylacyclouridine) with an in vitro K_i value of 100 nM for Urd substrate.[32,33] In the present study, we report the design, synthesis, and determination of kinetic and thermodynamic parameters for a new class of potent hUP1 inhibitors. The effect of these inhibitors on viability of normal and tumor cells, and their effect on 5-FU toxicity are also described.

RESULTS AND DISCUSSION

Design and Chemistry. First, in our strategy to obtain novel compounds with hUP1 inhibitory activity, we maintained the 2,6-dihydroxyl groups on the pyridine ring. This type of substitution on an aromatic ring, such as pyridine, preserves the substituents of the uracil base and serves as a classic bioisosteric replacement for six-membered rings.[34] In addition, the importance of these chemical groups has been illustrated by the analysis of the main inhibitors of UP (both human and not human) that have been previously reported. The importance of these groups is also supported by crystallographic studies, which have shown that hydrogen bonds form between these substituents at a molecular recognition level in the active site of hUP1.[28,35] Indeed, both BAU and 5-FU establish polar contacts involving the uracil rings and the Gln217 and Arg219 residues.[28,35]

It was thus deemed appropriate to test as an initial hit for hUP1 enzyme inhibition the commercially available 6-hydroxy-1*H*-pyridin-2-one (**1**) compound (Figure 1). This compound

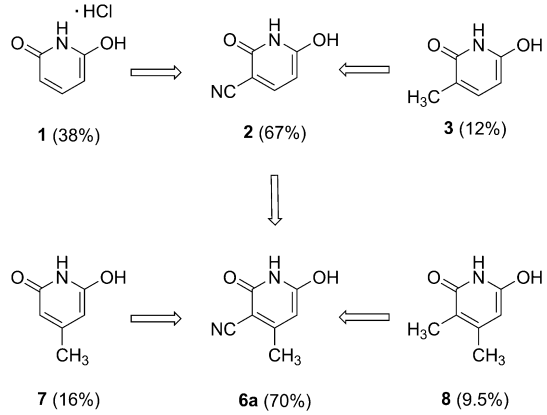

Figure 1. Scaffold evolution from 6-hydroxy-1*H*-pyridin-2-one (**1**). Inhibitory activity presented between brackets for 1 μM final concentration of compounds.

(**1**) was able to inhibit the activity of hUP1 by 38% when tested at a final concentration of 1 μM (Table 1). In the first attempt

Table 1. Observed in Vitro Inhibitory Activities over hUP1 Catalyzed Reaction

compd	inhibitory activity (%)[a]	compd	inhibitory activity (%)[a]
1	38	**6j**	60
2	67	**7**	16
3	12	**8**	9.5
6a	70	**10a**	80
6b	25	**10b**	82
6c	16	**10c**	78
6d	31	**10d**	81
6e	42	**10e**	25
6f	2	**10f**	49
6g	ND[b]	**10g**	51
6h	12	**11**	2
6i	43		

[a]Assigned at compounds final 1 μM concentrations in assay mixture. [b]Nondetected inhibitory activity.

to improve the inhibitory activity of compound **1**, we analyzed the contacts made by 5-FU at the site of hUP1 according to diffractometry studies. From these observations, one can note that N-1 of 5-FU is positioned 4.1 Å and 3.8 Å from residue Thr141, whereas the 5-fluoro moiety is directed toward the hydrophobic cavity formed by Leu272, Leu273, and Ile281. On the basis of these distances, the sum of the van der Walls radii and geometry, N-1 does not appear to form hydrogen bonds with hUP1. In contrast, the 5-fluoro substituent makes a polar contact with Ser142.[35] Our hypothesis was that 6-hydroxy-1*H*-pyridin-2-one nitrile-containing compounds can correctly place a hydrogen bond acceptor in proximity to Thr141 or participate in interactions with the cavity occupied by the fluorine of 5-FU because both the 3- and 5-positions are identical in this aromatic structure. Moreover, the electron-withdrawing effect caused by the nitrile group could facilitate the formation of hydrogen bonds with residues of hUP1 because of the reduction in the pK_a values of compounds as the conjugated

dx.doi.org/10.1021/jm401389u | J. Med. Chem. XXXX, XXX, XXX−XXX

base is stabilized. As the polar nitrile group places the nitrogen atom at 2.6 Å from C-3 of the 1*H*-pyridin-2-one ring, according to the data for the energy-minimized structure, there would be room for interaction with either Thr141, or Ser142, Leu272, and Leu273. This group is present in several drugs in clinical use and undergoing clinical trials, and it typically makes compounds more metabolically stable than their counterparts.[36] The greater stability conferred by the nitrile group is particularly important in 1*H*-pyridin-2-one **1** because this compound can readily undergo oxidation by 2,6-dihydroxypyridine-3-hydroxylase to yield 2,3,6-trihydroxypyridine.[37] Therefore, 1*H*-pyridin-2-one **2** was synthesized according to reported methodologies[38] and its hUP1 inhibitory activity was 67% at 1 μM (Figure 1 and Table 1). The replacement of the nitrile group with a methyl substituent at the 3-position demonstrated the importance of the nitrile group to the compound's inhibitory activity because 1*H*-pyridin-2-one **3** inhibited the activity of hUP1 by only 12% (Figure 1 and Table 1). As the C≡N unit is approximately 8 times smaller than a methyl group (**3**),[36] these results suggest that bulkier groups at this position are not likely to be better hUP1 inhibitors. To evaluate the effect of chemical substitutions at different positions, a series of 6-hydroxy-1*H*-pyridin-2-one-3-carbonitriles were synthesized via the cyclocondensation of β-ketoesters **4a−4i** with cyanoacetamide **5** in a basic reaction medium (Scheme 1).

Scheme 1

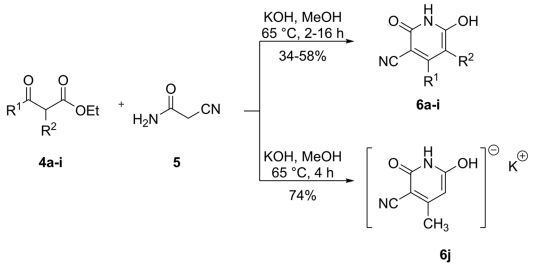

Compounds 4,6	R^1	R^2	Yield (%)
a	Me	H	52
b	Et	H	41
c	Pr	H	54
d	^{i}Pr	H	39
e	Ph	H	58
f	Bn	H	55
g	Me	Et	47
h	Me	Ph	34
i	Me	Bn	39

The alkyl and aryl chains attached to C-4 and C-5 on the 1*H*-pyridin-2-one-3-carbonitrile ring were varied, and the synthesis was performed according to reported methodologies,[39−41] yielding compounds **6a−6i** in 34−58% yields with reaction times of 2−16 h. When the acid work up was not performed, the compounds could be isolated in their salt forms.[39] The potassium salt **6j** was isolated in 74% yield (Scheme 1). All the synthesized compounds had spectroscopic data that were in agreement with the proposed structures. The hUP1 enzyme inhibition data for compounds **6a−6j** (Table 1) show that only **6a** displayed a better inhibitory activity as compared to the parent compound **2** (Figure 1 and Table 1). To assess the role of 3-nitrile and 4-methyl groups of 6-hydroxy-1*H*-pyridin-2-one ring of **6a**, the inhibitory activity of commercially available compounds **7** and **8** (Figure 1) were evaluated. The absence of the nitrile group or its replacement with a methyl group led to a dramatic decrease in the inhibitory activity. Alkyl, phenyl, and benzyl substitutions at C4 (**6b−6f**) resulted in weaker inhibitory activity (Table 1). Ethyl, phenyl, and benzyl substitutions at C5 of 4-methyl 6-hydroxy-1*H*-pyridin-2-one ring (**6g−6i**) were also detrimental to the inhibitory activity (Table 1) of the parent compound (**6a**). On the basis of this preliminary screening, compound **6a** was employed in the next round of chemical modifications. It appears worth mentioning that the compounds that were synthesized may be obtained in three tautomeric forms in both solid and liquid state.[38,39,42] On the basis of differences in stability, the most probable tautomer is the 1*H*-pyridin-2-one form. Semiempirical calculations for **6a** using the AM1 method[43] showed that this form is 1.96 and 3.7 kcal mol^{-1} more stable than 1*H*-pyridin-6-one and 2,6-dihydroxypyridine forms, respectively. The stability of 1*H*-pyridin-2-one form permits to infer that this tautomer is obtained in almost 96% at 37 °C (Figure S1, Supporting Information). This observation was supported by experimental data as nitrile absorption was obtained in agreement with presence of an ortho-electron withdrawing group.[42] In addition, no signal of others tautomers was observed in both NMR and FTIR experiments.

Acyclic mimics of the ribooxacarbenium ion of the transition state analogues of purine nucleoside phosphorylases have been reported to inhibit the enzyme at low nanomolar concentrations.[44−46] In addition to their low inhibition constant values, these simplified analogues are readily accessible chemically, and several of them do not contain asymmetric carbon centers. We thus deemed appropriate to use this structural template to develop potent hUP1 inhibitors. Incidentally, formation of a ribooxacarbenium ion in the transition state has been proposed for *Escherichia coli* UP[47] and hUP1[28] enzymes. A bimolecular A_ND_N mechanism with an S_N2-like transition state, in which the ribosyl moiety possesses significant bond order to both nucleophile and leaving groups, has been proposed for the arsenolysis of uridine catalyzed by *Trypanosoma cruzi* UP.[48] Therefore, the classic Mannich reaction was performed using primary amino alcohols and secondary cyclic and acyclic amines to access the desired compounds. Compounds **10a−10g** were obtained after heating **6a** in the presence of the appropriate amino alcohol or secondary amine and paraformaldehyde using methanol as solvent (Scheme 2). The products were found in 44−80% yields, and the reaction times ranged from 4 to 16 h (Scheme 2). As previously reported,[44] the secondary amines led to compounds with yields that were higher than those of the amino alcohol derivatives. All the synthesized compounds had spectroscopic data that were in agreement with the proposed structures. The 6-hydroxy-1*H*-pyridin-2-one-3-carbonitriles **10a−10g** were assayed for their ability to inhibit the catalytic activity of hUP1, using a final-fixed concentration of 1 μM as initial screening (Table 1). Despite the limited number of compounds evaluated, some characteristics of the structure−activity relationship are apparent. The presence of the hydroxyl group on the alkyl chain was a feature of fairly active 6-hydroxy-1*H*-pyridin-2-one-3-carbonitriles (**10a−10c**). A uracil derivative **11** (Figure 2) was synthesized according to a reported protocol,[49] and its inhibitory activity was measured.

Inhibitors Selection and Time-Dependent Inhibitory Activity Measurements. The initial screening of 23

dx.doi.org/10.1021/jm401389u | J. Med. Chem. XXXX, XXX, XXX−XXX

Scheme 2[a]

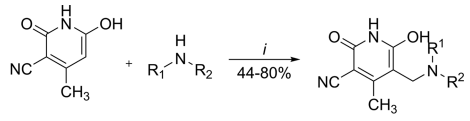

6a 9a-g 10a-g

Compounds 9,10	R^1	R^2	Yield (%)
a	CH_2CH_2OH	H	64
b	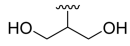	H	44
c	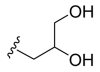	H	58
d	Me	Me	77
e	Et	Et	72
f	$CH_2(CH_2)_3CH_2$		76
g	$CH_2CH_2OCH_2CH_2$		80

[a]Reactants and conditions: i = $OH(CH_2O)_nH$, MeOH, 100 °C, 4−16 h.

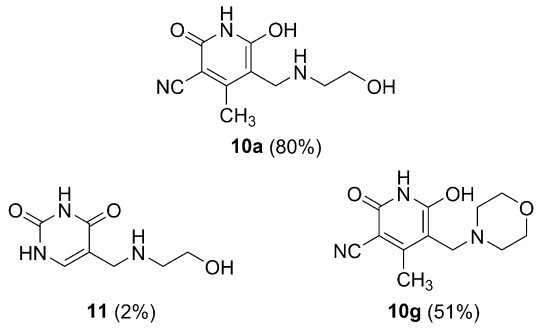

10a (80%) **11** (2%) **10g** (51%)

Figure 2. Structural modifications of compound **10a** with apparent requirements for potency. Percentage of inhibition of hUP1 activity showed between brackets for compound concentrations of 1 μM.

compounds showed that six compounds (**2**, **6a**, **10a**, **10b**, **10c**, and **10d**) displayed reasonably good inhibition (>60%) of hUP1 activity at final-fixed concentration of 1 μM (Table 1). The nitrile group on 3-position with (**6a**) or without (**2**) a methyl group on 4-position of the 6-hydroxy-1*H*-pyridin-2-one ring appears to be required for inhibitory activity of this class of compounds. The absence of the nitrile (**1**, **7**) or its replacement with a methyl group (**3**, **8**) at the 3-position of 6-hydroxy-1*H*-pyridin-2-one ring were detrimental to their inhibitory activity. Compounds in which the C4-methyl group was replaced with bulkier groups in the 6-hydroxy-1*H*-pyridin-2-one-3-carbonitriles (**6b**−**6f**) also showed decreased inhibitory activity. The ramifications attached to 5-position, absent in **2** and **6a**−**6f**, resulted in different inhibitory effects, namely compounds **10a**−**10d** displayed improved inhibitory activity whereas **10e**−**10g** were less active (Table 1) as compared to the parent compound (**6a**). It is noteworthy that the simplest amino alcohol led to the most potent series of inhibitors (**10a**−**10c**). The subtlety of the interactions with hUP1 can be assessed by the differing inhibitory activities of compounds **10d** (81%) and **10e** (25%) at 1 μM. The effects of constraining the side chain of **10a** using a morpholine derivative were tested based on the hypothesis that this approach would reduce the entropic penalties, leading to a more potent inhibitor. However, compound **10g** (51%) was less potent than **10a** (80%) at 1 μM (Table 1). Ramifications on C5 of 6-hydroxy-1*H*-pyridin-2-one-3-carbonitrile participate in hydrogen and hydrophobic interactions with amino acids in hUP1 active site, as discussed below. The six best compounds (**2**, **6a**, **10a**−**10d**) and BAU showed no time-dependent inhibition of hUP1 enzyme activity (data not shown). Accordingly, K_i measurements were carried out following classic Michaelis−Menten experiments. DMSO was investigated as a possible enzyme activity modulator, and no interference was observed at the maximum percentage of this solvent used to dissolve the compounds (1%).

Determination of K_i for Inhibitors of hUP1. The K_i values were determined for six selected compounds (**2**, **6a**, **10a**−**10d**) and BAU. The K_i of BAU was determined for both substrates and was compared with the K_i value for Urd in the literature.[32,33] The values determined corroborate the literature data and allowed a directed comparison of the inhibitory ability between the molecules here described and the best in vitro hUP1 inhibitor reported in the literature (BAU). Lineweaver−Burk plots (Figures S5−S11, Supporting Information) suggested the mode of inhibition (competitive, noncompetitive or uncompetitive) and data fitting to appropriate equations gave values for the inhibition constants (K_{is} and/or K_{ii}).[50,51] The inhibition data are summarized in Table 2. The best compounds in the series of synthesized analogues were **10a** with K_i values for Urd = 68 ± 10 nM and P_i = 127 ± 8 nM, and **10b** with K_i values for Urd = 94 ± 11 nM and P_i = 98 ± 6 nM. For both inhibitors, the types of inhibition were competitive toward Urd and uncompetitive to P_i. A steady-state ordered bi−bi kinetic mechanism has been proposed for hUP1, in which P_i binds first followed by the binding of Urd, and uracil dissociates first followed by R1P release.[27] The inhibition patterns for **10a** and **10b** indicate that the molecule binds to hUP1−P_i binary complex and competes with Urd binding en route to ternary complex formation, corroborating the ordered bi−bi mechanism proposed for hUP1.[27] Although one cannot assume that because an inhibitor displays the characteristic

Table 2. Inhibitory Constants of Selected Molecules on hUP1 Activity

compd	K_{is}/K_{ii} Urd (nM)	inhibition mode	K_{is}/K_{ii} P_i (nM)	inhibition mode
2	2610 ± 339/2546 ± 330	noncompetitive	565 ± 113/666 ± 59	noncompetitive
6a	375 ± 145/635 ± 91	noncompetitive	332 ± 32	uncompetitive
10a	68 ± 10	competitive	127 ± 8	uncompetitive
10b	94 ± 11	competitive	98 ± 6	uncompetitive
10c	109 ± 10	competitive	182 ± 7	uncompetitive
10d	99 ± 13	competitive	107 ± 7	uncompetitive
BAU[a]	130 ± 21	competitive	547 ± 44/317 ± 61	noncompetitive

[a]5-Benzyl-1-(2′-hydroxyethoxymethyl)uracil.

dx.doi.org/10.1021/jm401389u | J. Med. Chem. XXXX, XXX, XXX−XXX

signature of a competitive inhibitor that it necessarily binds to the enzyme active site,[50,51] the uncompetitive patterns for **10a** and **10b** toward P_i further suggest that these compounds bind to the Urd binding site of hUP1. For the design and synthesis of inhibitors, it is important to keep in mind the probable effect of these compounds in vivo, synthesizing molecules with different types of inhibition as their effectiveness (ability to produce a beneficial effect) depends on both the inhibitor binding affinity and the concentration of the natural ligands in the organism. It has been described that hUP1 activity as well as the enzymes in the salvage pathway are enhanced in tumor cells in contrast to normal cells because the tumor cells are constantly undergoing cell division thus requiring recycling of bases and nucleosides for RNA and DNA synthesis.[25,52] Owing to the importance of P_i and Urd in many cell processes, their balances are tightly controlled being vital for maintaining basic cellular function.[1,53−55] The P_i concentration is maintained at approximately 4.4 mM,[53] which is 2-fold larger than the K_m value for P_i (2.46 mM),[27] and the Urd levels in plasma and tissues are tightly maintained in the range 1−5 μM,[22,23] values lower than the K_m for Urd (51 μM) for the hUP1-catalyzed chemical reaction.[27] Accordingly, it is tempting to suggest that the competitive inhibition mode toward Urd and uncompetitive mode toward P_i bodes well to in vivo activity of **10a−10d** compounds. As intracellular P_i concentration is larger than its K_m value, formation of hUP1−P_i is likely and ensuing binding of **10a−10d** compounds to this binary complex feasible. In addition, these compounds would compete with an intracellular concentration of Urd that is lower than its K_m value, and displacement of inhibitors from hUP1 active site by Urd would thus be precluded.

Molecular docking experiments were performed to try to determine the interactions that occur upon enzyme−inhibitor complex formation. Interestingly, BAU showed a lower number of interactions than **10a** and **10b** (Figure 3). The substituents at the 5-position of **10a** and **10b** make hydrogen bonds with Thr141 (chain A) and Arg138 (chain A), and the ligand **10b** also participates in a hydrophobic interaction with Arg94 (chain B). The corresponding 1-hydroxyethoxymethyl group of BAU makes hydrogen contacts with Thr141 (chain A) and His36 (chain B) and a hydrophobic contact with Ser142 (chain A).[28] The benzyl ring of BAU makes hydrophobic interactions with Phe213 (chain A), Ile281 (chain A), Met110 (chain A), and Tyr35 (chain B).[28] The nitrile groups of **10a** and **10b** make hydrophobic interactions with Leu272 (chain A), Leu273 (chain A), Ser142 (chain A), and Gly143 (chain A). The nitrile of **10b** also makes a hydrophobic interaction with Phe213 (chain A). It has been shown that the fluorine moiety of 5-FU forms a hydrogen bond with Ser142 and hydrophobic interactions with Leu272, Leu273, and Ile281 residues.[35] The nitrile of **10a** and **10b** and the fluorine of 5-FU thus appear to bind to the same site of hUP1. The compounds without the ramification on 5-position (e.g., **2** and **6a**) do not make hydrogen bonds with Thr141 (chain A) and Arg138 (chain A) (data not shown), which is consistent with the larger K_i values for these compounds (Table 2).

Enzyme activity measurements were carried out to assess whether or not the compounds to which K_i and mode of inhibition of hUP1 were determined (Table 2) could also inhibit human thymidine phosphorylase enzyme (EC 2.4.2.4) activity. The IC_{50} values (concentration of inhibitor that reduces enzyme velocity by half) were >100 μM for compounds **2**, **6a**, and **10a−10d** (data not shown). These

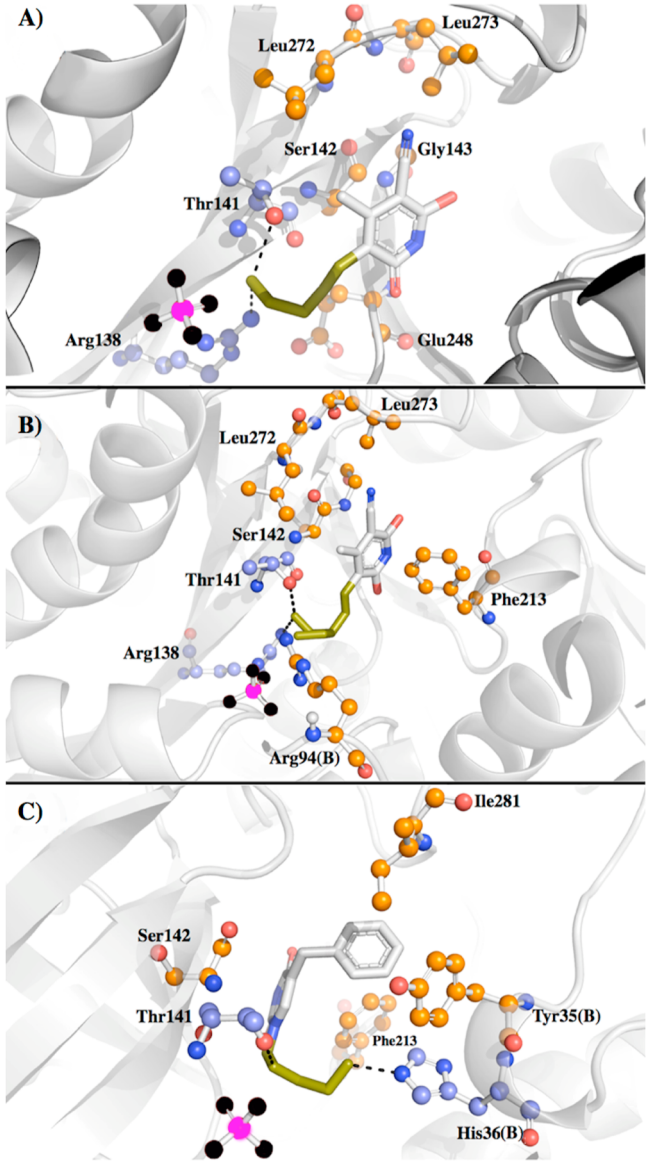

Figure 3. Three-dimensional representations of hUP1−ligands interactions. Docking simulations for hUP1−**10a** (A) and hUP1−**10b** (B). Crystal structure (PDB ID: 3EUF) of hUP1−BAU complex (C). The residues that are making contacts with **10a**, **10b**, and BAU are drawn as ball and sticks and colored as follows. Hydrophobic contacts: carbon (orange), nitrogen (blue), oxygen (red). Hydrogen bonds: carbon (light-blue), nitrogen (blue), oxygen (red). The 5-position of **10a** and **10b** and 1-position of BAU are colored in deep-olive and drawn as sticks. Phosphates are drawn as ball and stick representation and colored by atom (oxygen = black and phosphorus = pink). hUP1 tertiary structure is represented as cartoon. Figures prepared using PyMol (www.pymol.org).

results lend support to the specificity of compounds tested toward hUP1 enzyme as has been reported for pyrimidine acyclonucleosides inhibitors.[29,30] As thymidine phosphorylase may play a role in the therapeutic application of 5-FU because it is known to catalyze the conversion of 5-FU to 5′-fluoro-2′-deoxyuridine by the addition of 2-deoxyribose-1-phosphate, the specificity of the compounds here described for hUP1 activity appears to be a desirable feature to not interfere with antitumor activity of 5-FU. The low K_i values of **10a** and **10b** (in the same range as BAU), the mode of inhibition and specificity for hUP1 warranted further experimental efforts.

dx.doi.org/10.1021/jm401389u | J. Med. Chem. XXXX, XXX, XXX−XXX

Table 3. Thermodynamics Parameters for Free Enzyme and for the hUP1−P_i and hUP1−R1P Complexes at 310.15 K (37 °C)[a]

compd	hUP1 or complex	$\Delta H°$ (kcal/mol)	$-T\Delta S°$ (kcal/mol/K)	$\Delta G°$ (kcal/mol)	K_d (nM)
2	hUP1	−9.6 ± 0.3	1.7 ± 0.3	−7.8 ± 1.5	2900 ± 554
	hUP1−P_i				
	hUP1−R1P 50 μM	−15 ± 0.1	5.7 ± 0.9	−9.8 ± 1.6	108 ± 18
	hUP1−R1P 150 μM	−18 ± 0.5	8.5 ± 3.2	−9.7 ± 3.7	127 ± 48
6a	hUP1				
	hUP1−P_i	−19 ± 1.3	12 ± 1.4	−6.9 ± 0.8	12000 ± 1395
	hUP1−R1P 50 μM	−31 ± 1.2	22 ± 5.4	−8.3 ± 2.0	1400 ± 341
	hUP1−R1P 150 μM	−21 ± 0.1	11 ± 1.5	−9.8 ± 1.4	40 ± 5.0
	hUP1−R1P 200 μM	−22 ± 0.1	11 ± 1.3	−11 ± 1.3	20 ± 2.0
10a	hUP1	−23 ± 0.5	14 ± 1.5	−8.0 ± 0.9	2000 ± 221
	hUP1−P_i	−16 ± 0.2	6.4 ± 1.4	−9.5 ± 2.1	151 ± 34
	hUP1−R1P 50 μM	−17 ± 0.6	9.5 ± 1.7	−8.0 ± 1.5	2300 ± 423
	hUP1−R1P 150 μM	−30 ± 1.5	23 ± 3.3	−7.6 ± 1.1	3800 ± 553
10b	hUP1	−24 ± 0.6	16 ± 2.0	−7.4 ± 1.0	5300 ± 674
	hUP1−P_i	−14 ± 0.2	5.0 ± 0.8	−9.0 ± 1.5	502 ± 83
	hUP1−R1P 50 μM	−18 ± 0.4	10 ± 1.0	−7.3 ± 0.7	7000 ± 661
	hUP1−R1P 150 μM	−10 ± 1.0	3.3 ± 1.0	−7.3 ± 2.2	7000 ± 2115
10c	hUP1	−22 ± 2.2	15 ± 2.0	−6.7 ± 0.9	20000 ± 2633
	hUP1−P_i	−19 ± 0.1	10 ± 1.0	−9.3 ± 0.9	263 ± 26
	hUP1−R1P 50 μM	−22 ± 0.5	14 ± 1.0	−7.5 ± 0.5	4600 ± 344
	hUP1−R1P 150 μM	−18 ± 0.8	11 ± 1.2	−7.1 ± 0.8	9400 ± 1037
10d	hUP1	−6.7 ± 0.2	0.8 ± 0.1	−7.6 ± 1.1	4200 ± 602
	hUP1−P_i	−12 ± 0.2	2.6 ± 0.6	−9.1 ± 2.1	312 ± 73
	hUP1−R1P 50 μM	−22 ± 0.4	14 ± 0.7	−7.2 ± 0.4	7400 ± 381
	hUP1−R1P 150 μM	−23 ± 0.1	16 ± 2.1	−7.0 ± 0.9	10000 ± 1325
BAU[b]	hUP1	−10 ± 0.1	1.5 ± 0.2	−8.4 ± 1.0	1200 ± 150
	hUP1−P_i	−13 ± 0.3	4.6 ± 0.8	−8.2 ± 1.4	1400 ± 239
	hUP1−R1P 50 μM	−12 ± 0.3	4.3 ± 0.9	−8.2 ± 1.7	1200 ± 244
	hUP1−R1P 150 μM	−20 ± 0.7	12 ± 1.6	−7.3 ± 1.0	6600 ± 898

[a]Cells in which no data are given are for interaction processes that yielded no reliable data. [b]5-Benzyl-1-(2′-hydroxyethoxymethyl)uracil.

Determination of Thermodynamic Parameters by Isothermal Titration Calorimetry (ITC). The interaction phenomenon can be monitored by ITC measuring the differential heat (released or absorbed) among the sample and reference cells during a binding reaction, yielding values for the following thermodynamic parameters: enthalpy change ($\Delta H°$), entropy change ($\Delta S°$), Gibbs free energy change ($\Delta G°$), and association constant (K_a). The binding processes for compounds **2**, **6a**, **10a**−**10d**, and BAU to hUP1 were assessed by ITC (Table 3). The experimental data were analyzed in the differential mode, displaying sigmoidal plots (Figures S12−S18, Supporting Information). The differential mode treats each injection as an independent point and is plotted as heat evolved per injection vs molar ratio (ratio of total ligand concentration to hUP1 concentration).[56] The binding interactions between hUP1 and ligands were characterized by exothermic reactions and favorable Gibbs free energy changes, as negative values were observed for both $\Delta H°$ and $\Delta G°$ (Table 3). Compounds **2**, **6a**, and **10a**−**10d** exhibited a rather frequent problem in biological systems on the course of lead optimization, namely the enthalpy−entropy compensation ($\Delta H°-\Delta S°$) behavior.[57−59] This compensatory system leads to a linear relationship between the change in enthalpy and in entropy, resulting in no affinity gains ($\Delta G°$). Interestingly, the parent compound (**6a**) displayed a more favorable enthalpy of binding to hUP1−P_i (−19 kcal mol^{-1}) than the derivatives **10a** (−16 kcal mol^{-1}), **10b** (−14 kcal mol^{-1}), and **10d** (−12 kcal mol^{-1}), except **10c** (−19 kcal mol^{-1}). However, the more pronounced entropic penalty for **6a** as compared to **10a**−**10d** resulted in lower values for the dissociation constant of the latter compounds and more favorable $\Delta G°$ values (Table 3). These results are in agreement with lower inhibition constant values for **10a**−**10d** as compared to **6a** obtained from enzyme activity measurements (Table 2). The lower dissociation constant values for **10a**−**10d** binding to hUP1−P_i as compared to binding to free enzyme (Table 3) lends further support to the uncompetitive mode of inhibition toward P_i (Table 2). Interestingly, the ITC data for compounds **2** and **6a** show that there exists an increase in affinity (lower dissociation constant values) for binding to hUP1−R1P binary complex as compared to binding to free hUP1 for **2** and to hUP1−P_i for **6a** (Table 3). Compound **6a**, in particular, displays increasing affinity as a function of increasing R1P concentration (Table 3), thereby suggesting formation of a dead-end complex. On the other hand, compounds **10a**−**10d** showed decreasing affinity as a function of increasing R1P

dx.doi.org/10.1021/jm401389u | J. Med. Chem. XXXX, XXX, XXX−XXX

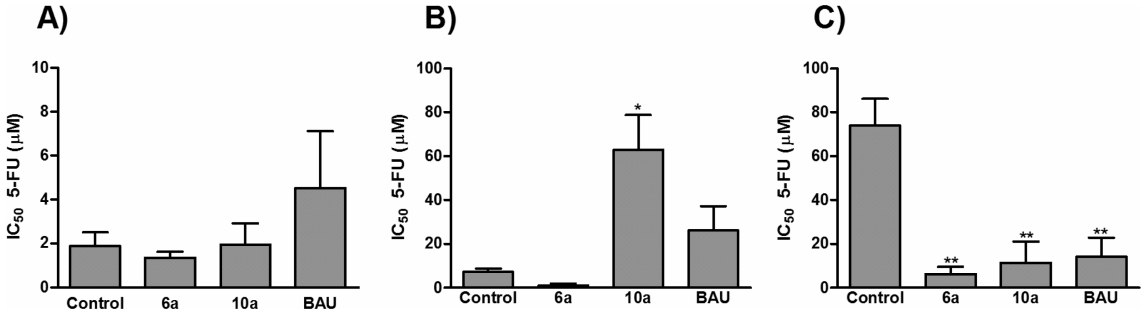

Figure 4. The (A) HaCat, (B) HT-29, and (C) SW-620 cell lineages were cultured and treated with different concentrations of 5-FU followed by 72 h of incubation with 30 μM of the compounds **6a**, **10a**, or BAU. Control cells were exposed only to culture medium or culture medium with 1% DMSO. Data are shown as mean ± standard error of mean of three independent experiments performed in quadruplicate. The statistical analysis was performed by one-way ANOVA followed by Bonferroni's post hoc test. * Significantly different from the control group ($p < 0.05$).

concentration (Table 3), suggesting overlapping binding sites. In addition, the stoichiometry (n) of the reaction was different for some inhibitors. The hUP1 enzyme is dimeric in solution, with the two active sites in the interface of the monomers,[28] consequently the n of the binding assays should be 1. The compounds **2**, **6a**, and **10c** showed n = 0.5, suggesting a negative cooperativity in which the binding of one molecule of inhibitor cause a conformational change that locks the protein in a disable form, weakening the binding affinity of the other active site of the enzyme.[60] The thermodynamics parameters of **6a** and **10a−10d** show more favorable $\Delta H°$ values as compared to BAU (Table 3), indicating a larger stability value for the protein−ligand complex (less energy is required for complex formation) due to the thermodynamic of noncovalent interaction profile (hydrogen bonds and van der Waals redistribution), suggesting a better complementarity between the protein and ligands.[58,59] On the other hand, the entropic contributions of **6a** and **10a−10c** (except **10d**) are less favorable as compared to BAU (Table 3). These results suggest that addition of hydrophobic groups could improve the entropic contributions of these compounds, perhaps on 3-position of the pyridine ring. According to previous reports, which were confirmed by hUP1 crystallographic structure, there is a hydrophobic pocket adjacent to the uracil binding site that is formed by amino acids of the two subunits.[28,32] There are differences between the interaction of BAU and compounds **10a−10b** with the hUP1 active site (Figure 3). These differences include contacts with Arg94 of chain B for **10b** (Figure 3B) and a hydrogen bond with His36 of chain B and a hydrophobic contact with Tyr35 of chain B for BAU (Figure 3C); the latter is consistent with the more favorable entropic contribution for BAU (Table 3). However, there is a limit to refine the hydrophobic nature of the analogues, such as solubility of the compounds, which can reduce oral bioavailability. For some compounds, it was not possible to determine the thermodynamic parameters for all experimental conditions tested due to low affinity of the molecule for some forms of enzyme in solution (either in complex or free).

Cytotoxicity of hUP1 Inhibitors on Normal and Tumor Cells. The possible in vitro cytotoxicity of the lead molecule (**6a**) and the best in vitro inhibitor of hUP1 (**10a**) was evaluated in normal and tumor cell lines using the 3-(4,5-dimethylthiazol-2-yl)-2,5-diphenyltetrazolium bromide (MTT) assay. The in vitro incubation of the selected compounds (1−100 μM) did not significantly affect cell viability of either normal or tumor cells (Figure S19, Supporting Information).

Influence of hUP1 Inhibitors on 5-FU IC_{50}. A concentration−response curve for 5-FU was performed in presence or absence of the compounds **6a** and **10a** to determine the influence of these inhibitors on the cytotoxicity of 5-FU in normal and tumor cell lines, using BAU as positive control.[61] The IC_{50} values for 5-FU in both the presence and absence of **6a**, **10a**, and BAU are expressed as the concentrations that corresponded to a reduction of cellular growth by 50%. The 5-FU IC_{50} for HaCat and HT-29 were similar to values previously described in the literature,[61,62] with mean values (accompanied by the 95% confidence interval) of, respectively, 1.3 (6.9−0.27) and 6.9 (9.5−5.0) μM (Figure 4). However, the IC_{50} value for the tumor SW-620 cell line [81 (107−61) μM] was significantly different from a previously reported value (15.3 ± 0.8 μM),[62] probably because the published assay was performed after only 24 h of exposure. The analysis showed that HaCat cells were equally sensitive to 5-FU with or without the compounds (Figure 4A), suggesting that the inhibitors have no effect on cytotoxicity of 5-FU for normal cells, as expected for BAU.[61] Similarly, for HT-29 tumor cells, the incubation of compound **6a** or BAU (30 μM) did not cause a significant alteration of IC_{50} values when compared to control cells (Figure 4B). However, the coexposure of these cells to 5-FU and compound **10a** (30 μM) produced an increase of about 9-fold in IC_{50} values, suggesting a protective effect for HT-29 cells (Figure 4B). Interestingly, when the more aggressive cell line SW-620 was exposed to increasing concentrations of 5-FU, in the presence of the inhibitors, the cells were far more sensitive to 5-FU, with a decrease in IC_{50} values of 12-fold for **6a** and 6-fold for **10a** (Figure 4C). 5-FU has multiple possible mechanisms of interference with the proliferative activity of cells.[13−16] It is tempting to suggest that inhibition of hUP1 by **6a** and **10a** decreased the conversion rate of 5-FU into 5-FUridine in the tumor cells, resulting in increased 5-FU concentration that would thus inhibit the TS enzyme activity and cause the DNA damage, responsible for the therapeutic effect of the chemotherapy.[17−19] However, determination of intracellular concentrations of these metabolites in the presence of **6a** and **10a** should be assessed to provide a solid basis for these proposals. At any rate, both the low cytotoxicity and the lower IC_{50} values for 5-FU (more so for **6a**) appear to warrant further efforts to be pursued.

■ CONCLUSIONS

The interest in the search for compounds that are able to decrease 5-FU toxic effects on normal cells is not recent. The initial studies were performed using exogenous Urd and its pro-

dx.doi.org/10.1021/jm401389u | J. Med. Chem. XXXX, XXX, XXX−XXX

drugs, but interest in these approaches diminished due to pharmacokinetic problems. One promising approach is the use of hUP inhibitors, which appears to be the best option to raise and maintain the Urd levels by an endogenous process. There are many classes of drug targets, and enzymes comprise an important category. The pharmaceutical industry has a great interest in the production of enzyme-targeted drugs due to the catalysis advantage for the drug design beyond the binding property, and until 2005 the FDA had approved 317 drugs that had enzymes as targets.[63] The hUP1 inhibitors have a potential utility in cancer chemotherapy regimens as modulators of the host toxicity of 5-FU. In this study, we synthesized a new potent class of hUP1 inhibitors and determined the kinetic and thermodynamic properties of these inhibitors. Data on cell culture suggested that the use of hUP1 inhibitors allow the reduction of 5-FU concentration, resulting in less damage to the normal cells and fewer side effects for the patient. The data here presented may provide key information to in vivo action and could be used to design new molecules for cancer chemotherapy.

EXPERIMENTAL SECTION

Chemistry. Compounds **1**, **3**, **7**, and **8**, starting materials, and solvents were used as obtained from commercial suppliers without further purification. Although compounds **6a−b**, **6d−6e**, **6g**, and **6i** are commercially available, they were synthesized by our research group. All melting points were measured using a Microquímica MQAPF-302 apparatus. ^{1}H NMR spectra were acquired on a Bruker DPX 400 (Federal University of Santa Maria, UFSM/Brazil) or Anasazi EFT-60 spectrometer (^{1}H at 400.13 MHz or 60.13 MHz, respectively) at 25 °C, for DPX400, and 30 °C for EFT-60, in 5 mm sample tubes. DMSO-d_6 or D_2O were used as solvent. For molecules solubilized in DMSO-d_6, TMS was used as internal standard. Chemical shifts were expressed in ppm, and J values were given in Hz. High-resolution mass spectra (HRMS) were obtained for all compounds on an LTQ Orbitrap Discovery mass spectrometer (Thermo Fisher Scientific). This hybrid system combines an LTQ XL linear ion trap mass spectrometer and an Orbitrap mass analyzer. The experiments were performed via direct infusion of the samples in phosphoric acid 0.1% acetonitrile/water (1:1, v/v) in positive-ion mode using electrospray ionization (ESI); flow rate of 10 μL min^{-1}. Elemental composition calculations were carried out using the specific tool included in the Qual Browser module of Xcalibur (Thermo Fisher Scientific, release 2.0.7). Fourier transform infrared (FTIR) spectra were recorded using a universal attenuated total reflectance (UATR) attachment on a PerkinElmer Spectrum 100 spectrometer in the wavenumber range of 650−4000 cm^{-1} with a resolution of 4 cm^{-1}. Purity of compounds was determined by HPLC using an Äkta HPLC system (GE Healthcare Life Sciences). HPLC analysis conditions: RP column 5 μm Nucleodur C-18 (250 mm × 4.6 mm); flow rate 1.5 mL min^{-1}; UV detection at 270 and 254 nm; 100% water (0.1% acetic acid) for 7 min, followed by linear gradient from 100% water (0.1% acetic acid) to 90% acetonitrile/methanol (1:1, v/v) in 16 min; the last partition was maintained by 15 min and subsequently returned to 100% water (0.1% acetic acid) in 5 min, remaining for an additional 6 min. All evaluated compounds were >95% pure.

*General Procedure for Preparation of 6-Hydroxy-1H-pyridin-2-one-3-carbonitriles **6**. Selected Example for Compound 6-Hydroxy-4-propyl-1H-pyridin-2-one-3-carbonitrile (**6c**).* To a solution of β-ketoester **4c** (0.791 g, 5 mmol) and cyanoacetamide **5** (0.420 g, 5 mmol) in methanol (8 mL) was added potassium hydroxide (0.421 g, 7.5 mmol) in methanol (8 mL). The mixture was stirred at 65 °C for 8 h. After cooling to room temperature, the amorphous solid formed was filtered off and washed with cold methanol (2 × 15 mL). The solid obtained was dissolved in warm water (20 mL), filtered, cooled in an ice bath, and acidified with concentrated hydrochloric acid. The resultant solid was then washed with cold water (2 × 10 mL) and methanol (2 × 10 mL). Finally, the product was dried under reduced pressure for at least 24 h to give 0.481 g (54%) of **6c** as white powder. No further purification was needed. Melting point 247−249 °C. HPLC 96.6% (t_R = 16.72 min). ^{1}H NMR (60 MHz, DMSO-d_6): δ 0.93 (t, 3H, CH_3), 1.54 (quint, 2H, CH_2), 2.53 (t, 2H, CH_2), 5.64 (s, 1H, CH), 11.45 (br s, 2H). FT-IR (UATR): 2874, 2222, 1599, 1292, 840. HRMS (ESI) calcd for $C_9H_{10}N_2O_2$ + H, 179.0815; found, 179.0814 (M + H)$^+$.

*General Procedure for Preparation of 6-Hydroxy-1H-pyridin-2-one-3-carbonitriles **10**. Selected Example for Compound 6-Hydroxy-5-(((2-hydroxyethyl)amino)methyl)-4-methyl-1H-pyridin-2-one-3-carbonitrile (**10a**).* The mixture of 6-hydroxy-4-methyl-1*H*-pyridin-2-one-3-carbonitrile (**6a**) (1.0 mmol, 0.150 g), ethanolamine (**9a**) (1.0 mmol, 0.061 g), and paraformaldehyde (0.030 g) in methanol (10 mL) was heated in a Fisher−Porter vessel at 100 °C for 16 h. After cooling to room temperature, the solvent was evaporated under reduced pressure. The solid obtained was washed with water (10 mL) and cold diethyl ether (10 mL). Finally, the product was crystallized from methanol, using carbon black, and subsequently was dried under reduced pressure to give 0.153 g (64%) of **10a** as pale white solid. Melting point 219−221 °C (dec). HPLC 95.8% (t_R = 11.73 min). ^{1}H NMR (400 MHz, DMSO-d_6): δ 2.13 (s, 3H, CH_3), 2.97 (t, 2H, CH_2), 3.65 (t, 2H, CH_2), 3.86 (s, 2H, CH_2), 5.05 (br s, 1H), 7.98 (br s, 2H), 10.00 (br s, 1H, NH). FT-IR (UATR, cm^{-1}): 3189, 2937, 2775, 2202, 1572, 1338, 1302, 704. HRMS (ESI) calcd for $C_{10}H_{13}N_3O_3$ + H, 224.1030; found, 224.1032 (M + H)$^+$.

Expression, Purification, and Enzyme Activity Assay. Production and isolation of recombinant hUP1 were as described in a previous study as well as hUP1 enzyme activity assay.[27] In brief, pET-23a(+)::hUP1 recombinant plasmid was transformed into *Escherichia coli* Rosetta (DE3) host cells, cultured in Terrifc Broth medium and grown for 36 h at 30 °C. The isolation of the recombinant hUP1 was by a single-step HPLC protocol using a cation exchange column, and the homogeneous protein was stored at −80 °C. Recombinant protein concentration was determined by the Bradford's method.[63,64] The enzyme assay was performed under initial rate conditions in which hUP1 activity was linear function of both time and protein concentration, monitoring a decrease change in absorbance at 280 nm upon conversion of Urd to uracil using a spectrophotometer (UV-2550 UV/Visible, Shimadzu). The assay mixture contained 100 mM Tris buffer pH 7.4, 100 nM of recombinant hUP1, Urd, and P_i concentrations at their K_m values (50 μM and 2 mM, respectively) in a final volume of 500 μL. The inhibitors were added to the mixture in a final concentration of 1 μM. All the compounds that inhibited more than 60% of the initial enzyme activity were selected. Assays were carried out at 37 °C for 60 s. For the compounds that were dissolved in DMSO, a control reaction was performed to evaluated DMSO effect at a maximum final concentration of 1%.

Time-Dependent Inhibitory Effect. Before embarking on determination of inhibition dissociation constants, the presence of time-dependent inhibitory activity was evaluated. For this analysis, 100 nM of recombinant hUP1 was preincubated with 1 μM of inhibitor (final concentration), which was then added at different times (up to 30 min) to the reaction mixture described above. The change in initial velocity with time was monitored and the percentage of inhibition was calculated.

Determination of K_i for Selected Inhibitors of hUP1. The determination of K_i values and the mode of inhibition (competitive, noncompetitive, or uncompetitive) were performed for each selected inhibitor and BAU toward both hUP1 substrates. The inhibition studies were carried out at varying concentration of one substrate, fixed concentration of other substrate (K_m value), and four different concentrations of inhibitor (0.1 to 5 μM). For Urd substrate analysis, the experiment was repeated with Urd concentrations ranging from 20 to 600 μM and P_i at 2 mM, and for P_i substrate analysis, P_i concentrations ranging from 0.1 to 12 mM with Urd fixed at 50 μM. The enzyme concentration was constant at 100 nM throughout the assays. The K_{is} and K_{ii} values were estimated from the slope and intercepts, respectively, of Lineweaver−Burk plot,[65] and the mode of inhibition was determined from the straight line patterns.[65] The data

dx.doi.org/10.1021/jm401389u | J. Med. Chem. XXXX, XXX, XXX−XXX

were fitted to the following equations for competitive, noncompetitive, or uncompetitive, respectively:

$$v = VA/[K_a(1 + I/K_{is}) + A]$$

$$v = VA/[K_a(1 + I/K_{is}) + A(1 + K_{ii})]$$

or

$$v = VA/[A(1 + I/K_{ii}) + K_a]$$

where V is the maximum velocity V_{max}, A is the substrate concentration, K_a is the Michaelis–Menten constant (K_m), I is the inhibitor concentration, K_{is} is the equilibrium dissociation constant for enzyme–inhibitor complex, and K_{ii} is the equilibrium constant dissociation constant for enzyme–substrate–inhibitor complex.[66] All measurements were performed in duplicate.

Determination of Thermodynamics Parameters by Isothermal Titration Calorimetry (ITC). The binding interaction between the enzyme and ligands was performed by ITC using ITC200 microcalorimeter (MicroCal, Inc., Northampton, MA). All assays were performed under initial rate conditions at 310.15 K (37 °C), 56 μM of recombinant hUP1 in Tris HCl 50 mM, pH 7.4, 10 mM of P_i (final concentration), and R1P concentrations ranging from 50 to 200 μM (final concentration). The reference cell (200 μL) was loaded with MilliQ water for all assays. The compounds **2**, **10a–10d**, and BAU were first dissolved in DMSO and then diluted in buffer (Tris HCl 50 mM pH 7.4), and the compound **6a** was diluted only in buffer. The same percentage of DMSO in the final stock was added to the sample cell (200 μL) containing the reaction mixture. The formation of either binary or ternary complex was carried out by one injection of 0.5 μL (excluded of the analysis), followed by 26 injections of 1.5 μL of each inhibitor to a solution containing either free enzyme, hUP1–P_i , or hUP1–R1P binary complexes in the sample cell. Nonspecific contributions arising from dilution effects of the P_i or R1P and protein were corrected for by subtracting the small heat changes at the end of titrations.[56] The thermodynamics parameters $\Delta H°$ (enthalpy of binding) and K_{eq} (affinity constant at equilibrium) and stoichiometry of binding (n) were obtained from fitting the data to one set of sites binding model. The $\Delta S°$ (entropy of binding) and $\Delta G°$ (Gibbs free energy of binding) were calculated by the following equations:

$$\Delta G° = \Delta H° - T\Delta S°$$

$$\Delta G° = -RT \ln K_{eq}$$

where R is the gas constant (1.98 cal K^{-1} mol^{-1} or 8.314 J K^{-1} mol^{-1}), T is the temperature in Kelvin (T = °C + 273.15), and ln K_{eq} is the natural logarithm of equilibrium constant.

The dissociation constant at equilibrium (K_d) was calculated by the following equation:

$$K_d = 1/K_{eq}$$

Molecular Docking of the Selected Compounds. Molecular docking experiments were performed to analyze the interaction mode of the selected compounds with the receptor hUP1. The receptor and ligand structures were prepared using AutoDockTools1.5.2, while docking simulations were performed with AutoDock4.2, allowing flexibility to the ligands.[67,68] The crystal structure of hUP1 associated with BAU (PDB ID: 3EUF) was used as template. Because hUP1 is biologically active as a dimer, this form was used to perform all docking experiments. For all simulations, the 3D-grid dimension used to define the hUP1 active site and to evaluate the scoring function was 60 × 60 × 60, with spacing of 0.375 Å. The Lamarckian Genetic Algorithm (LGA) was employed as the docking algorithm with 50 runs and the remaining parameters set to their default values, except for ga_num_evals, which was set to 2500000. All docking experiments were performed with the most stable tautomeric form of the compounds assessed by chemical synthesis analyses (NMR and FT-IR) and semiempirical calculations.

Cell Culture. The human keratinocyte cell line HaCat was cultured in Dulbecco's Modified Eagle's Medium (DMEM, Invitrogen), supplemented with 10% (v/v) fetal bovine serum (FBS, Invitrogen) and antibiotics, and the human colon cancer cell lines HT-29 and SW-620 were cultured on RPMI-1640 (Invitrogen) supplemented with 10% (v/v) FBS and antibiotics. The cells were incubated in plastic culture dishes at 37 °C, a minimum relative humidity of 95%, and an atmosphere of 5% CO_2 in air. The medium was replaced with fresh one every 48 h. When ∼80% the confluence was reached, cells were treated with trypsin (2 mL) to separate them from the dishes, counted, and the appropriate culture medium volume added before being seeded. All the assays had as experimental control cultured cells with medium only and medium with 1% of DMSO.

Cytotoxicity of hUP1 Inhibitors on Normal and Tumor Cells. For cytotoxicity assays, 7 × 10^3 cells were seeded onto 96-well plates and incubated for 48 or 24 h (HaCat or HT-29 and SW-620, respectively) before drug treatments to promote their adhesion to the plate. Thereafter, the medium cultured was removed, replaced with varying concentrations of the inhibitors **6a** and **10a** (1–100 μM), and exposed for 72 h. For the analysis of cell viability, the medium was removed, the cells were washed with calcium magnesium-free buffer, and 100 μL of 10% (v/v) MTT solution was added to the cells and incubated for 3 h. The formazan crystals formed were dried at room temperature for at least 24 h and then dissolved with 100 μL of DMSO. The absorbance was measured at 495 nm (Spectra Max M2e, Molecular Devices). The formazan concentration is directly proportional to the number of live cells with active mitochondria. The percentage of cell viability was calculated according to the following equation:

$$\text{cell viability (\%)} = \text{AbsT/AbsC} \times 100$$

where AbsT is the absorbance of treated cells and AbsC is the absorbance of control (untreated) cells. The cell viability was reported as the mean of three different experiments ± standard error mean and each experiment was performed as quadruplicate. One-way ANOVA was used as statistical analysis for cytotoxicity followed by Bonferroni's post hoc test. A p value <0.05 was considered statistically significant. Values are reported as the mean ± standard error mean in Figure S19, Supporting Information.

Influence of hUP1 Inhibitors on 5-FU IC_{50}. For the 5-FU concentration–response curve, 7 × 10^3 cells were seeded onto 96-well plates and grown as described above. The cells were exposed for 72 h to increasing concentrations of 5-FU: HaCat (0.25–20 μM), HT-29 (0.25–50 μM), and SW-620 (0.5–150 μM). The same concentration–response curve was performed in the presence of 30 μM of the compounds **6a**, **10a**, and also BAU as a positive control.[62] Analysis of cell sensitivity to the 5-FU, in the presence or absence of inhibitors, was performed by MTT assay (described above) and expressed by IC_{50}, which was calculated from a semilogarithmic concentration–response curve by nonlinear regression using Prism software (GraphPad 5.0). Experiments were carried out in quadruplicate and repeated three times. One-way ANOVA was used as statistical analysis for IC_{50} analysis followed by Bonferroni's post hoc test. A p value <0.05 was considered statistically significant. Values are reported as the mean accompanied by the 95% confidence interval.

■ ASSOCIATED CONTENT

Supporting Information

Synthesis and characterization of compounds (^{1}H NMR, FTIR, and high resolution mass spectrometry), tautomeric equilibrium of **6a**, Lineweaver–Burk plots of compounds **2**, **6a**, **10a–10d**, and BAU, isothermal titration calorimetry of compounds **2**, **6a**, **10a–10d**, and BAU, and cell viability. This material is available free of charge via the Internet at http://pubs.acs.org.

■ AUTHOR INFORMATION

Corresponding Authors

*For L.A.B.: phone/fax, +55-51-33203629; E-mail, luiz.basso@pucrs.br.
*For D.S.S.: E-mail, diogenes@pucrs.br.

Author Contributions

The manuscript was written through contribution of all authors. All authors have given approval to the final version of the manuscript.

Funding

This work was supported by the National Institute of Science and Technology on Tuberculosis, (DECIT/SCTIE/MS-MCT-CNPq-FNDCT-CAPES) awarded to D.S.S. and L.A.B. L.A.B. and D.S.S. also acknowledge financial support awarded by FAPERGS-CNPq-PRONEX-2009. L.A.B., D.S.S., O.N.S., A.A.S., and R.R. are Research Career Awardees of the National Research Council of Brazil (CNPq). R.R. acknowledges funds awarded to the National Institute for Translational Medicine. R.R. is also supported by CNPq research grants 303703/2009-1 and 484185/2012-8. D.R. and L.A.R. are recipients of a Ph.D. scholarship awarded by CNPq.

Notes

The authors declare no competing financial interest.

■ ABBREVIATIONS USED

BAU, 5-benzylacyclouridine or 5-benzyl-1-(2′-hydroxyethoxymethyl)uracil; FBS, fetal bovine serum; 5-FU, 5-fluorouracil; FUTP, fluorouridine 5′-triphosphate; MTT, 3-(4,5-dimethylthiazol-2-yl)-2,5-diphenyltetrazolium bromide; P_i, inorganic phosphate; ITC, isothermal titration calorimetry; Urd, uridine; UP, uridine phosphorylase; TS, thymidylate synthase

■ REFERENCES

(1) Connolly, G. P.; Duley, J. A. Uridine and its Nucleotides: Biological Actions, Therapeutic Potentials. *Trends Pharmacol. Sci.* **1999**, *20*, 218−225.

(2) Cardini, C. E.; Caputto, R.; Paladini, A. C.; Leloir, L. F. Uridine Diphosphate Glucose: The Coenzyme of the Galactose−Glucose Phosphate Isomerization. *Nature* **1950**, *165*, 191−192.

(3) Cardini, C. E.; Leloir, L. F.; Chiriboga, J. The Biosynthesis of Sucrose. *J. Biol. Chem.* **1955**, *214*, 149−155.

(4) Persson, B. E.; Sjöman, M.; Niklasson, F.; Ronquist, G. Uridine, Xanthine and Urate Concentrations in Prostatic Fluid and Seminal Plasma of Patients with Prostatitis. *Eur. Urol.* **1991**, *19*, 253−256.

(5) Peters, G. J.; van Groeningen, C. J.; Laurensse, E. J.; Lankelma, J.; Leyva, A.; Pinedo, H. M. Uridine-Induced Hypothermia in Mice and Rats in Relation to Plasma and Tissue Levels of Uridine and its Metabolites. *Cancer Chemother. Pharmacol.* **1987**, *20*, 101−108.

(6) Connolly, G. P.; Harrison, P. J.; Stone, T. W. Action of Purine and Pyrimidine Nucleotides on the Rat Superior Cervical Ganglion. *Br. J. Pharmacol.* **1993**, *110*, 1297−1304.

(7) Choi, J. W.; Shin, C. Y.; Choi, M. S.; Yoon, S. Y.; Ryu, J. H.; Lee, J.; Kim, W.; el Kouni, M. H.; Ko, K. H. Uridine Protects Cortical Neurons from Glucose Deprivation-Induced Death: Possible Role of Uridine Phosphorylase. *J. Neurotrauma* **2008**, *25*, 695−707.

(8) Leyva, A.; van Groeningen, C. J.; Kraal, I.; Gall, H.; Peters, G. J.; Lankelma, J.; Pinedo, H. M. Phase I and Pharmacokinetic Studies of High-Dose Uridine Intended for Rescue from 5-Fluorouracil Toxicity. *Cancer Res.* **1984**, *44*, 5928−5933.

(9) Martin, D. S.; Stolfi, R. L.; Sawyer, R. C.; Spiegelman, S.; Young, C. W. High-Dose 5-Fluorouracil with Delayed Uridine "Rescue" in Mice. *Cancer Res.* **1982**, *42*, 3964−3970.

(10) al Safarjalani, O. N.; Rais, R.; Naguib, F. N. M.; el Kouni, M. H. Potent Combination Therapy for Human Breast Tumors with High Doses of 5-Fluorouracil: Remission and Lack of Host Toxicity. *Cancer Chemother. Pharmacol.* **2012**, *69*, 1449−1455.

(11) Heidelberger, C.; Chaudhuri, N. K.; Dannerberg, P.; Mooren, P.; Griesbach, L.; Duschinsky, R.; Schnitzer, R. J.; Pleven, E.; Scheiner, J. Fluorinated Pyrimidines, a New Class of Tumor-Inhibitory Compounds. *Nature* **1957**, *179*, 663−666.

(12) Pinedo, H. M.; Peters, G. J. Fluorouracil: Biochemistry and Pharmacology. *J. Clin. Oncol.* **1988**, *6*, 1653−1664.

(13) Longley, D. B.; Harkin, D. P.; Johnston, P. G. 5-Fluorouracil: Mechanisms of Action and Clinical Strategies. *Nature* **2003**, *3*, 330−338.

(14) Rich, T. A.; Shepard, R. C.; Mosley, S. T. Four Decades of Continuing Innovation with Fluorouracil: Current and Future Approaches to Fluorouracil Chemoradiation Therapy. *J. Clin. Oncol.* **2004**, *22*, 2214−2232.

(15) van Groeningen, C. J.; Peters, G. J.; Pinedo, H. M. Modulation of Fluorouracil Toxicity with Uridine. *Semin. Oncol.* **1992**, *19*, 148−154.

(16) Grem, J. L. 5-Fluorouracil: Forty-Plus and Still Ticking. A Review of Its Preclinical and Clinical Development. *Invest. New Drugs* **2000**, *18*, 299−313.

(17) Houghton, J. A.; Houghton, P. J.; Wooten, R. S. Mechanism of Induction of Gastrointestinal Toxicity in the Mouse by 5-Fluorouracil, 5-Fluorouridine, and 5-Fluoro-2′-deoxyuridine. *Cancer Res.* **1979**, *39*, 2406−2413.

(18) al Safarjalani, O. N.; Rais, R.; Shi, J.; Schinazi, R. F.; Naguib, F. N. M.; el Kouni, M. H. Modulation of 5-Fluorouracil Host-Toxicity and Chemotherapeutic Efficacy Against Human Colon Tumors by 5-(Phenylthio)acyclouridine, a Uridine Phosphorylase Inhibitor. *Cancer Chemother. Pharmacol.* **2006**, *58*, 692−698.

(19) Wan, L.; Cao, D.; Zeng, J.; Yan, R.; Pizzorno, G. Modulation of Uridine Phosphorylase Gene Expression by Tumor Necrosis Factor-α Enhances the Antiproliferative Activity of the Capecitabine Intermediate 5′-Deoxy-5-fluorouridine in Breast Cancer Cells. *Mol. Pharmacol.* **2006**, *69*, 1389−1395.

(20) al Safarjalani, O. N.; Zhou, X.; Rais, R. H.; Shi, J.; Schinazi, R. F.; Naguib, F. N. M.; el Kouni, M. H. 5-(Phenylthio)acyclouridine: a Powerful Enhancer of Oral Uridine Bioavailability: Relevance to Chemotherapy with 5-Fluorouracil and Other Uridine Rescue Regimens. *Cancer Chemother. Pharmacol.* **2005**, *55*, 541−551.

(21) Pizzorno, G.; Yee, L.; Burtness, B. A.; Marsh, J. C.; Darnowski, J. W.; Chu, M. Y. W.; Chu, S. H.; Chu, E.; Leffert, J. J.; Handschumacher, R. E.; Calabresi, P. Phase I Clinical and Pharmacological Studies of Benzylacyclouridine, a Uridine Phosphorylase Inhibitor. *Clin. Cancer Res.* **1998**, *4*, 1165−1175.

(22) Ashour, O. M.; Naguib, F. N. M.; Goudgaon, N. M.; Schinazi, R. F.; el Kouni, M. H. Effect of 5-(Phenylselenenyl)acyclouridine, an Inhibitor of Uridine Phosphorylase, on Plasma Concentration of Uridine Released from 2′,3′,5′-Tri-*O*-acetyluridine, a Prodrug of Uridine: Relevance to Uridine Rescue in Chemotherapy. *Cancer Chemother. Pharmacol.* **2000**, *46*, 235−240.

(23) Gasser, T.; Moyer, J. D.; Handschumacher, R. E. Novel Single-Pass Exchange of Circulating Uridine in Rat Liver. *Science* **1981**, *213*, 777−778.

(24) Cardine, C. E.; Paladini, A. C.; Caputto, R.; Leloir, L. F. Liver Uridine Phosphorylase. *Acta Physiol. Lat. Am.* **1950**, *1*, 57−63.

(25) Liu, M.; Cao, D.; Russel, R.; Handschumacher, R. E.; Pizzorno, G. Expression, Characterization, and Detection of Human Uridine Phosphorylase and Identification of Variant Phosphorolytic Activity in Selected Human Tumors. *Cancer Res.* **1998**, *58*, 5418−5424.

(26) Johansson, M. Identification of a Novel Human Uridine Phosphorylase. *Biochem. Biophys. Res. Commun.* **2003**, *307*, 41−46.

(27) Renck, D.; Ducati, R. G.; Palma, M. S.; Santos, D. S.; Basso, L. A. The Kinetic Mechanism of Human Uridine Phosphorylase 1: Towards the Development of Enzyme Inhibitors for Cancer Chemotherapy. *Arch. Biochem. Biophys.* **2010**, *497*, 35−42.

(28) Roosild, T. P.; Castronovo, S.; Fabbiani, M.; Pizzorno, G. Implications of the Structure of Human Uridine Phosphorylase 1 on the Development of Novel Inhibitors for Improving the Therapeutic Window of Fluoropyrimidine Chemotherapy. *BMC Struct. Biol.* **2009**, *16*, 9−14.

(29) Niedzwicki, J. G.; el Kouni, M. H.; Chu, S. H.; Cha, S. Pyrimidine Acyclonucleosides, Inhibitors of Uridine Phosphorylase. *Biochem. Pharmacol.* **1981**, *15*, 2097−2101.

(30) Naguib, F. N. M.; Levesque, D. L.; Wang, E.; Panzica, R. P.; el Kouni, M. H. 5-Benzylbarbituric Acid Derivatives, Potent and Specific Inhibitors of Uridine Phosphorylase. *Biochem. Pharmacol.* **1993**, *46*, 1273−1283.
(31) Goudgaon, N. M.; Naguib, F. N. M.; el Kouni, M. H.; Schinazi, R. F. Phenylselenenyl- and Phenylthio-substituted Pyrimidines as Inhibitors of Dihydrouracil Dehydrogenase and Uridine Phosphorylase. *J. Med. Chem.* **1993**, *39*, 4250−4254.
(32) Cha, S. Development of Inhibitors of Pyrimidine Metabolism. *Yonsei Med. J.* **1989**, *30*, 315−326.
(33) Temmink, O. H.; de Bruin, M.; Turksma, A. W.; Cricca, S.; Laan, A. C.; Peters, G. J. Activity and Substrate Specificity of Pyrimidine Phosphorylase and their Role in Fluoropyrimidine Sensitivity in Colon Cancer Cell Lines. *Int. J. Biochem. Cell Biol.* **2007**, *39*, 565−575.
(34) Lima, L. M.; Barreiro, E. L. Bioisosterism: A Useful Strategy for Molecular Modification and Drug Design. *Curr. Med. Chem.* **2005**, *12*, 23−49.
(35) Roosild, T. P.; Castronovo, S. Active Site Conformational Dynamics in Human Uridine Phosphorylase 1. *PLoS One* **2010**, *5*, 1−6.
(36) Fleming, F. F.; Yao, L.; Ravikumar, P. C.; Funk, L.; Shook, B. C. Nitrile-Containing Pharmaceuticals: Efficacious Roles of the Nitrile Pharmacophore. *J. Med. Chem.* **2010**, *53*, 7902−7917.
(37) Treiber, N.; Schulz, G. E. Structure of 2,6-Dihydroxypyridine 3-Hydroxylase from a Nicotine-Degrading Pathway. *J. Mol. Biol.* **2008**, *379*, 94−104.
(38) Hirohashi, M.; Kido, M.; Yamamoto, Y.; Kojima, Y.; Jitsukawa, K.; Fujii, S. Synthesis of 5-Fluorouracil Derivatives Containing an Inhibitor of 5-Fluorouracil Degradation. *Chem. Pharm. Bull.* **1993**, *41*, 1498−1506.
(39) Mijin, D. Z.; Uscumlic, G. S.; Valentic, N. V. Synthesis and Investigation of Solvent Effects on the Ultraviolet Absorption Spectra of 5-Substituted-4-methyl-3-cyano-6-hydroxy-2-pyridones. *J. Serb. Chem. Soc* **2001**, *66*, 507−516.
(40) Bobbitt, J. M.; Scola, D. A. Synthesis of Isoquinoline Alkaloids. II. The Synthesis and Reactions of 4-Methyl-3-pyridinecarboxaldehyde and other 4-Methyl-3-substituted Pyridines. *J. Org. Chem.* **1960**, *25*, 560−564.
(41) Pevet, I.; Brulé, C.; Tizot, A.; Gohier, A.; Cruzalegui, F.; Boutin, J. A.; Goldstein, S. Synthesis and Pharmacological Evaluation of Thieno[2,3-*b*]pyridine Derivatives as Novel c-Src Inhibitors. *Bioog. Med. Chem.* **2011**, *19*, 2517−2528.
(42) Portnoy, S. Fluorinated Nitrogen Heterocycles via Cyclization. I. Trifluoromethyl-2-pyridones from Fluorinated 1,3-Dicarbonyls and Cyanoacetamide. *J. Org. Chem.* **1965**, *30*, 3377−3380.
(43) Dewar, M. J. S.; Zoebisch, E. G.; Healy, E. F.; Stewart, J. J. P. Development and Use of Quantum Mechanical Molecular Models. 76. AM1: A New General Purpose Quantum Mechanical Molecular Model. *J. Am. Chem. Soc.* **1985**, *107*, 3902−3909.
(44) Semeraro, T.; Lossani, A.; Botta, M.; Ghiron, C.; Alvarez, R.; Manetti, F.; Mugnaini, C.; Valensin, S.; Focher, F.; Corelli, F. Simplified Analogues of Immucillin-G Retain Potent Human Purine Nucleoside Phosphorylase Inhibitory Activity. *J. Med. Chem.* **2006**, *49*, 6037−6045.
(45) Taylor, E. A.; Clinch, K.; Kelly, P. M.; Li, L.; Evans, G. B.; Tyler, P. C.; Schramm, V. L. Acyclic Ribooxacarbenium Ion Mimics as Transition State Analogues of Human and Malarial Purine Nucleoside Phosphorylases. *J. Am. Chem. Soc.* **2007**, *129*, 6984−6985.
(46) Clinch, K.; Evans, G. B.; Fröhlich, R. F. G.; Furneaux, R. H.; Kelly, P. M.; Legentil, L.; Murkin, A. S.; Li, L.; Schramm, V. L.; Tyler, P. C.; Woolhouse, A. D. Third-Generation Immucillins: Syntheses and Bioactivities of Acyclic Immucillin Inhibitors of Human Purine Nucleoside Phosphorylase. *J. Med. Chem.* **2009**, *52*, 1126−1143.
(47) Caradoc-Davies, T. T.; Cutfield, S. M.; Lamont, I. L.; Cutfield, J. F. Crystal Structure of *Escherichia coli* Uridine Phosphorylase in Two Native and Three Complexed Forms Reveal Basis of Substrate Specificity, Induced Conformational Changes and Influence of Potassium. *J. Mol. Biol.* **2004**, *337*, 337−354.
(48) Silva, R. G.; Vetticatt, M. J.; Merino, E. F.; Cassera, M. B.; Schramm, V. L. Transition-State Analysis of *Trypanosoma cruzi* Uridine Phosphorylase-Catalyzed Arsenolysis of Uridine. *J. Am. Chem. Soc.* **2011**, *133*, 9923−9931.
(49) Delia, T. J.; Scovill, J. P.; Munslow, W. D.; Burckhalter, J. H. Synthesis of 5-Substituted Aminomethyluracils via the Mannich Reaction. *J. Med. Chem.* **1976**, *19*, 344−346.
(50) Copeland, R. A. *Evaluation of Enzyme Inhibitors in Drug Discovery: A Guide for Medicinal Chemists and Pharmacologists*, 1st ed.; John Wiley & Sons: Hoboken, NJ, 2005; pp 48−81.
(51) Schön, A.; Lam, S. Y.; Freire, E. Thermodynamics-Based Drug Design: Strategies for Inhibiting Protein−Protein Interactions. *Future Med. Chem.* **2011**, *3*, 1129−1137.
(52) Pizzorno, G.; Cao, D.; Leffert, J. J.; Russell, R. L.; Zhang, D.; Handschumacher, R. E. Homeostatic Control of Uridine and the Role of Uridine Phosphorylase: A Biological and Clinical Update. *Biochim. Biophys. Acta* **2002**, *1587*, 133−144.
(53) Khoshniat, S.; Bourgine, A.; Julien, M.; Weiss, P.; Guicheux, J.; Beck, L. The Emergence of Phosphate as a Specific Signaling Molecule in Bone and Other Cell Types in Mammals. *Cell. Mol. Life Sci.* **2011**, *68*, 205−218.
(54) Traut, T. W. Physiological Concentrations of Purines and Pyrimidines. *Mol. Cell. Biochem.* **1994**, *140*, 1−22.
(55) Griffiths, L.; Stratford, I. J. Platelet-Derived Endothelial Cell Growth Factor Thymidine Phosphorylase in Tumour Growth and Response to Therapy. *Br. J. Cancer* **1997**, *76*, 689−693.
(56) Perozzo, R.; Folkers, G.; Scapozza, L. Thermodynamics of Protein−Ligand Interactions: History, Presence, and Future Aspects. *J. Recept. Signal Transduction Res.* **2004**, *24*, 1−52.
(57) Eftink, M. R.; Anusiem, A. C.; Biltonen, R. L. Enthalpy−Entropy Compensation and Heat Capacity Changes for Protein−Ligand Interactions: General Thermodynamic Models and Data for the Binding of Nucleotides to Ribonuclease A. *Biochemistry* **1983**, *22*, 3884−3896.
(58) Ladbury, J. E.; Klebe, G.; Freire, E. Adding Calorimetric Data to Decision Making in Lead Discovery: A Hot Tip. *Nature Rev. Drug Discovery* **2010**, *9*, 23−27.
(59) Kawasaki, Y.; Freire, E. Finding a Better Path to Drug Selectivity. *Drug Discovery Today* **2011**, *16*, 985−990.
(60) Copeland, R. A. *Enzymes: A Practical Introduction to Structure, Mechanism, and Data Analysis*, 2nd ed.; John Wiley & Sons: Hoboken, NJ, 2000; pp 367−383.
(61) Temmink, O. H.; de Bruin, M.; Turksma, A. W.; Cricca, S.; Laan, A. C.; Peters, G. J. Activity and Substrate Specificity of Pyrimidine Phosphorylases and Their Role in Fluoropyrimidine Sensitivity in Colon Cancer Cell Lines. *Int. J. Biochem. Cell Biol.* **2007**, *39*, 565−575.
(62) Mans, D. R. A.; Grivicich, I.; Peters, G. J.; Schwartsmann, G. Sequence-Dependent Growth Inhibition and DNA Damage Formation by the Irinotecan-5-fluorouracil Combination in Human Colon Carcinoma Cell Lines. *Eur. J. Cancer* **1999**, *35*, 1851−1861.
(63) Robertson, J. G. Enzymes as a Special Class of Therapeutical Target: Clinical Drugs and Modes of Action. *Curr. Opin. Struct. Biol.* **2007**, *17*, 674−679.
(64) Bradford, M. M. A Rapid and Sensitive Method for the Quantitation of Microgram Quantities of Protein Utilizing the Principle of Protein−Dye Binding. *Anal. Biochem.* **1976**, *72*, 248−254.
(65) Lineweaver, H.; Burk, D. The Determination of Enzyme Dissociation Constant. *J. Am. Chem. Soc.* **1934**, *56*, 658−666.
(66) Copeland, R. A. *Enzymes: A Practical Introduction to Structure, Mechanism, and Data Analysis*, 2nd ed.; John Wiley & Sons, Inc.: Hoboken, NJ, 2000; pp 266−304.
(67) Morris, G. M.; Huey, R.; Lindstrom, W.; Sanner, M. F.; Belew, R. K.; Goodsell, D. S.; Olson, A. J. AutoDock4 and AutoDockTools4: Automated Docking with Selective Receptor Flexibility. *J. Comput. Chem.* **2009**, *30*, 2785−2791.
(68) Goodsell, D. S.; Olson, A. J. Automated Docking of Substrates to Proteins by Simulated Annealing. *Proteins* **1990**, *8*, 195−202.

Supporting Information

Design of a novel series of potent inhibitors of human uridine phosphorylase-1: synthesis, inhibition studies, and *in vitro* influence on 5-fluorouracil cytotoxicity.

Daiana Renck[1,2], Pablo Machado[1,2], André A. Souto[2,3], Leonardo A. Rosado[1,2], Thais Erig[4,5], Maria M. Campos[2,4,6], Caroline B. Farias[7,8], Rafael Roesler[7,8,9], Luis F. S. M. Timmers[2,10], Osmar N. de Souza[2,10], Diógenes S. Santos[1,2,5], Luiz A. Basso[1,2*]*

TABLE OF CONTENTS

EXPERIMENTAL SECTION

1. Synthetic procedures and structural data

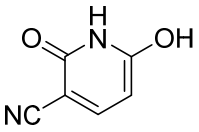

6-hydroxy-1*H*-pyridin-2-one-3-carbonitrile (2). The compound was synthesized in accordance to reported procedure.[1] Yield: 62%; M.p. 251-253°C (dec); HPLC 95.9% (t_R = 13.27 min); ^{1}H NMR (60 MHz, DMSO-d_6): δ 5.64 (d, J = 8 Hz, 1H, H-5), 7.78 (d, J = 8 Hz, 1H, H-4), 9.90 (br, 2H); FT-IR (UATR, cm^{-1}): 2883, 2741, 2223, 1596, 807, 760; HRMS (ESI) calcd for $C_6H_4N_2O_2$+Na: 159.0165. Found 159.0166 $(M + Na)^+$.

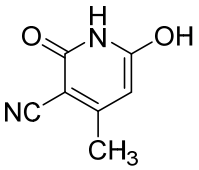

6-hydroxy-4-methyl-1*H*-pyridin-2-one-3-carbonitrile (6a). To a solution of ethyl 3-oxobutanoate (**4a**) (0.651 g, 5 mmol) and cyanoacetamide **5** (0.420 g, 5 mmol) in methanol (8 mL) was added potassium hydroxide (0.421 g, 7.5 mmol) in methanol (8 mL). The mixture was stirred at 65 °C for 4 h. After cooling to room temperature the amorphous solid formed was filtered off and washed with cold methanol (2 × 15 mL). The solid obtained was dissolved in warm water (20 mL), filtered, cooled in an ice bath and acidified with concentrated hydrochloric acid. After, the resultant solid was washed with cold water (2 × 10 mL) and methanol (2 × 10 mL). Finally, the product was dried under reduced pressure to give 0.390 g (52 %) of **6a** as white powder. No further purification was needed. M.p. 302-306°C (dec); HPLC 96.9% (t_R = 14.07 min); ^{1}H NMR (400 MHz, DMSO-d_6): δ 2.20 (s, 3H, CH_3), 5.54 (s, 1H, H-5); NMR (125 MHz, DMSO-d_6): δ 20.6 (CH_3), 88.7 (C3), 92.8 (C5), 117.2 (CN), 160.1 (C6), 161.1 (C4), 161.9 (C2); FT-IR (UATR, cm^{-1}): 2882, 2223, 1597, 1303, 835; HRMS (ESI) calcd for $C_7H_6N_2O_2$+K: 189.0061. Found 189.0068 $(M + K)^+$.

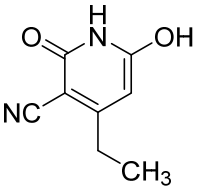

4-ethyl-6-hydroxy-1*H*-pyridin-2-one-3-carbonitrile (6b). Compound **6b** was prepared in 41% yield (0.336 g) by a procedure similar to that used to prepare compound **6a**. The reaction mixture of ethyl 3-oxopentanoate (**4b**) and cyanoacetamide **5** was stirred at 65 °C for 2 h. M.p. 299-301°C; HPLC 95.3% (t_R = 16.62 min); ^{1}H NMR (400 MHz, $CDCl_3$): δ 1.16 (t, 3H, CH_3), 2.54 (q, 2H, CH_2), 5.64 (s, 1H, CH), 7.56 (br, 2H); FT-IR (UATR): 2880, 2222, 1595, 1292, 835; HRMS (ESI) calcd for $C_8H_8N_2O_2$+K: 203.0217. Found 203.0222 $(M + K)^+$.

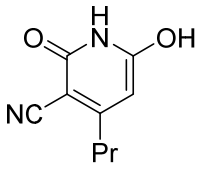

6-hydroxy-4-propyl-1*H*-pyridin-2-one-3-carbonitrile (6c). The procedure and spectra data were describe in the main text.

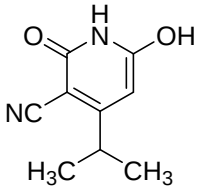

6-hydroxy-4-isopropyl-1*H*-pyridin-2-one-3-carbonitrile (6d). Compound **6d** was prepared in 39% yield (0.347 g) by a procedure similar to that used to prepare compound **6a**. The reaction mixture of ethyl 4-methyl-3-oxopentanoate (**4d**) and cyanoacetamide **5** was stirred at 65 °C for 8 h. M.p. 202-204°C; HPLC 97.6% (t_R = 16.63 min), ^{1}H NMR (60 MHz, DMSO-d$_6$): δ 1.17 (d, 6H, 2CH$_3$), 2.98 (quin, 1H, CH), 5.65 (s, 1H, CH), 7.95 (br, 2H); FT-IR (UATR): 2971, 2870, 2216, 1575, 1314, 736; HRMS (ESI) calcd for $C_9H_{10}N_2O_2$+H: 179.0815. Found 179.0805 (M + H)$^+$.

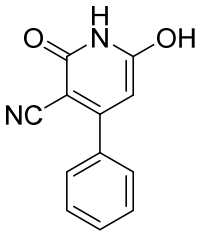

6-hydroxy-4-phenyl-1*H*-pyridin-2-one-3-carbonitrile (6e). Compound **6e** was prepared in 58% yield (0.615 g) by a procedure similar to that used to prepare compound **6a**. The reaction mixture of ethyl 3-oxo-3-phenylpropanoate (**4e**) and cyanoacetamide **5** was stirred at 65 °C for 8 h. M.p. >350°C; HPLC 95.2% (t_R = 17.98 min); ^{1}H NMR (400 MHz, DMSO-d$_6$): δ 5.01 (s, 1H, CH), 7.36-7.44 (m, 5H, C$_6$H$_5$), 9.74 (br, 1H, NH); FT-IR (UATR, cm^{-1}): 3075, 2933, 2749, 2194, 1591, 1376, 748, 692; HRMS (ESI) calcd for $C_{12}H_8N_2O_2$+2K: 289.9854. Found 289.9848 (M + 2K)$^+$.

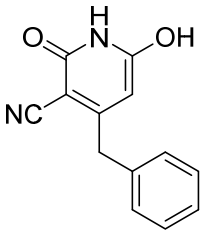

4-benzyl-6-hydroxy-1*H*-pyridin-2-one-3-carbonitrile (6f). Compound **6f** was prepared in 55% yield (0.622 g) by a procedure similar to that used to prepare compound **6a**. The reaction mixture of ethyl 3-oxo-4-phenylbutanoate (**4f**) and cyanoacetamide **5** was stirred at 65 °C for 16 h. M.p. 259-263°C (dec); HPLC 96.4% (t_R = 18.09 min); ^{1}H NMR (60 MHz, DMSO-d$_6$): δ 3.88

(s, 2H, CH_2), 5.49 (s, 1H, CH), 7.29-7.34 (m, 5H, C_6H_5); FT-IR (UATR, cm^{-1}): 2889, 2224, 1588, 1295, 696; HRMS (ESI) calcd for $C_{13}H_{10}N_2O_2$+K: 265.0374. Found 265.0382 $(M + K)^+$.

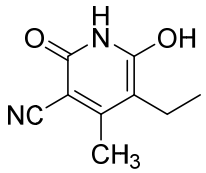

5-ethyl-6-hydroxy-4-methyl-1*H*-pyridin-2-one-3-carbonitrile (6g). Compound **6g** was prepared in 47% yield (0.419 g) by a procedure similar to that used to prepare compound **6a**. The reaction mixture of ethyl 2-ethyl-3-oxobutanoate (**4g**) and cyanoacetamide **5** was stirred at 65 °C for 16 h. M.p. 216-218°C; HPLC 95.8% (t_R = 16.85 min); ^{1}H NMR (60 MHz, DMSO-d_6): δ 0.97 (t, 3H, CH_3), 2.28 (s, 3H, CH_3), 2.44 (q, 2H, CH_2), 10.10 (Br, 2H); FT-IR (UATR, cm^{-1}): 2973, 2218, 1567, 1309, 862; HRMS (ESI) calcd for $C_8H_{10}N_2O_2$+H: 179.0815. Found 179.0807 $(M + H)^+$.

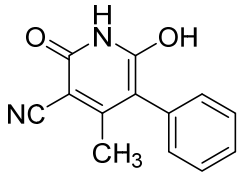

6-hydroxy-4-methyl-5-phenyl-1*H*-pyridin-2-one-3-carbonitrile (6h). Compound **6h** was prepared in 34% yield (0.384 g) by a procedure similar to that used to prepare compound **6a**. The reaction mixture of ethyl 3-oxo-2-phenylbutanoate (**4h**) and cyanoacetamide **5** was stirred at 65 °C for 16 h. M.p. >350°C; HPLC 96.1 % (t_R = 18.92 min); ^{1}H NMR (60 MHz, DMSO-d_6): δ 3.59 (s, 3H, CH_3), 7.29 (s, 5H, C_6H_5); FT-IR (UATR, cm^{-1}): 3199, 2220, 1634, 1404, 1315, 675; HRMS (ESI) calcd for $C_{13}H_{10}N_2O_2$+H: 227.0815. Found 227.0819 $(M + H)^+$.

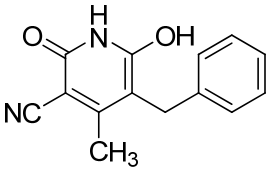

5-benzyl-6-hydroxy-4-methyl-1*H*-pyridin-2-one-3-carbonitrile (6i). Compound **6i** was prepared in 39% yield (0.468 g) by a procedure similar to that used to prepare compound **6a**. The reaction mixture of ethyl 2-benzyl-3-oxobutanoate (**4i**) and cyanoacetamide **5** was stirred at 65 °C for 16 h. M.p. 209-211°C; HPLC 96.1% (t_R = 18.70 min); ^{1}H NMR (60 MHz, DMSO-d_6): δ 2.27 (s, 3H, CH_3), 3.87 (s, 2H, CH_2), 7.25-7.30 (m, 5H, C_6H_5); FT-IR (UATR, cm^{-1}): 3409, 2911, 2222, 1630, 1362, 1180; HRMS (ESI) calcd for $C_{14}H_{12}N_2O_2$+H: 241.0972. Found 241.0974 $(M + H)^+$.

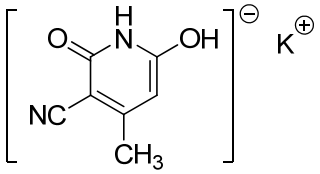

6-hydroxy-4-methyl-1*H*-pyridin-2-one-3-carbonitrile, potassium salt (6j). To a solution of ethyl 3-oxobutanoate (**4a**) (0.651 g, 5 mmol) and cyanoacetamide **5** (0.420 g, 5 mmol) in methanol (8 mL) was added potassium hydroxide (0.421 g, 7.5 mmol) in methanol (8 mL). The mixture was stirred at 65 °C for 4 h. After cooling to room temperature the amorphous solid formed was filtered off and washed with cold methanol (3 × 20 mL). After, the product was dried under reduced pressure to give 0.700 g (74 %) of **6j** as white powder. No further purification was needed. M.p. 292-294°C (dec); HPLC 97.1% (t_R = 16.16 min); ^{1}H NMR (60 MHz, D_2O): δ 2.19 (s, 3H, CH_3), 5.50 (s, 1H, H-5); FT-IR (UATR, cm^{-1}): 2937, 2197, 1594, 1373, 745; HRMS (ESI) calcd for $C_7H_6N_2O_2$+K: 189.0061. Found 189.0064 $(M + K)^+$.

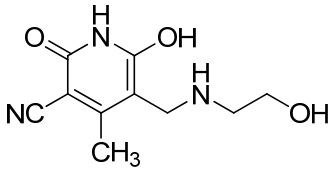

6-hydroxy-5-(((2-hydroxyethyl)amino)methyl)-4-methyl-1*H*-pyridin-2-one-3-carbonitrile (10a). The procedure and spectra data were describe in the main text.

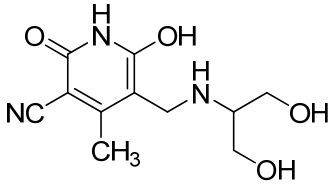

5-((1,3-dihydroxypropan-2-ylamino)methyl)-6-hydroxy-4-methyl-1*H*-pyridin-2-one-3-carbonitrile (10b). The mixture of 6-hydroxy-4-methyl-1*H*-pyridin-2-one-3-carbonitrile (**6a**) (1.0 mmol, 0.150 g), 2-aminopropane-1,3-diol (**9b**) (1.0 mmol, 0.091 g) and paraformaldehyde (0.030 g) in methanol (10 mL) was heated in a Fisher-Porter vessel at 100 °C for 16 h. After cooling to room temperature the solvent was evaporated under reduced pressure. The solid obtained was washed with water (10 mL) and cold diethyl ether (10 mL). Finally, the product was crystallized from methanol, using carbon black, and subsequently was dried under reduced pressure to give 0.111 g (44 %) of **10a** as beige solid. M.p. 204-207°C (dec); HPLC 95.6% (t_R = 11.79 min); ^{1}H NMR (400 MHz, DMSO-d$_6$): δ 2.13 (s, 3H, CH_3), 3.10 (qui, 1H, CH), 3.58 (d, 2H, CH_2), 3.61 (d, 2H, CH_2), 3.95 (s, 2H, CH_2), 5.16 (br, 2H), 8.04 (br, 2H), 10.06 (br, 1H, NH); FT-IR (UATR, cm^{-1}): 3387, 2932, 2203, 1571, 1376, 1045, 711; HRMS (ESI) calcd for $C_{11}H_{15}N_3O_4$+H: 254.1135 Found 254.1129 $(M + H)^+$.

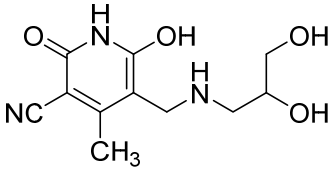

5-((2,3-dihydroxypropylamino)methyl)-6-hydroxy-4-methyl-1*H*-pyridin-2-one-3-carbonitrile (10c). Compound **10c** was prepared in 58% yield (0.147 g) by a procedure similar to that used to prepare compound **10b**. M.p. 201-203°C; HPLC 95.9% (t_R = 11.71 min); ^{1}H NMR (400 MHz, DMSO-d$_6$): δ (*J*, Hz) 2.13 (s, 3H, CH_3), 2.68-2.82 (m, 2H, CH_2), 2.96 (dd, 1H, *J* = 13, *J* = 3, CH_2), 4.56 (dd, 1H, *J* = 13, *J* = 3, CH_2), 3.29-3.35 (m, 1H, CH), 3.86 (s, 2H, CH_2), 5.30 (br, 2H), 8.00 (br, 2H), 10.12 (br, 1H, NH); FT-IR (UATR, cm^{-1}): 3310, 2883, 2197, 1588,

1386, 1057, 933, 704; HRMS (ESI) calcd for $C_{11}H_{15}N_3O_4$+H: 254.1135 Found 254.1130(M + H)$^+$.

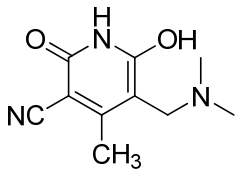

5-((dimethylamino)methyl)-6-hydroxy-4-methyl-1*H*-pyridin-2-one-3-carbonitrile (10d). Compound **10d** was prepared in 77% yield (0.159 g) by a procedure similar to that used to prepare compound **10b**. The reaction mixture was stirred at 100 °C for 4 h. M.p. 191-194°C (dec); HPLC 95.4% (t_R = 11.92 min); ^{1}H NMR (400 MHz, DMSO-d$_6$): δ 2.14 (s, 3H, CH_3), 2.67 (s, 6H, $N(CH_3)_2$), 3.91 (s, 2H, CH_2), 10.03 (br, 1H, NH); FT-IR (UATR, cm^{-1}): 3411, 3052, 2934, 2848, 2760, 2189, 1587, 910; HRMS (ESI) calcd for $C_{10}H_{13}N_3O_2$+H: 208.1081. Found 208.1080 (M + H)$^+$.

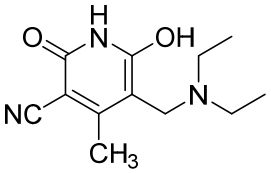

5-((diethylamino)methyl)-6-hydroxy-4-methyl-1*H*-pyridin-2-one-3-carbonitrile (10e). Compound **10e** was prepared in 72% yield (0.169 g) by a procedure similar to that used to prepare compound **10b**. The reaction mixture was stirred at 100 °C for 4 h. M.p. 108-111°C; HPLC 96.2% (t_R = 12.57 min); ^{1}H NMR (60 MHz, $CDCl_3$): δ 1.25 (t, 6H, $2CH_3$), 2.28 (s, 3H, CH_3), 3.14 (q, 4H, $2CH_2$), 3.91 (s, 2H, CH_2), 11.90 (br, 1H, NH); FT-IR (UATR, cm^{-1}): 2926, 2190, 1575, 1367, 791, 709; HRMS (ESI) calcd for $C_{12}H_{17}N_3O_2$+H: 236.1394. Found 236.1440 (M + H)$^+$.

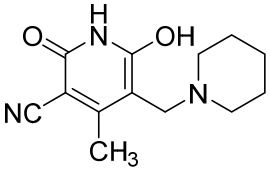

6-hydroxy-4-methyl-5-(piperidin-1-ylmethyl)-1*H*-pyridin-2-one-3-carbonitrile (10f). Compound **10f** was prepared in 76% yield (0.188 g) by a procedure similar to that used to prepare compound **10b**. The reaction mixture was stirred at 100 °C for 4 h. M.p. 210-212°C; HPLC 95.9% (t_R = 12.89 min), ^{1}H NMR (60 MHz, DMSO-d$_6$): δ 1.61 (br, 6H, $(CH_2)_3$), 2.15 (s, 3H, CH_3), 3.04 (br, 4H, $(CH_2)_3$), 3.92 (s, 2H, CH_2), 10.03 (br, 1H, NH); FT-IR (UATR, cm^{-1}): 3633, 3473, 2925, 2739, 2197, 1588, 1380, 927; HRMS (ESI) calcd for $C_{13}H_{17}N_3O_2$+H: 248.1394. Found 248.1397 (M + H)$^+$.

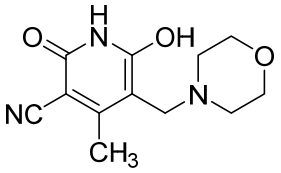

6-hydroxy-4-methyl-5-(morpholinomethyl)-1*H*-pyridin-2-one-3-carbonitrile (10g). Compound **10g** was prepared in 80% yield (0.199 g) by a procedure similar to that used to prepare compound **10b**. The reaction mixture was stirred at 100 °C for 4 h. M.p. 212-214°C; HPLC 96.3% (t_R = 12.43 min); ^{1}H NMR (60 MHz, DMSO-d_6): δ 2.16 (s, 3H, CH_3), 3.20 (br, 4H, $(CH_2)_2$), 3.81 (br, 4H, $(CH_2)_2$), 3.98 (s, 2H, CH_2), 10.1 (br, 1H, NH); FT-IR (UATR, cm^{-1}): 2927, 2192, 1591, 1362, 936; HRMS (ESI) calcd for $C_{12}H_{15}N_3O_3$+H: 250.1186. Found 250.1189 $(M + H)^+$.

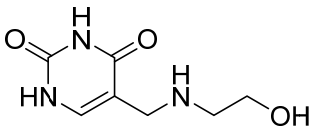

5-((2-hydroxyethylamino)methyl)pyrimidine-2,4(1H,3H)-dione (11). The compound was synthesized in accordance to reported procedure.[2] Yield: 71%; HPLC 96.7% (t_R = 11.05 min); ^{1}H NMR (60 MHz, DMSO-d_6): δ 2.54 (t, 2H, CH_2), 3.22 (s, 2H, CH_2), 3.47 (t, 2H, CH_2), 7.43 (s, 1H, CH), 10.74 (br, 2H, NH); HRMS (ESI) calcd for $C_7H_{11}N_3O_3$+H: 186.0873. Found 186.0873 $(M + H)^+$.

2. Tautomeric forms of 6-hydroxy-4-methyl-1H-pyridin-2-one-3-carbonitrile (6a)

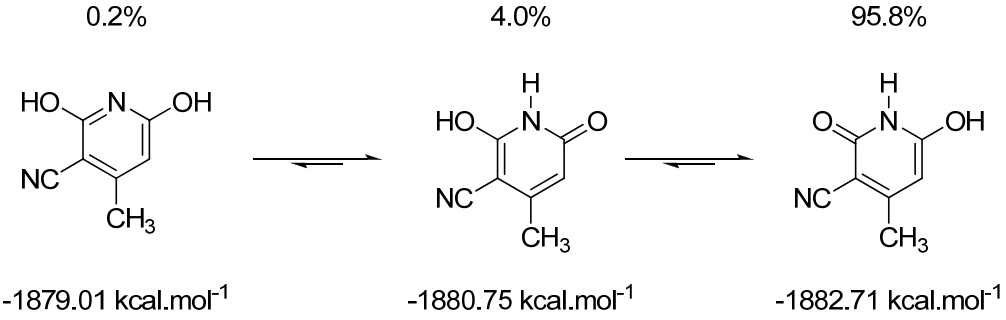

Figure S1. Energy of tautomeric forms of 6-hydroxy-4-methyl-1*H*-pyridin-2-one-3-carbonitrile (**6a**) calculated on minimized structures using the HyperChem 7.52 package (2002) (HYPERCHEM$^{(TM)}$ Professional 7.52 (2002), Hypercube, Inc.). Optimisation was accomplished using the semi-empirical AM1 method without fixing any parameter, thus bringing all geometric variables to equilibrium. The energy minimisation protocol employed the Polak-Ribiere conjugated gradient algorithm. Convergence to a local minimum was achieved when the energy gradient was ≤ 0.01 kcal·mol^{-1}. The RHF (*Restricted Hartree-Fock)* method was used for spin pairing with the electrons occupying the same spatial orbital.

3. ^{1}H NMR spectra of compounds 6a, 10a-b:

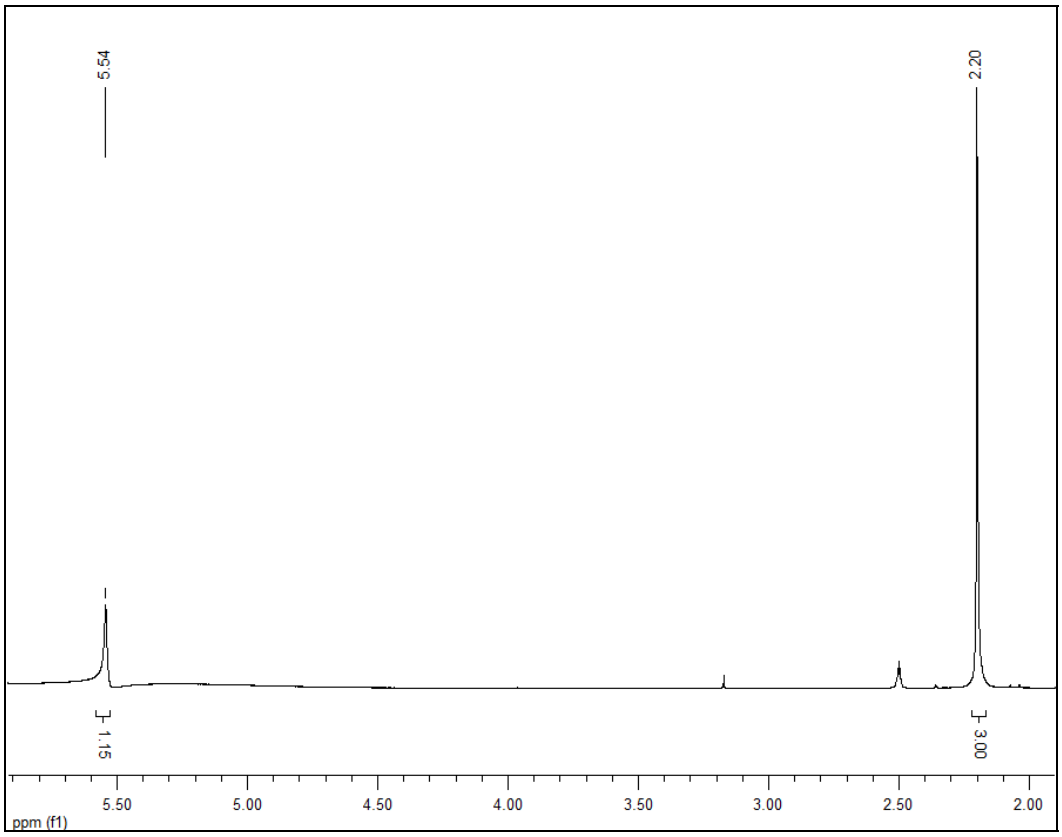

Figure S2. ^{1}H NMR spectra of compound **6a.**

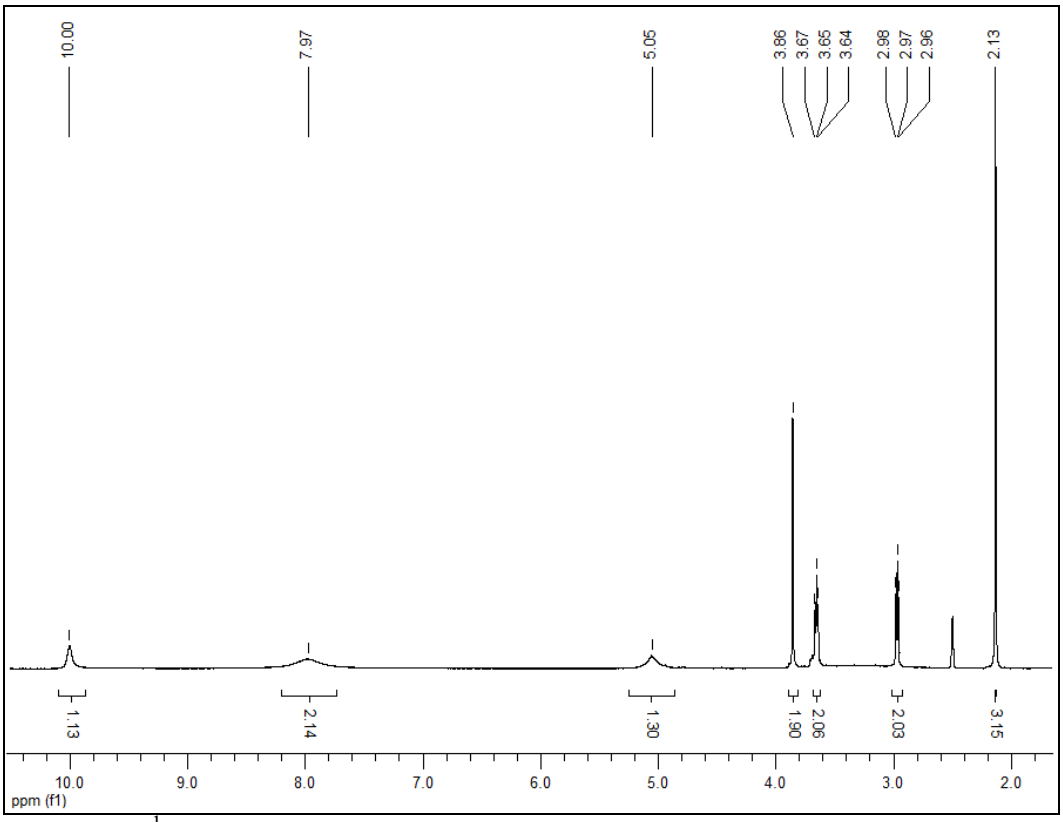

Figure S3. ^{1}H NMR spectra of compound **10a.**

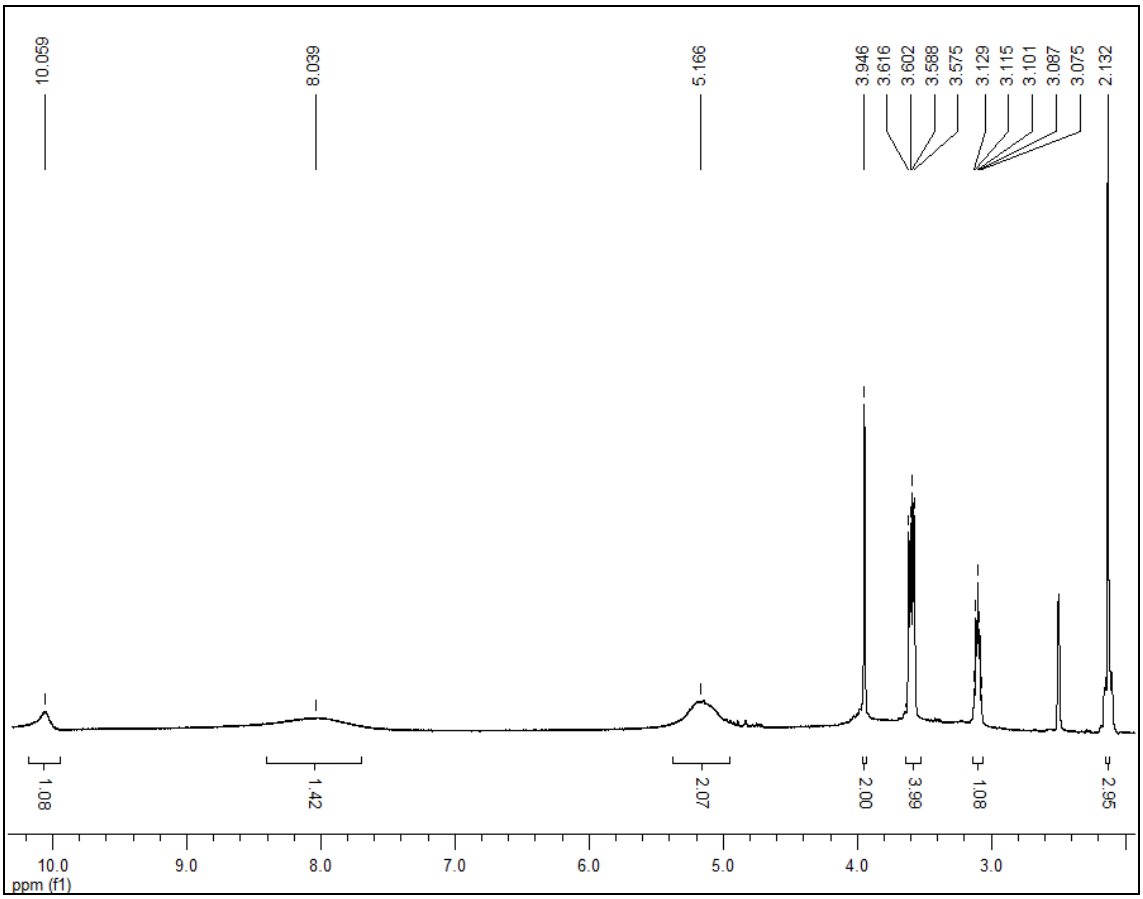

Figure S4. ^{1}H NMR spectra of compound **10b.**

4. Lineweaver-Burk plots of compounds 2, 6a, 10a-10d, and BAU

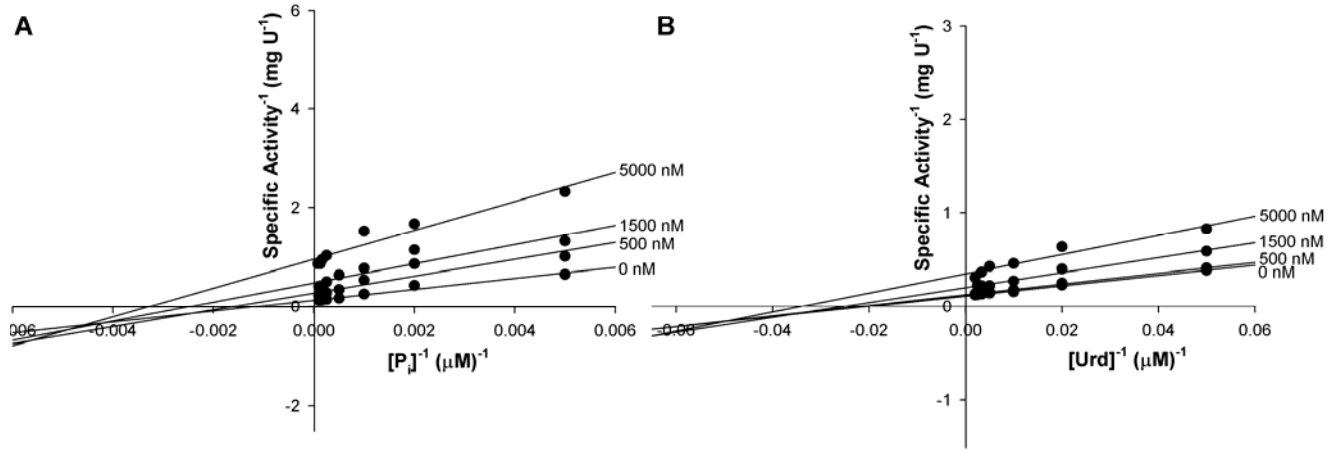

Figure S5. Double-reciprocal plots of inhibition assays for compound **2** (0-5000 nM). Pattern of intersecting lines at left of *y*-axis indicate non-competitive inhibition towards P_i (A) and Urd (B).

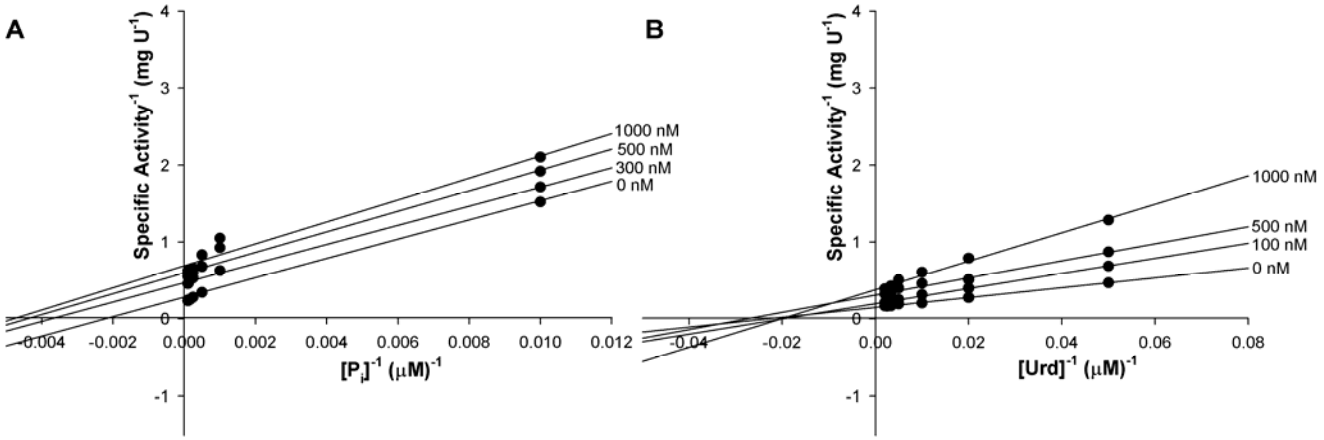

Figure S6. Double-reciprocal plots of inhibition assays for compound **6a** (0-1000 nM). Pattern of parallel lines indicate uncompetitive inhibition towards P_i (A), whereas pattern of intersection at left of *y*-axis indicate non-competitive inhibition towards Urd (B).

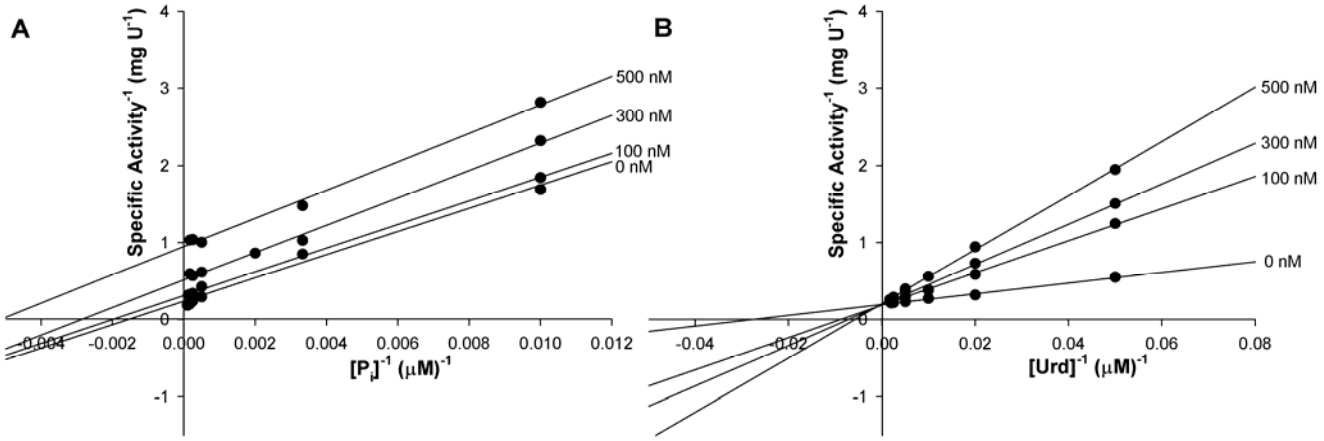

Figure S7. Double-reciprocal plots of inhibition assays for compound **10a** (0-500 nM). Pattern of parallel lines indicate uncompetitive inhibition towards P_i (A), whereas pattern of intersection at *y*-axis indicate competitive inhibition towards Urd (B).

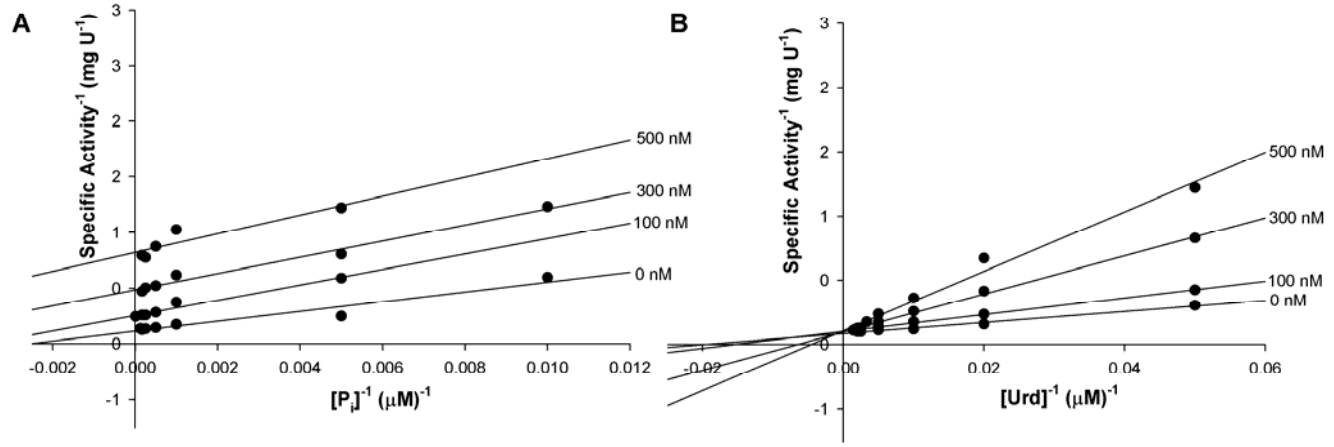

Figure S8. Double-reciprocal plots of inhibition assays for compound **10b** (0-500 nM). Pattern of parallel lines indicate uncompetitive inhibition towards P_i (A), whereas pattern of intersection at *y*-axis indicate competitive inhibition towards Urd (B).

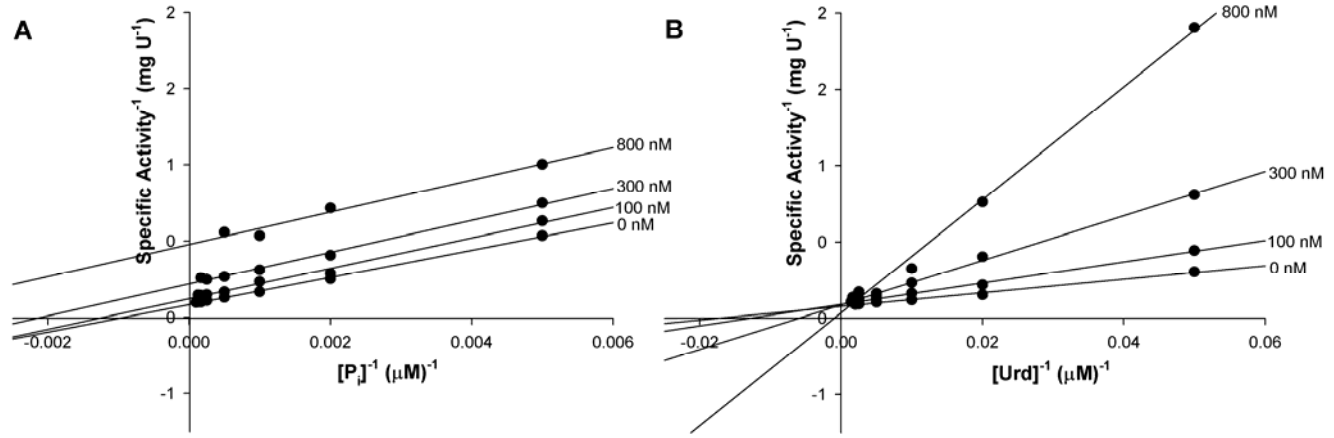

Figure S9. Double-reciprocal plots of inhibition assays for compound **10c** (0-800 nM). Pattern of parallel lines indicate uncompetitive inhibition towards P_i (A), whereas pattern of intersection at *y*-axis indicate competitive inhibition towards Urd (B).

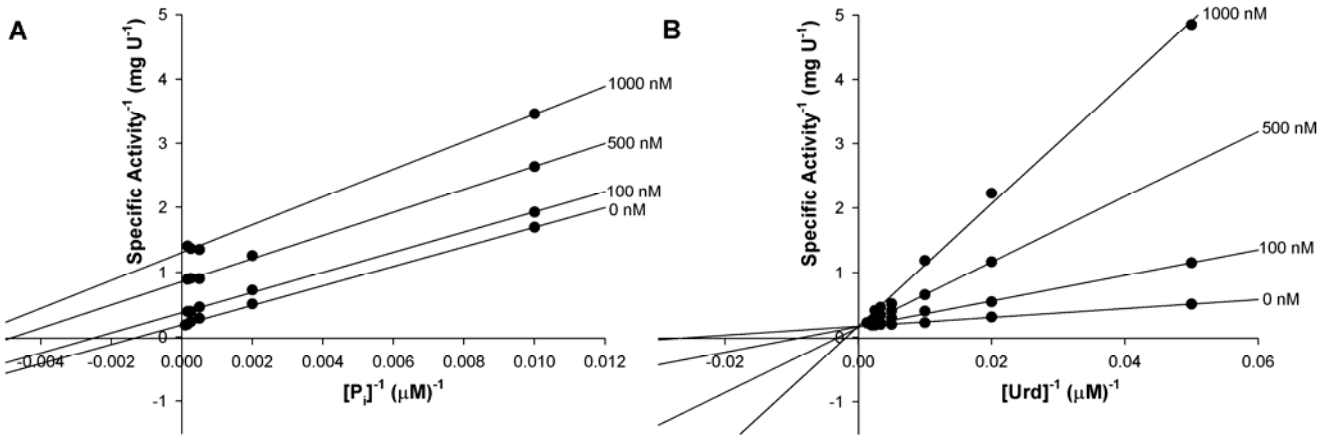

Figure S10. Double-reciprocal plots of inhibition assays for compound **10d** (0-1000 nM). Pattern of parallel lines indicate uncompetitive inhibition towards P_i (A), whereas pattern of intersection at *y*-axis indicate competitive inhibition towards Urd (B).

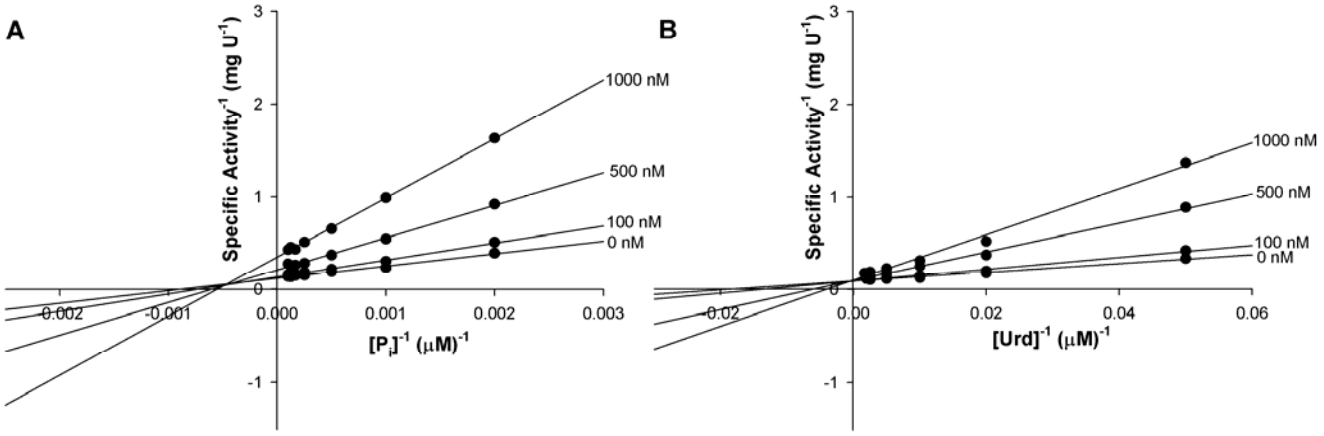

Figure S11. Double-reciprocal plots of inhibition assays for compound BAU (5-benzyl-1-(2'-hydroxyethoxymethyl)uracil) (0-1000 nM). Pattern of intersecting lines at left of y-axis indicate non-competitive inhibition towards P_i (A), whereas pattern of intersection at *y*-axis indicate competitive inhibition towards Urd (B).

5. Isothermal titration calorimetry (ITC) of compounds 2, 6a, 10a-10d, and BAU

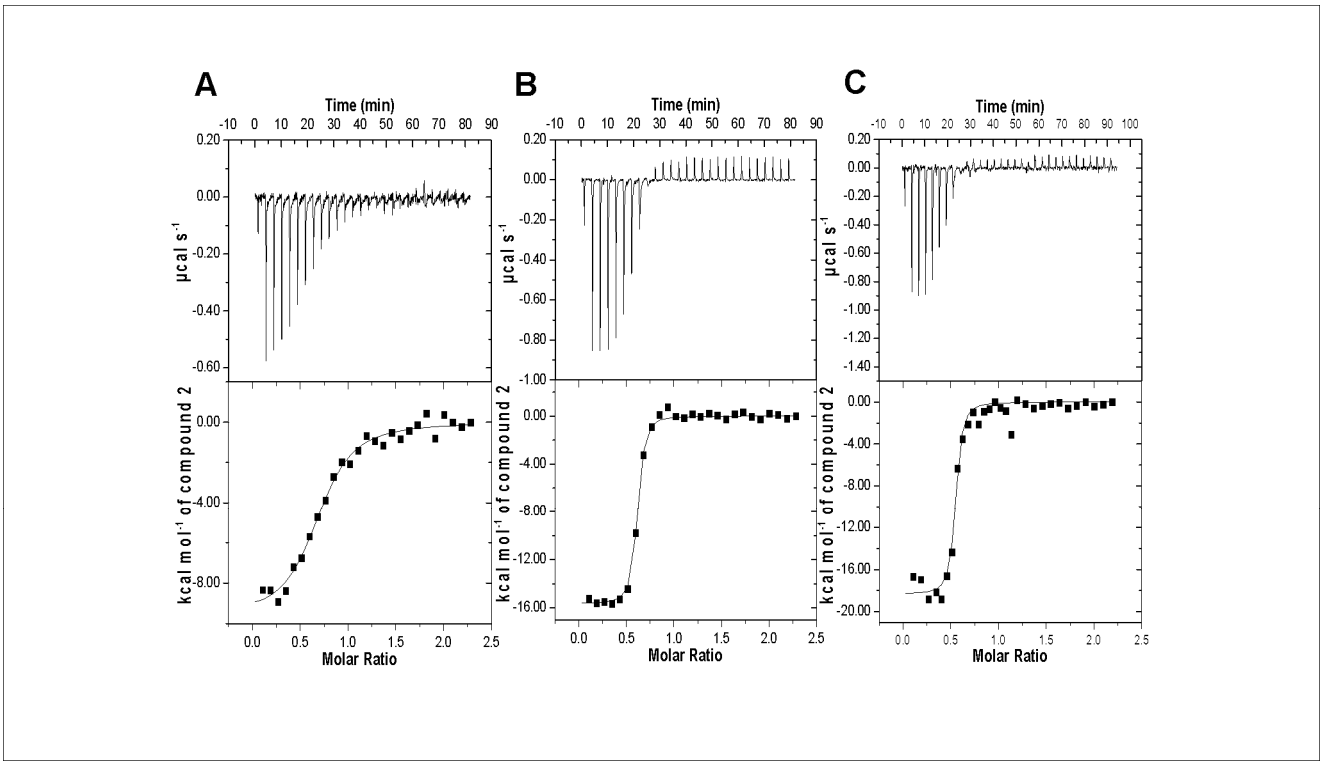

Figure S12. ITC binding assays of compound **2** on hUP1 (A), hUP1-R1P 50 µM (B), and hUP1-R1P 150 µM (C). The binding isotherms were fitted to one set of sites binding model.

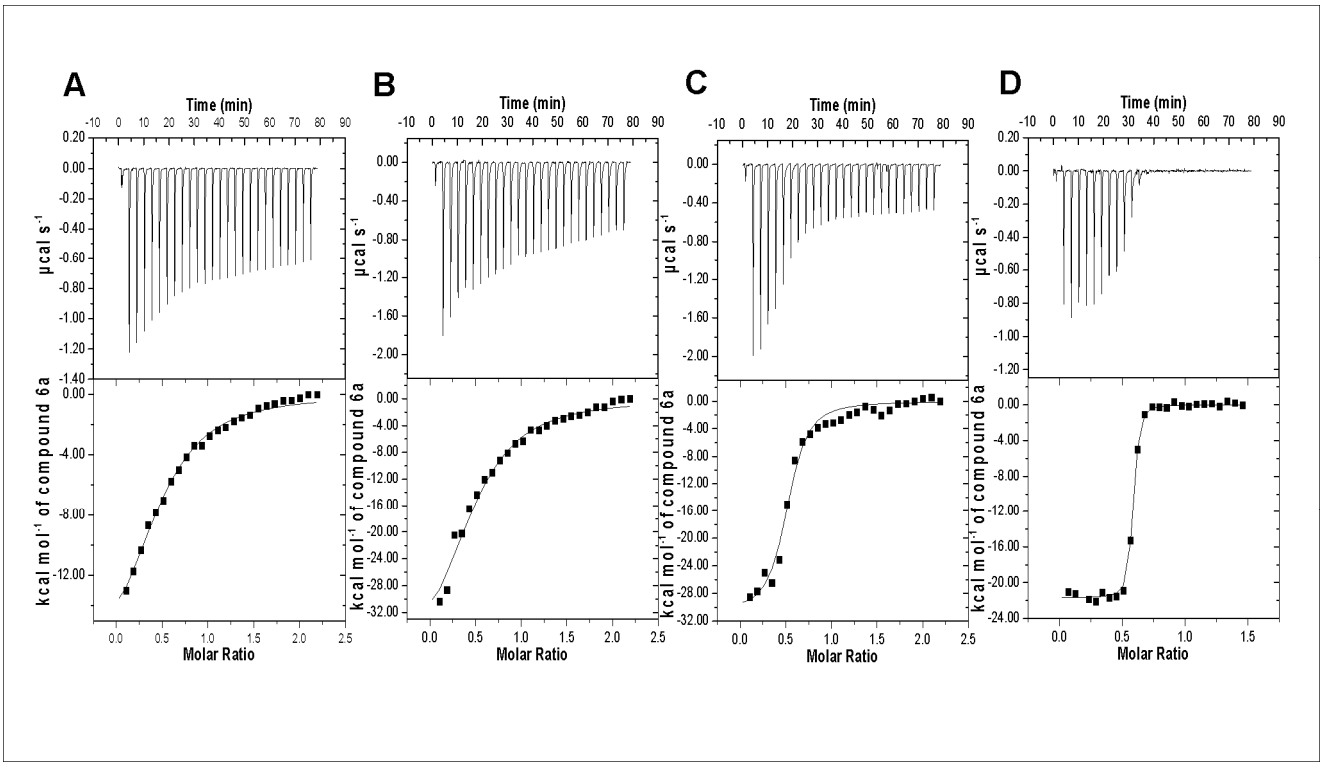

Figure S13. ITC binding assays of compound **6a** on hUP1-P_i (A), hUP1-R1P 20 µM (B), hUP1-

R1P 50 μM (C), and hUP1-R1P 150 μM (D). The binding isotherms were fitted to one set of sites model.

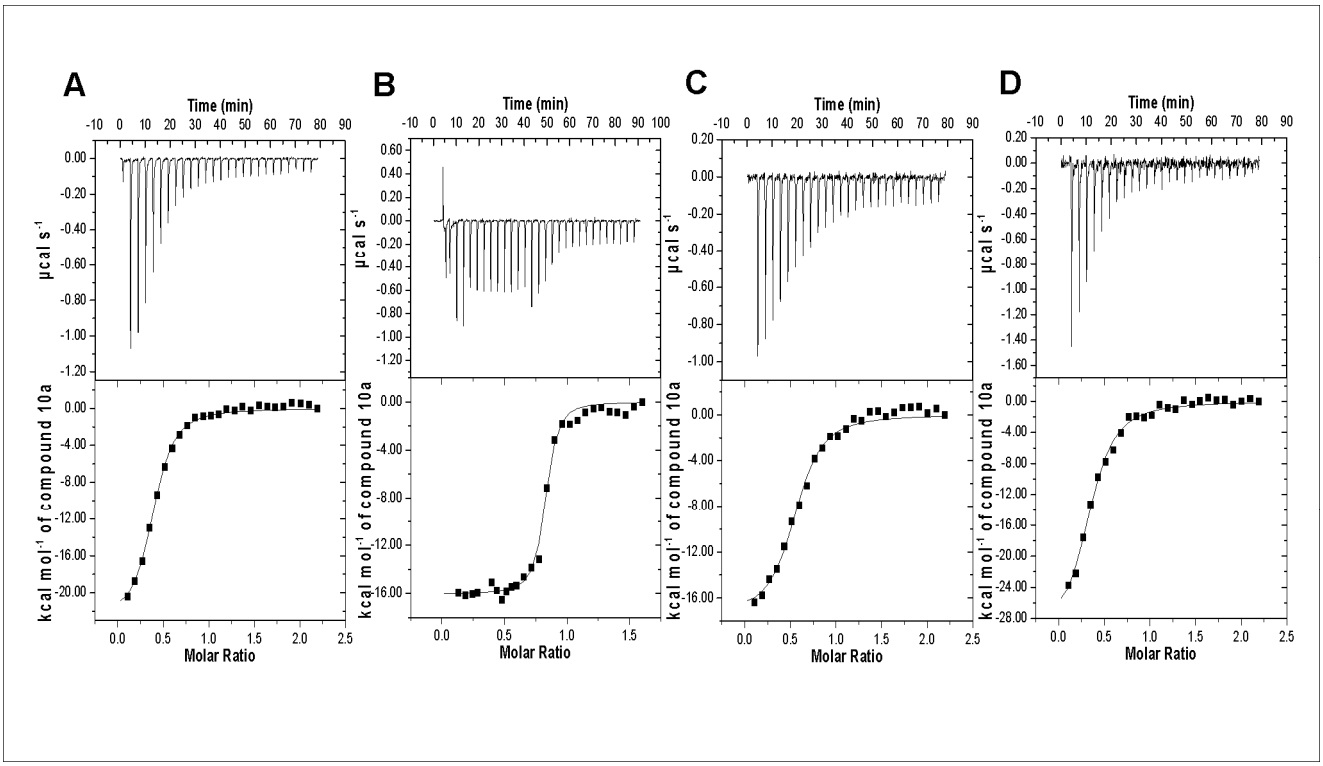

Figure S14. ITC binding assays of compound **10a** on hUP1 (A), hUP1-P_i (B), hUP1-R1P 50 μM (C), and hUP1-R1P 150 μM (D). The binding isotherms were fitted to one set of sites model.

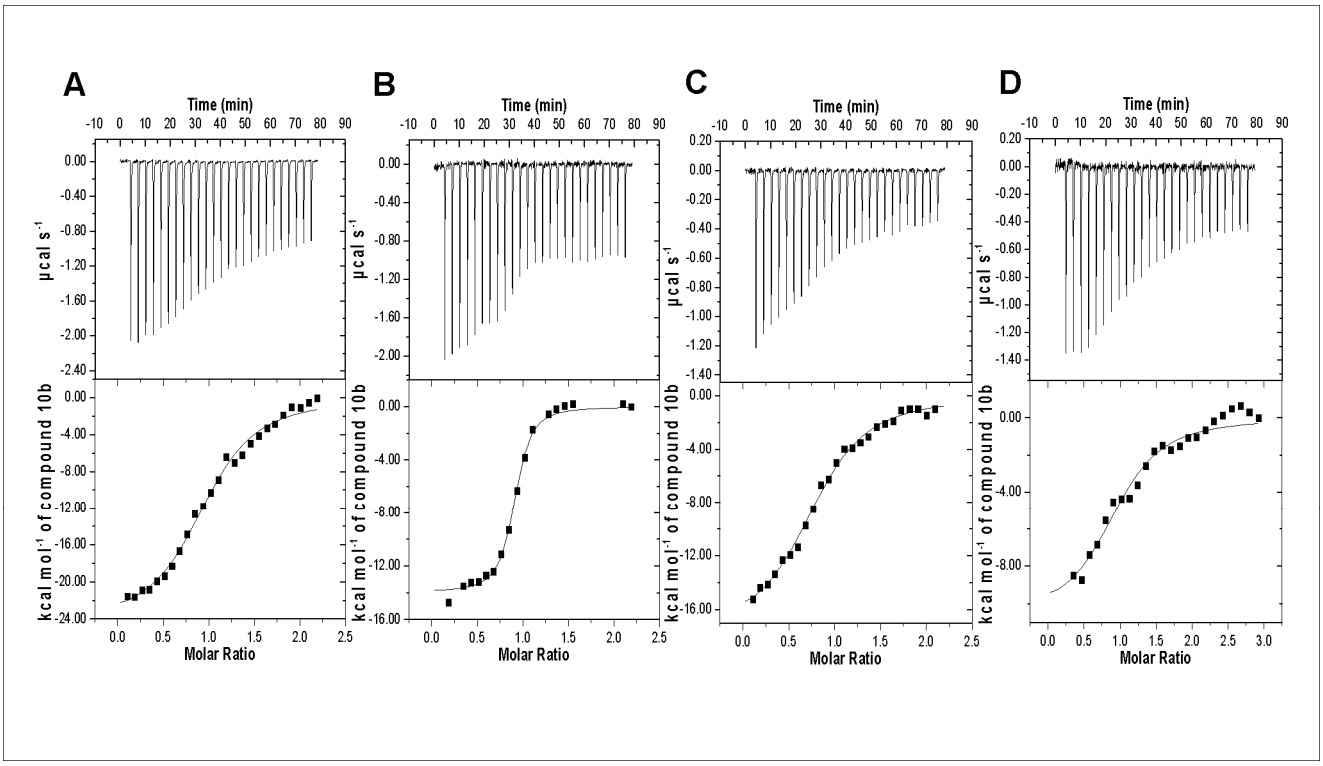

Figure S15. ITC binding assays of compound **10b** on hUP1 (A), hUP1-P_i (B), hUP1-R1P 50 µM (C), and hUP1-R1P 150 µM (D). The binding isotherms were fitted to one set of sites model.

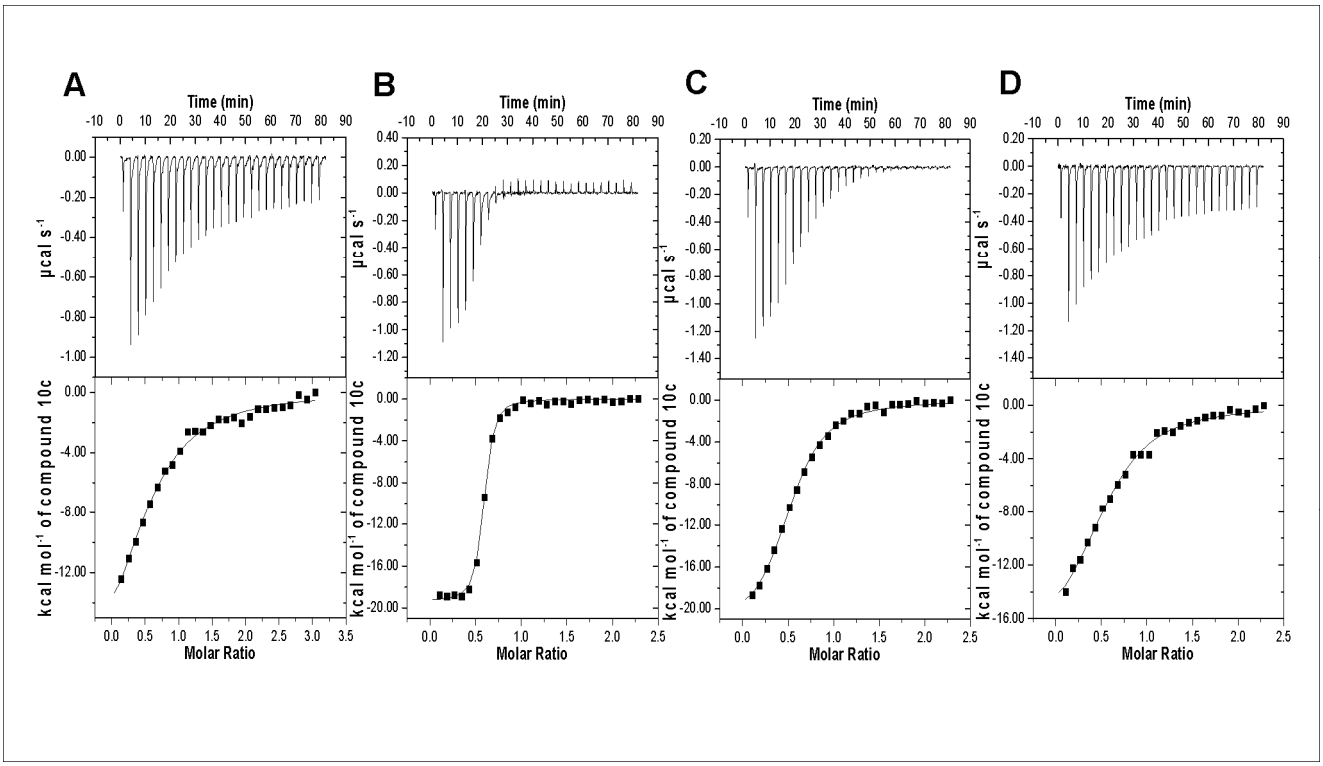

Figure S16. ITC binding assays of compound **10c** on hUP1 (A), hUP1-P_i (B), hUP1-R1P 50 µM (C), and hUP1-R1P 150 µM (D). The binding isotherms were fitted to one set of sites model.

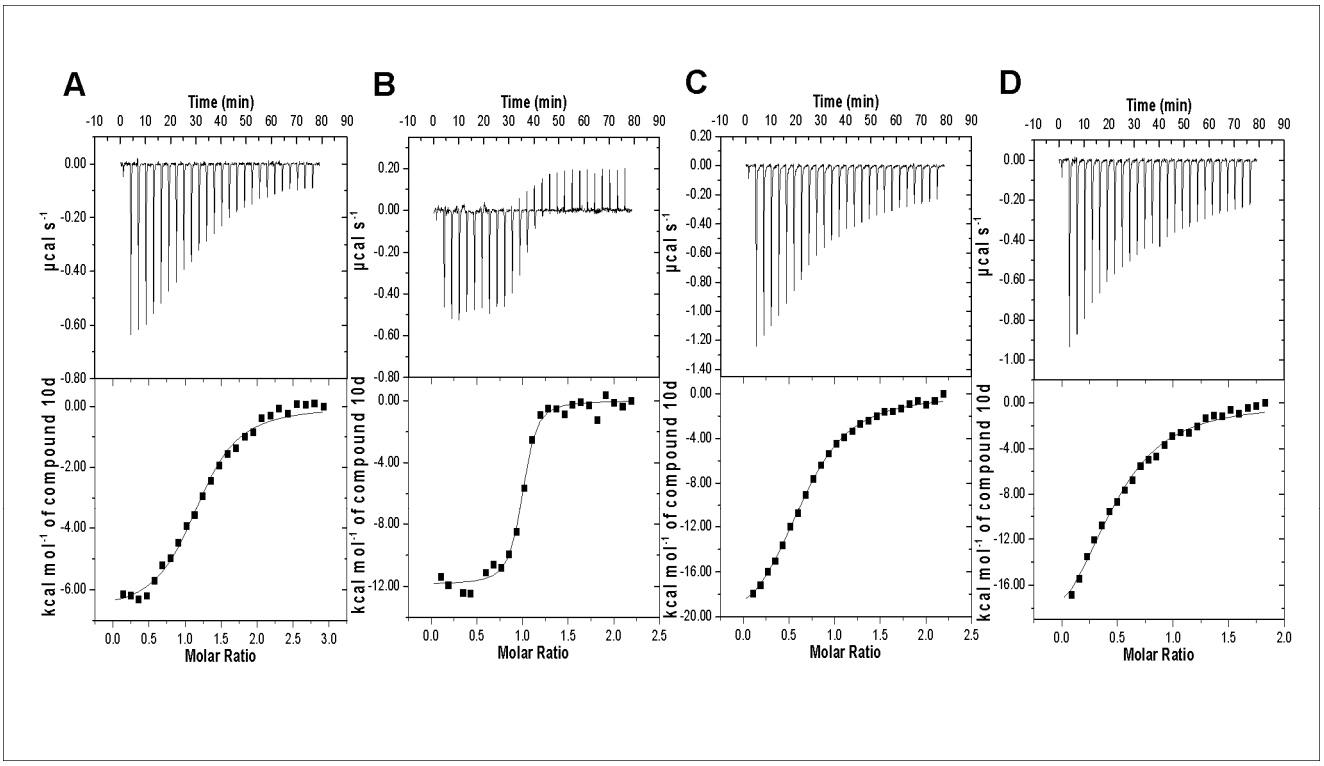

Figure S17. ITC binding assays of compound **10d** on hUP1 (A), hUP1-P_i (B), hUP1-R1P 50 µM (C), and hUP1-R1P 150 µM (D). The binding isotherms were fitted to one set of sites model.

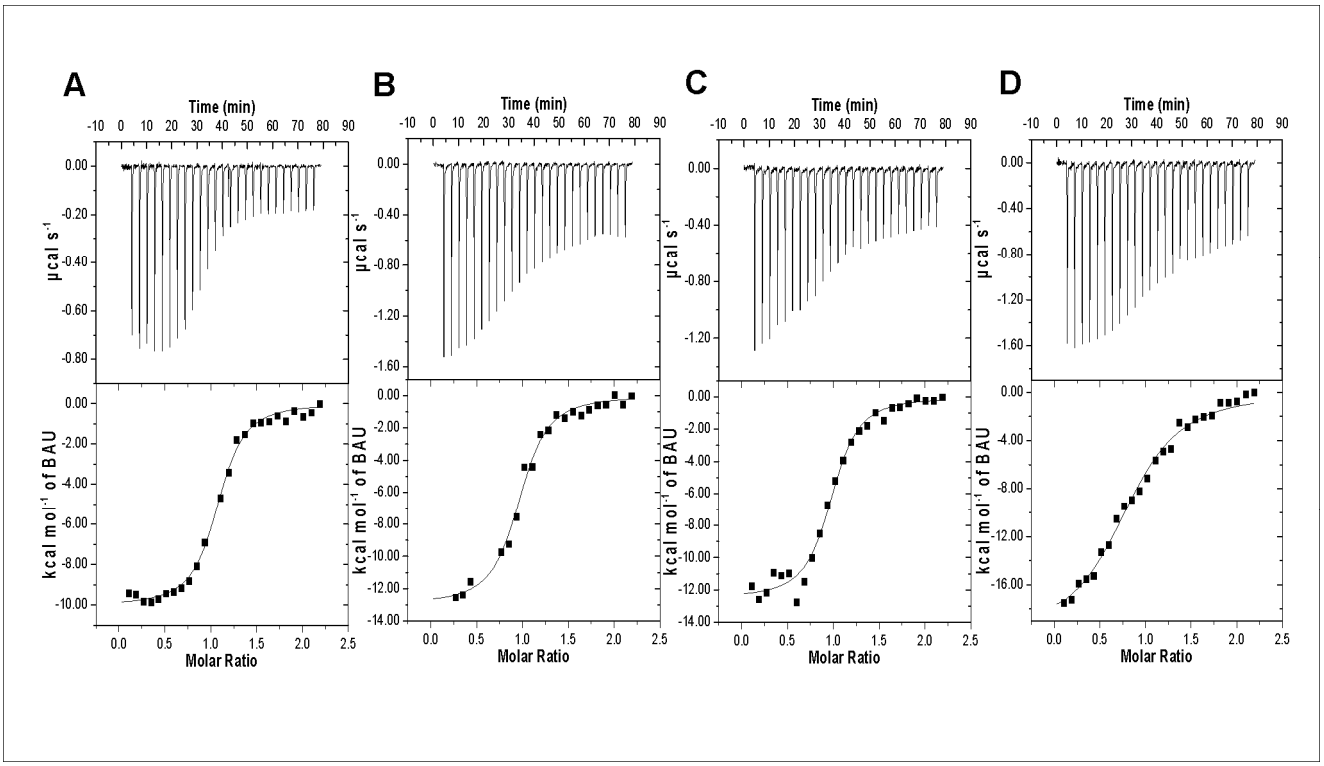

Figure S18. ITC binding assays of BAU (5-benzyl-1-(2'-hydroxyethoxymethyl)uracil) on hUP1 (A), hUP1-P_i (B), hUP1-R1P 50 μM (C), and hUP1-R1P 150 μM (D). The binding isotherms were fitted to one set of sites model.

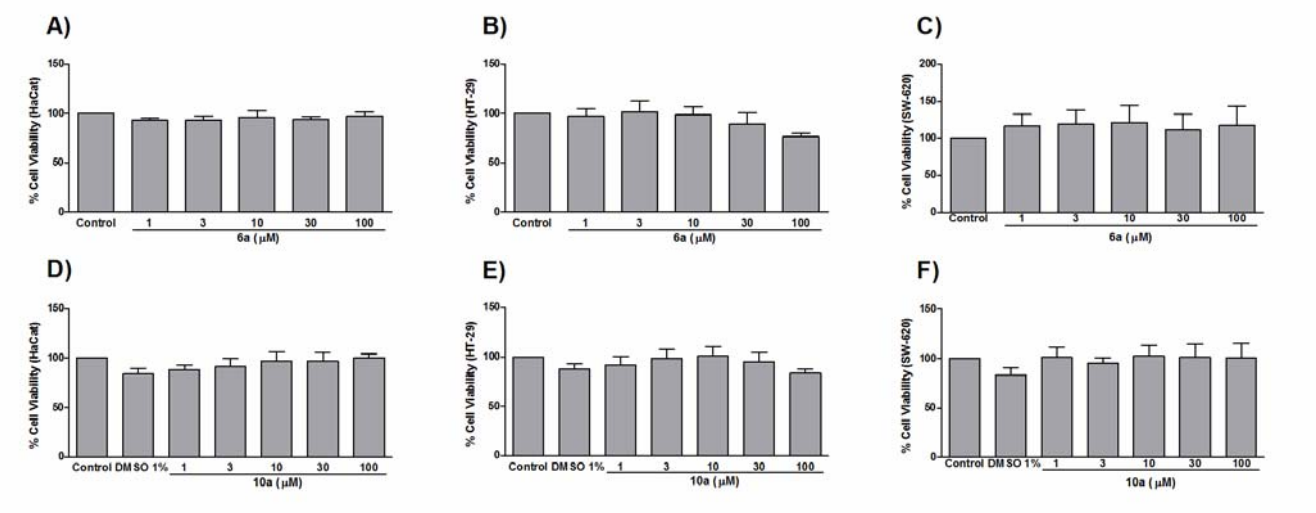

Figure S19. Evaluation of cell viability in HaCat (A and D), HT-29 (B and E), and SW-620 (C and F) cell lines. The cells were exposed to compounds (**6a** and **10a**) at varying concentrations (1-100 μM) followed by 72 h of incubation. Control cells were incubated with either culture medium (for **6a**) or culture medium with DMSO 1% (for **10a**). Data are shown as mean + standard error of mean of three independent experiments performed in quadruplicate. The statistical analysis was performed by one-way ANOVA followed by Bonferroni's post hoc test.

References:

1. Hirohashi, M.; Kido, M.; Yamamoto, Y.; Kojima, Y.; Jitsukawa, K.; Fujii, S. Synthesis of 5-Fluorouracil Derivatives Containing an Inhibitor of 5-Fluorouracil Degradation. *Chem. Pharm. Bull*. **1993**, *41*, 1498-1506.

2. Delia, T. J.; Scovill, J. P.; Munslow, W. D.; Burckhalter, J. H. Synthesis of 5-Substituted Aminomethyluracils via the Mannich Reaction. *J Med Chem*. **1976**, *19*, 344-346.

Capítulo 3

"Human uridine phosphorylase-1 inhibitors: a new approach for 5-fluorouracil-induced intestinal mucositis"

Manuscrito submetido no periódico *Cancer Chemotherapy and Pharmacology*, 2013.

Human uridine phosphorylase-1 inhibitors: a new approach to ameliorate 5-fluorouracil-induced intestinal mucositis

Daiana Renck[1,2], André A. Santos Jr[2,3], Pablo Machado[1,2], Guilherme O. Petersen[1,2], Tiago G. Lopes[4], Diógenes S. Santos[1,2], Maria M. Campos[3,5], Luiz A. Basso[1,2]

M.M. Campos and L.A. Basso (Corresponding Authors). E-mails: camposmmartha@yahoo.com, maria.campos@pucrs.br, luiz.basso@pucrs.br Phones: +55 51 33203677 and +55-51-33203629

[1]Centro de Pesquisas em Biologia Molecular e Funcional (CPBMF), Instituto Nacional de Ciência e Tecnologia em Tuberculose (INCT-TB), Pontifícia Universidade Católica do Rio Grande do Sul (PUCRS), Porto Alegre, RS, Brazil.

[2]Programa de Pós-Graduação em Biologia Celular e Molecular, Pontifícia Universidade Católica do Rio Grande do Sul (PUCRS), Porto Alegre, RS, Brazil.

[3]Instituto de Toxicologia e Farmacologia (INTOX), Pontifícia Universidade Católica do Rio Grande do Sul (PUCRS), Alegre, RS, Brazil.

[4]Instituto de Pesquisas Biomédicas (IPB), Pontifícia Universidade Católica do Rio Grande do Sul, Porto Alegre, RS, Brazil.

[5]Faculdade de Odontologia, Pontifícia Universidade Católica do Rio Grande do Sul (PUCRS), Porto Alegre, RS, Brazil.

Abstract

Purpose 5-fluorouracil (5-FU) has been broadly used to treat solid tumors for more than 50 years. One of the major side effects of fluoropyrimidines therapy is oral and intestinal mucositis. Human uridine phosphorylase (hUP) inhibitors have been suggested as modulators of 5-FU toxicity. Therefore, the present study aimed to test the ability of novel hUP blockers in preventing mucositis induced by 5-FU.

Methods We induced intestinal mucositis in Wistar rats with 5-FU, and the intestinal damage was evaluated in presence or absence of two hUP1 inhibitors characterized previously. We examined the loss of weight and diarrhea following the treatment, the villus integrity, uridine levels in plasma, and the neutrophil migration by MPO activity.

Results We found that one of the compounds, namely **6a** was efficient to promote intestinal mucosa protection and to inhibit the hUP1 enzyme, increasing the uridine levels in the plasma of animals. However, the loss of body weight, diarrhea intensity or neutrophil migration remained unaffected.

Conclusion Our results bring support to the hUP1 inhibitor strategy as a novel possibility of prevention and treatment of mucositis during the 5-FU chemotherapy, based on the approach of uridine accumulation in plasma and tissues.

Keywords: 5-fluorouracil, mucositis, uridine, human uridine phosphorylase-1 inhibitors.

Introduction

The fluoropyrimidine antimetabolite agent 5-fluorouracil (5-FU) was developed in 1957 [1] and since then, this agent has been broadly used in the treatment of cancer, mainly solid tumors including breast and colorectal cancers [2]. 5-FU acts by inhibiting the cell division processes through DNA and RNA damage, resulting in a decrease of cellular proliferation [2, 3]. This mechanism occurs via 5-FU active metabolites that cause RNA damage by fluorouridine 5'-triphosphate (FUTP) incorporation or DNA damage by irreversible inhibition of thymidylate synthase, reducing the production of deoxynucleotides [2, 4]. Chemotherapy-induced intestinal and oral mucositis is a well-recognized serious collateral effect associated with high- and standard-doses of 5-FU-containing regimens. This is a major problem caused during treatment of cancer being a dose-limiting factor for 5-FU chemotherapy [5]. Mucosal injury is the result of a number of sequential biological processes in small intestine and oral epithelium, and the last phase is the ulcerative event that is aggravated by local bacterial colonization [6, 7]. Intestinal mucositis has been reported to occur in 40-80 % of the patients who receive 5-FU [8], and it is characterized by a decrease in villus length and architecture disorder, as well as, an inflammatory process [9, 10]. Mucositis is manifested by a range of symptoms, including nausea, vomiting, severe diarrhea, dehydration, decrease in food intake, and in some cases, serious bacterial infection that cause severe pain, and may contribute to poor prognosis [5, 6]. Its presence during the chemotherapy cycle might require a dose reduction of the anticancer drug, changes in the nutritional diet (being necessary the replacement by total parenteral nutrition), and antibiotics therapy for the patients who develop bacterial infection. All of these represent a significant increase of investments per patient per cycle of chemotherapy, affecting the total hospitalization costs [11].

Although a variety of strategies have been employed to prevent, treat or attenuate this side effect, none of these approaches have been demonstrated to be totally effective, with no efficient treatment in clinical use, leading to the use of basic standard protocols that include oral hygiene care and drugs for the control of pain and diarrhea [12, 13]. The human enzyme uridine phosphorylase (EC 2.4.2.3, hUP) is responsible for the uridine homeostasis control in plasma and tissues, and its inhibitors have been proposed to decrease 5-FU toxicity, by increasing uridine levels [14, 15]. The excess of uridine produces more uridine triphosphate that will compete with FUTP for RNA incorporation, diminishing the rate of incorporation of the fluorinated nucleotide, and reducing the RNA damage responsible for the side effects [4, 14]. A previous study conducted by our research group [data under review] pointed out novel compounds that are potent inhibitors of hUP1 *in vitro*, and presented interesting data in cell culture, in which the compounds improved the susceptibility of colon tumor cells HT-29 and SW-620 to 5-FU, without modifying the viability of normal keratinocytes. However, the relationship between cancer chemotherapy-induced mucositis and protection by enhancing uridine in plasma has not been elucidated. Here, two lead compounds (**6a** and **10a**) were assessed for their ability to reduce the intestinal mucositis in an animal model of mucositis induced by 5-FU administration.

Material and Methods

Compounds

The compounds tested in this study (**6a** and **10a**) were synthesized as described by Renck et al., 2013 [data under review], and were solubilized in 0.9 % saline (vehicle) or vehicle with 1 % of dimethyl sulfoxide (DMSO), respectively. All solutions were prepared in the day of treatments and were administered in suspension form.

Animals

Female Wistar rats (4-5 per group, 160-200 g) were obtained from the Central Biotery of Universidade Federal of Pelotas (Brazil). Animals were housed in cages in a temperature- (22 ± 1 °C) and humidity-controlled (60-70 %) room under a 12 h light-dark cycle. Food and water were available *ad libitum*. Animal treatment and surgical procedures were performed in accordance with "Principal of Laboratory Animal Care" from National Institute of Health and were approved by the Institutional Animal Ethics Committee (CEUA 10/00199-PUCRS). All the administrations were carried out at 01:00 PM to avoid a possible influence of circadian cycle variation on hUP1 activity [16].

Induction of intestinal mucositis by 5-FU

Intestinal mucositis was induced as described by Saegusa et al [17], with some modifications. The animals were treated by intraperitoneal (i.p.) injection of 5-FU (Eurofarma, São Paulo, Brazil) at a dose of 50 mg kg^{-1} day^{-1}. Separated groups of animals were treated with the compounds **6a** (50 mg kg^{-1} day^{-1} or 150 mg kg^{-1} day^{-1}) and **10a** (60 mg kg^{-1} day^{-1} or 180 mg kg^{-1} day^{-1}) by oral gavage, 30 min before 5-FU administration. The treatment schedule continued by additional 5 days and the disease severity was assessed daily by measuring body weight and intensity of diarrhea. The euthanasia was performed on the 6^{th} day with isoflurane (Cristália, Itapira, Brazil); groups that were treated with the compounds received an additional dose 2 h before euthanasia and the other groups received vehicle. As positive control of mucositis, the animals were treated with 5-FU only, and as a negative control of the side effects, other animals received vehicle only. To determine any possible nonspecific toxicological effect of the test compounds, additional groups of animals received the highest dose of each compound.

Intestinal histological assessment

For the assessment of intestinal mucositis induced by 5-FU, the initial portion of the small intestine was surgically removed and stored in 10 % phosphate-buffered formalin for 2 days to histological analysis. The samples were then embedded in paraffin, cut into 5 μm thick sections, and stained with Hematoxylin and Eosin. Measurement of villus heights was performed from the baseline to the villus tip, and crypt length was measured from the baseline to the submucosa. The images were captured by Zeiss AxioImager M2 and analyzed through the Image-Pro Plus 4.0 software (Media Cybernetics L.P). About ten independent measurements from four different longitudinal sections of intact and well-oriented villus and crypts were counted per rat.

Plasma uridine concentration

For plasma uridine levels analysis, blood was collected by cardiac puncture into K2 ethylenediamine tetraacetic acid (EDTA) tubes (BD Vacutainer). The blood was then centrifuged at 5000 rpm for 20 min, and the recovered plasma was immediately stored at -20 °C until analysis by High Performance Liquid Chromatography Diode Array Detector (Thermo Scientific). Calibration curve was performed from 0.625 to 20 μM with uridine standard (Sigma-Aldrich) in blank plasma as matrix, followed by dilution with ultrapure water (1:1), and centrifuged at 13000 rpm for 30 min in microtubes Amicon (3 kDa molecular weight cutoff). The samples (100 μL) were injected on a Sephasil Peptide C18 ST 250 x 4.6 mm, 5 μm, 100 Å column (GE HealthCare) maintained at 20 °C, flow rate set at 0.5 mL min^{-1} with a mobile phase of 0.1 % acetic acid. Under these conditions, the retention time of uridine was 31.7 min with a linear relationship ($r > 0.99$) between the peak area and the uridine concentration, normalized by saline group concentration. The plasma extracts of each group were processed by the same protocol and the peak area was used to determine the uridine concentration.

Intestinal myeloperoxidase (MPO) activity

Neutrophil recruitment was quantified indirectly by determining MPO activity, according to the method described before [18]. The animals were treated with **6a** (50 mg kg^{-1} day^{-1}) for 4 days in an 8-8 h schedule by oral gavage, and 5-FU (50 mg kg^{-1} day^{-1} by i.p.) was administered on days 3 and 4, 30 min after administration of compound. The euthanasia was performed on the 5^{th} day with isoflurane, the initial portion of the small intestine was removed, and immediately stored at -20 °C. Briefly, the frozen tissues were homogenized at 5 % (w v^{-1}) in 20 mM $NaPO_4$ EDTA/NaCl buffer (pH 4.7) and centrifuged at 5000 rpm, 20 min, at 4 °C. The supernatant was removed and the pellet was resuspended in 200 µL of 20 mM $NaPO_4$ EDTA/NaCl buffer pH 4.7 + 0.2 % NaCl for 30 s, and after the addition of 1.5 mL of 1.6 % NaCl + 5 % glucose, the sample was centrifuged. The pellet was resuspended in 5 % (w v^{-1}) 50 mM $NaPO_4$ EDTA/NaCl buffer containing 0.5 % hexadecyltrimethyl ammonium bromide (pH 5.7), homogenized, and 1 mL was collected and centrifuged (5000 rpm, 30 min, at 4 °C). Duplicate 25-µL samples of the resulting supernatant were added into a 96-well plate. For the assay, 1.6 mM tetramethylbenzidine, and 0.3 mM hydrogen peroxide was added on the plate, and the samples were rapidly stirred and incubated at 37 °C for 5 min. The absorbance was measured at 595 nm, and the results are expressed as optical density per mg of tissue.

Statistical analysis

The results are reported as means ± standard error of the mean for each group. One-way ANOVA was performed followed by Bonferroni's test. A p value < 0.05 was considered statistically significant.

Results and Discussion

The most frequent side effect of chemotherapy are gastrointestinal symptoms, mainly nausea, vomiting, and diarrhea. Patients that are treated with 5-FU commonly develop other severe toxic effects that represent a leading cause of morbidity and mortality during the treatment of cancer: mucositis [8, 9]. In the murine model, 5-FU-induced diarrhea was intense on days 4 and 5 after the onset of chemotherapy administration (data not shown), and the presence of hUP1 inhibitors (**6a** and **10a**) did not prevent this side effect, that likely contributed to the observed body weight loss. Thus, during the experimental period (5 days), 5-FU treatment significantly reduced the body weight, independent on the administration of compounds **6a** and **10a**, in contrast with the animals that received vehicle or compounds only that clearly had body weight gains (Table 1).

In this study, we found that the compound **6a** appeared to reduce the severity of 5-FU-induced intestinal toxicity, according to the histological examination of small intestine. 5-FU caused a loss of architecture and integrity of the intestinal mucosa, as seen by a significant villi shortening with vacuolated cells, and inflammatory infiltration in the intestinal initial portion compared with the negative control group (saline) (Fig. 1a and 1b). Additionally, the normal crypt architecture was lost but with no damage on the crypt depth. In contrast, when the animals were pre-treated with the inhibitor **6a**, the histological features of mucositis were significantly reduced ($p < 0.01$) for both tested doses (50 and 150 mg kg^{-1} day^{-1}) (Fig. 2a). The villi were longer and well-ordered in compound **6a**-treated animals (Fig. 1a), in comparison to the damage of positive control group (5-FU alone), as saline group. There was no significant difference on crypts depths between the groups of animals but the normal crypt architecture was preserved on the groups that were treated with the compound (data not shown). The animals that were treated only with 150 mg kg^{-1} day^{-1} of compound **6a** did not present any toxic effect, such as body mass reduction, diarrhea, changes on food or water

intake, as well as intestinal damage, discarding nonspecific effects of the compound *per se*. This group showed a significant increase of the villi height when compared with the negative group, corroborating the protective effect on intestinal mucosa. We previously demonstrated [under review] that compound **6a** improved the cytotoxic effect of the 5-FU in colon tumor cells, without any influence on half maximal inhibitory concentration in normal cells (keratinocytes). These data will be important for future evaluation on the influence of this compound in a tumor model in rats treated with 5-FU, supporting further investments in this molecule, which also presents an interesting mucosal protection. On the other hand, mucositis was not decreased by the administration of the other hUP1 inhibitor, compound **10a** (Fig. 1b). The animals treated with 5-FU and the compound (on both doses) developed severe diarrhea, and intestinal damage with no significant difference with the positive damage control group (Fig. 2c). There were probably difficulties in absorption of the molecule due to its insoluble characteristic in polar vehicle and by the limiting concentration of DMSO, avoiding the inhibition of the enzyme and ensuing uridine accumulation.

The increase of uridine in plasma and tissues is well discussed in literature to prevent side effects as well as to improve the effects of fluoropyrimidines [4, 14, 16]. The compound **6a** was not efficient to reduce the diarrhea and the loss of weight of the animals treated with 5-FU, however, the intestinal mucosa was preserved. The analysis of plasma uridine levels revealed that animals treated with compound **6a** had an increase about 4-fold in plasma uridine concentration (Fig. 2b), demonstrating that the molecule was absorbed and inhibited the enzyme hUP1, as expected. We can correlate this uridine accumulation with the intestinal mucosa preservation during the chemotherapeutic schedule. This hypothesis is strongly strengthened by the negative outcome of compound **10a**, that failed to inhibit the enzyme *in vivo*, maintaining the plasma uridine concentration at normal levels (Fig 2d) and it was reflected on the inability to decrease mucositis. Therefore, our results suggest that the increase

of uridine concentration in plasma and tissues is an interesting approach for attenuating chemotherapy-induced intestinal damage that leads to discontinued treatment.

As we demonstrated that compound **6a** was able to significantly decrease the intestinal damage elicited by 5-FU, we also decided to investigate the inflammatory process. MPO is an enzyme that is primarily expressed in azurophilic neutrophil granules, and it is commonly used as a biochemical marker of inflammation, including for the gastrointestinal tract [5]. The intestinal inflammatory process caused by 5-FU administration was also characterized by an increase in MPO activity in groups that received the chemotherapeutic agent compared with saline group ($p < 0.01$), corroborating the literature data [5, 18]. However, the treatment with 5-FU lasted 2 days only, in contrast with the 5 days of the mucositis model, because we have noted that on the day of euthanasia, the primary inflammatory response had been lost, and no difference in MPO activity was detected between control and 5-FU groups (data not shown). The pre-treatment with the hUP1 inhibitor (**6a**, 50 mg kg^{-1} day^{-1}) did not display any significant effect on MPO activity, showing that beneficial effects of this compound do not appear to rely on the interference with neutrophil migration allied to 5-FU administration (Online Resource 1). The neutrophil migration might well be related to the reduction of body mass and severe diarrhea that is observed in all animals that received 5-FU, suggesting a directional protective effect on intestinal mucosa dependent on uridine concentration.

Conclusions

Oral and gastrointestinal mucositis is a common side effect following cancer chemotherapy, and researchers and pharmaceutical industry have attempted to develop new interventions to avoid this toxic effect, although it remains an unmet medical problem. Many different strategies have been proposed to eliminate this side effect and to improve the life quality of patients, including interleukin receptor antagonism [11], insulin-like growth factor-I [19],

minocycline [9], platelet-activating factor [5], omeprazole and ranitidine [6], among others. Since 1981, hUP inhibitors are proposed as promising agents to reduce 5-FU toxicity by reducing FUTP incorporation into RNA [14, 20]. However, until today, there is no experimental evidence indicating that hUP inhibitors provide intestinal protection against mucositis. Here, we present two hUP1 inhibitors as candidates to oral drugs to decrease mucositis during 5-FU treatment. We provide convincing pieces of evidence that compound **6a** has a beneficial effect against intestinal damage, probably via increased uridine concentration. Thereby, hUP1 inhibitors might represent potential targets for drug design to decrease the oral and gastrointestinal damage caused by 5-FU. Future *in vivo* assays employing a tumor animal model would be critical for evaluating the influence of the combination therapy. Furthermore, experiments with different anticancer drugs can also contribute to determine the range of use of this class of compounds. Owing to the aging of population and lifestyle changes, the global cancer incidence is predicted to be significantly increased in the next years, and also the toxic manifestations arising from the treatment. For this reason, it still is essential to continue to focus on developing antimucotoxics therapies by identification and validation of novel targets.

Abbreviations

5-FU: 5-fluorouracil

DMSO: dimethyl-sulfoxide

FUTP: fluorouridine 5'-triphosphate

hUP: human uridine phosphorylase

MPO: myeloperoxidase

Acknowledgments

This work was supported by the National Institute of Science and Technology on Tuberculosis, (DECIT/SCTIE/MS-MCT-CNPq-FNDCT-CAPES) awarded to D.S.S. and L.A.B. L.A.B and D.S.S. also acknowledge financial support awarded by FAPERGS-CNPq-PRONEX-2009. L.A.B., D.S.S. and M.M.C. are Research Career Awardees of the National Research Council of Brazil (CNPq). D.R. and G.O.P. are recipients of a PhD scholarship awarded by CNPq and A.A.S.Jr. is recipient of a PhD scholarship awarded by CAPES.

References

1. Heidelberger C, Chaudhuri NK, Danneberg P, Mooren D, Griesbach L, Duschinsky R, Schnitzer RJ, Pleven E, Scheiner J (1957) Fluorinated pyrimidines, a new class of tumour-inhibitory compounds. Nature 179:663-666
2. Longley DB, Harkin DP, Johnston PG (2003) 5-fluorouracil: mechanisms of action and clinical strategies. Nat Rev Cancer 3:330-338
3. Grem JL (2000) 5-fluorouracil: forty-plus and still ticking. A review of its preclinical and clinical development. Invest New Drugs 18:299-313
4. van Groeningen CJ, Peters GJ, Pinedo HM (1992) Modulation of fluorouracil toxicity with uridine. Semin Oncol 19:148-154
5. Soares PMG, Mota JMSC, Gomes AS, Oliveira RB, Assreuy AMS, Brito GAC, Santos AA, Ribeiro RA, Souza MHLP (2008) Gastrointestinal dysmotility in 5-fluorouracil-induced intestinal mucositis outlasts inflammatory process resolution. Cancer Chemother Pharmacol 63:91-98
6. Rubenstein EB, Peterson DE, Schubert M, Keefe D, Mcguire D, Epstein J, Elting LS, Fox PC, Cooksley C, Sonis ST (2004) Clinical practice guidelines for the prevention and treatment of cancer therapy-induced oral and gastrointestinal mucositis. Cancer 100:2026-2046
7. Sonis ST (2010) New thoughts on the initiation of mucositis. Oral Dis 16:597-600
8. Sonis ST (2004) The pathobiology of mucositis. Nat Rev Cancer 4:277-284
9. Huang TY, Chu HC, Lin YL, Ho WH, Hou HS, Chao YC, Liao CL (2009) Minocycline attenuates 5-fluorouracil-induced small intestinal mucositis in mouse model. Biochem Biophys Res Commun 389:634-639
10. Sonis ST (2009) Mucositis: the impact, biology and therapeutic opportunities of oral mucositis. Oral Oncol 45:1015-1020

11. Bowen JM, Gibson RJ, Keefe DMK (2011) Animal models of mucositis: implications for therapy. J Support Oncol 9:161-168
12. Keefe DM, Schubert MM, Elting LS, Sonis ST, Epstein JB, Raber-Durlacher JE, Migliorati CA, McGuire DB, Hutchins RD, Peterson DE (2007) Updated clinical practice guidelines for the prevention and treatment of mucositis. Cancer 109:820-831
13. Melichar B, Kohout P, Bratova M, Solichova D, Kralickova P, Zadak Z (2001) Intestinal permeability in patients with chemotherapy-induced stomatitis. J Cancer Res Clin Oncol 127:314-318
14. Al Safarjalani ON, Rais R, Shi J, Schinazi RF, Naguib FNM, el kouni MH (2006) Modulation of 5-fluorouracil host-toxicity and chemotherapeutic efficacy against human colon tumors by 5-(Phenylthio)acyclouridine, a uridine phosphorylase inhibitor. Cancer Chemother Pharmacol 58:692-698
15. Leyva A, van Groeningen CJ, Kraal I, Gall H, Peter GJ, Lankelma J, Pinedo HM (1984) Phase I and Pharmacokinetic studies of high-dose uridine intended for rescue from 5-fluorouracil toxicity. Cancer Res 44:5928-5933
16. Al Safarjalani ON, Rais R, Naguib FNM, el Kouni MH (2012) Potent combination therapy for human breast tumors with high doses of 5-fluorouracil: remission and lack of host toxicity. Cancer Chemother Pharmacol 69:1449-1455
17. Saegusa Y, Ichikawa T, Iwai T, Goso Y, Ikezawa T, Nakano M, Shikama N, Saigenji K, Ishihara K (2008) Effects of acid antisecretory drugs on mucus barrier of the rat against 5-fluorouracil-induced gastrointestinal mucositis. Scand J Gastroenterol 43:531-537
18. Soares PMG, Lima-Junior RCP, Mota JMSC, Justino PFC, Brito GAC, Ribeiro RA, Cunha FQ, Souza MHLP (2011) Role of platelet-activating factor in the pathogenesis

of 5-fluorouracil-induced intestinal mucositis in mice. Cancer Chemother Pharmacol 68:713-720

19. Cool JC, Dyer JL, Xian CJ, Butler RN, Geier MS, Howarth GS (2004) Pre-treatment with insulin-like growth factor-I partially ameliorates 5-fluorouracil-induced intestinal mucositis in rats. Growth Horm IGF Res 15:72-82
20. Niedzwicki JG, el Kouni MH, Chu SH, Cha S (1981) Pyrimidine acyclonucleosides, inhibitors of uridine phosphorylase. Biochem Pharmacol 30:2097-2101

Table 1 Body weight changes in 5-FU treated animals

Treatment (mg/kg)	Weight (g) ± SE Day 1	Weight (g) ± SE Day 6
Saline + Saline	216 ± 6	219 ± 5
6a(150) + Saline	226 ± 4	223 ± 4
Saline + 5-FU(50)	241 ± 10	196 ± 5**
6a(50) + 5-FU(50)	236 ± 7	199 ± 8*
6a(150) + 5-FU(50)	239 ± 10	192 ± 6**
Saline + Saline	155 ± 4	172 ± 4*
DMSO1% + Saline	146 ± 2	159 ± 2
10a(180) + Saline	160 ± 3	177 ± 2
Saline + 5-FU(50)	155 ± 5	133 ± 3*
10a(60) + 5-FU(50)	165 ± 3	148 ± 9*
10a(180) + 5-FU(50)	154 ± 6	141 ± 6

SE standard error mean, *$p < 0.05$ and **$p < 0.01$ versus day 1.

Figure Captions

Fig. 1 Representative images of histological assessments of initial portion of the intestine after 5 days of 5-FU treatment or/and 5-FU and hUP1 inhibitor (**6a** on a, and **10a** on b). Sections were stained with Hematoxylin and Eosin and observed using light microscopy (magnification 10x).

Fig. 2 The influence of the compounds **6a** (a) and **10a** (c) in the intestinal morphometry of villus height from intestinal mucosa in the mucositis model caused by 5-FU. Ten independent measurements from four different longitudinal sections of intact and well-oriented villus were counted per rat. The values are shown as mean ± standard error. Values were compared statistically using One-way ANOVA followed by Bonferroni's post-test. $*p < 0.05$ and $***p < 0.0001$ denote the significant levels in comparison to positive control of damage (Saline + 5-FU) values; $\#p < 0.05$ and $\#\#\#p < 0.0001$ denote significant levels in comparison to Saline + Saline values. Uridine concentration in plasma of the animals treated with 5-FU and/or compounds **6a** (b) and **10a** (d). The values are shown as mean ± standard error. Values were compared statistically using One-way ANOVA followed by Bonferroni's post-test. $*p < 0.05$ denote the significant levels in comparison to Saline + Saline values. Graphic program used was GraphPad Prism 5.0.

Fig. 1

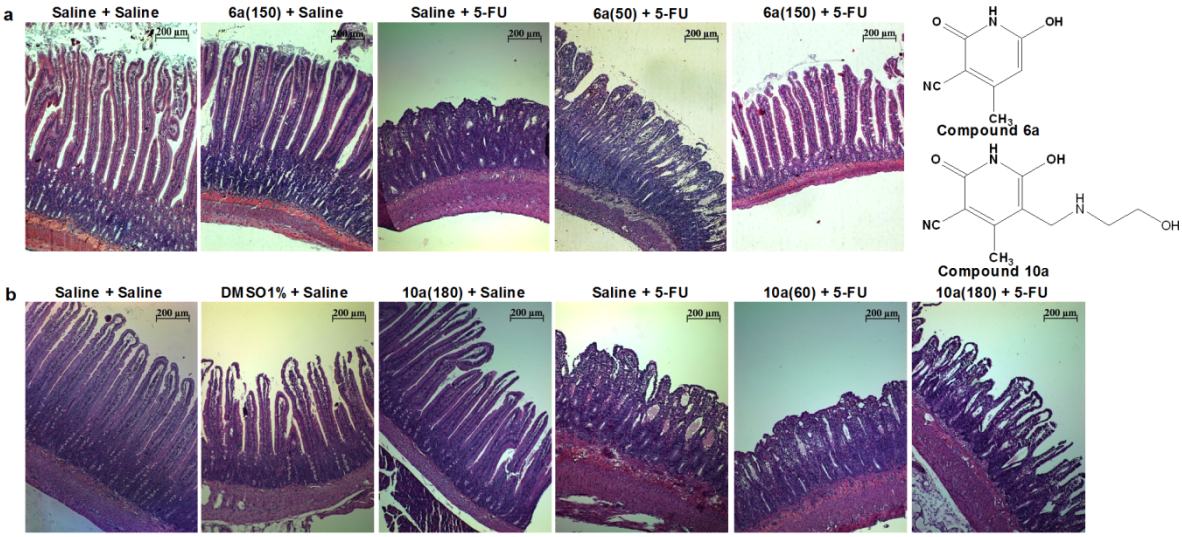
a
Saline + Saline
6a(150) + Saline
Saline + 5-FU
6a(50) + 5-FU
6a(150) + 5-FU
200 µm
Compound 6a
Compound 10a
b
Saline + Saline
DMSO1% + Saline
10a(180) + Saline
Saline + 5-FU
10a(60) + 5-FU
10a(180) + 5-FU

Fig. 2

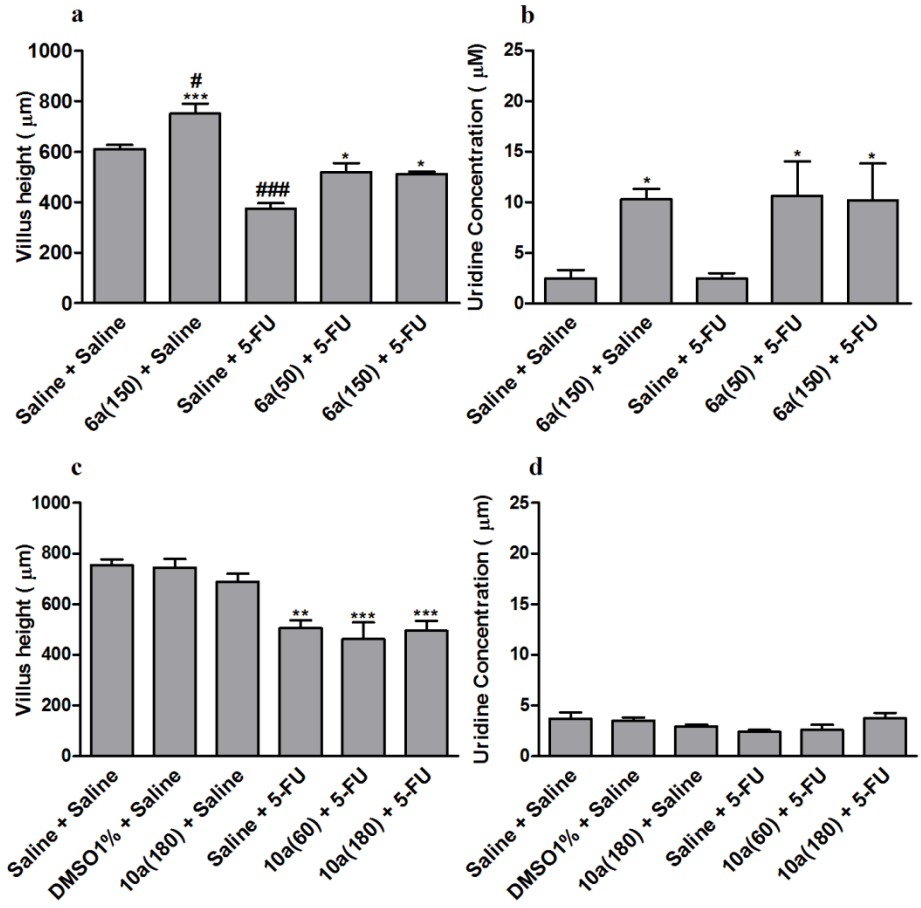
a
Villus height (μm)
1000
800
600
400
200
0
#
***
###
*
*
Saline + Saline
6a(150) + Saline
Saline + 5-FU
6a(50) + 5-FU
6a(150) + 5-FU
b
Uridine Concentration (μM)
25
20
15
10
5
0
*
*
*
Saline + Saline
6a(150) + Saline
Saline + 5-FU
6a(50) + 5-FU
6a(150) + 5-FU
c
Villus height (μm)
1000
800
600
400
200
0
**
***
***
Saline + Saline
DMSO1% + Saline
10a(180) + Saline
Saline + 5-FU
10a(60) + 5-FU
10a(180) + 5-FU
d
Uridine Concentration (μm)
25
20
15
10
5
0
Saline + Saline
DMSO1% + Saline
10a(180) + Saline
Saline + 5-FU
10a(60) + 5-FU
10a(180) + 5-FU

Online Resource 1

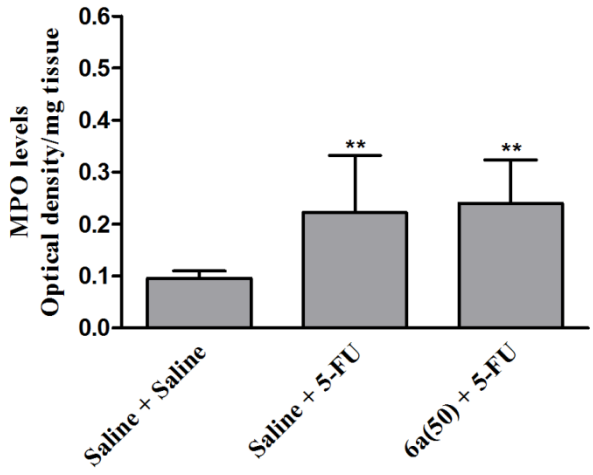

Figure Caption

Online Resource 1 Each column represents the mean of 4 animals. The values are shown as mean ± standard error. Values were compared statistically using One-way ANOVA followed by Bonferroni's post-test. $^{**}p < 0.01$, denote significant levels compared with Saline + Saline group. Graphic program used was GraphPad Prism 5.0

Capítulo 4

CONSIDERAÇÕES FINAIS

CONSIDERAÇÕES FINAIS

Por mais de 60 anos, a quimioterapia tem sido utilizada para o tratamento do câncer, assim como tumores metastáticos. Muitos dos agentes quimioterápicos foram descobertos sem conhecimento a respeito de mecanismos de ação bioquímicos e nos últimos anos uma estratégia racional foi introduzida para o desenho de fármacos e pró-fármacos. Essa estratégia se baseia em alvos moleculares definidos que façam parte de rotas metabólicas importantes para as células tumorais (72). Porém, ainda existem muitos alvos moleculares para serem estudados e caracterizados, assim como elucidar as funções que desempenham no processo de progressão tumoral (73). Além da necessidade de caracterização de novos alvos, outro problema no tratamento é a necessidade do uso da terapia combinada, com diversos agentes quimioterápicos e outras técnicas, como radioterapia e cirurgia, podendo levar a uma resistência a múltiplos fármacos quando o período de tratamento é prolongado e a um severo dano aos tecidos normais do paciente, entre outros fatores (74).

Os efeitos adversos gerados aos pacientes é um dos grandes desafios que ainda devem ser vencidos, sabendo-se que a qualidade de vida é um fator que influencia diretamente o sucesso do tratamento. O 5-FU foi um dos primeiros fármacos a serem desenvolvidos com base em observações bioquímicas no ano de 1957 (15) e desde então é amplamente utilizado na clínica para o tratamento de tumores sólidos, principalmente câncer de mama e colorretal (18). Além dos efeitos adversos comuns a quase todos os agentes quimioterápicos, o 5-FU induz mucosite em cerca de 40-80 % dos pacientes. Esse processo de destruição da mucosa ocorre tanto na boca quanto no intestino e pode ser um fator de risco para o paciente. A mucosite é caracterizada por ulcerações nessas mucosas, gerando dores severas, além de modificações na dieta e no esquema de administração do fármaco, interferindo substancialmente na eficiência do tratamento. Ao mesmo tempo, essas ulcerações podem se tornar portas de entrada para micro-organismos, gerando um quadro de infecção generalizada (sepse) e levando o paciente a óbito. Até hoje não existe nenhum tipo de tratamento para prevenir ou tratar a mucosite, havendo apenas procedimentos básicos como a administração de medicamentos para dor e intensa higienização bucal (24,25,26).

Os dados já existentes na literatura quanto à caracterização cinética da enzima hUP1 (42) foram de extrema importância para o desenvolvimento desse

trabalho, visto que a análise do mecanismo deve ser uma prioridade para o desenvolvimento de fármacos (49). Identificamos inibidores com afinidades e parâmetros termodinâmicos aprimorados em relação à nossa molécula líder ao fazermos uso de derivatização química em porções específicas da molécula. Além disso, nossos inibidores seguem o mesmo modo de ação do mecanismo cinético, necessitando da ligação prévia do P_i no sítio ativo para depois ocorrer a ligação da molécula no sítio de ligação da uridina. Esse fato corrobora a prioridade do entendimento do modo de ação das enzimas para o desenvolvimento de drogas. Esses dados ainda foram reforçados pelos resultados obtidos através dos ensaios de ligação utilizando a técnica de microcalorimetria, onde confirmamos a necessidade da ligação do P_i antes do inibidor competir pelo sítio ativo da uridina. Além disso, os dados termodinâmicos revelaram que nossa estratégia de desenho de novos compostos apresenta o problema mais comum e mais difícil de ser ultrapassado no processo de planejamento de uma nova série de moléculas: o sistema de compensação entalpia-entropia. Esse sistema de compensação surge da tentativa de melhorarmos uma porção da molécula com o objetivo de melhorar um parâmetro termodinâmico, interferindo de forma negativa no outro. Esse processo é caracterizado por valores de energia livre de Gibbs praticamente iguais, revelando que não houve praticamente nenhum ganho de afinidade com as modificações propostas (75). Os ensaios de cultura de células e os ensaios em roedores nos revelaram que a molécula líder é o nosso composto promissor, mesmo não possuindo as melhores características cinéticas e termodinâmicas. Verificamos que, ao ser administrado juntamente com o 5-FU, o composto afetou as células tumorais tornando-as mais sensíveis ao quimioterápico e, ao mesmo tempo, não influenciou a ação do fármaco nas células normais. Em modelo animal de mucosite intestinal, o composto parece proteger as vilosidades intestinais dos ratos, podendo protegendo sua mucosa através da elevação da concentração da uridina no plasma em aproximadamente 4 vezes, porém, o composto não foi capaz de reduzir o processo inflamatório e a diarreia severa, assim como alterações de peso e mais estudos são necessários para confirmar o papel protetor e o mecanismo pelo qual esse evento ocorre.

Os inibidores enzimáticos são uma das classes mais procuradas pela indústria farmacêutica, correspondendo à parcela de 25 % do mercado de medicamentos dos Estados Unidos (49,71). Assim, a constante busca por novas

moléculas inibitórias da hUP1 para o desenvolvimento de um possível fármaco que tenha como ação final melhorar a qualidade de vida dos pacientes que desenvolvem mucosite é fundamental. Os dados aqui apresentados reforçam essa estratégia do uso de inibidores da hUP1 como meio para elevar a concentração de uridina e além disso, são resultados importantes que poderão auxiliar no desenho e no modo de interação de novas moléculas.

REFERÊNCIAS

REFERÊNCIAS

1. The History of Cancer. American Cancer Society. 2012.

2. DeVita VT, Rosenberg AS. Two hundred years of cancer research. N Engl J Med. 2012;366(23):2207-2214.

3. World Health Organization, WHO. Endereço eletrônico: http://www.who.int/en/. Acessado em 10 de julho de 2013.

4. Hanahan D, Weinberg RA. Hallmarks of cancer: the next generation. Cell. 2011;144(5):646-674.

5. Cancer Fact & Figures. American Cancer Society. 2011.

6. Estimativa 2012, incidência de câncer no Brasil. Instituto Nacional de Câncer, INC, 2011. Endereço eletrônico: (http://www.inca.gov.br). Acessado em 10 de julho de 2013.

7. DeVita VT, Chu E. The history of cancer chemotherapy. Cancer Res. 2008;68(21):8643-8653.

8. American Cancer Society. Endereço eletrônico: (http://www.cancer.org/index). Acessado em 29 de outubro de 2013.

9. Voet D, Voet JG. Bioquímica. 4ª ed. 2013.

10. Shambaugh GE 3rd. Pyrimidine biosynthesis. Am J Clin Nutr. 1979;32(6):1290-1297.

11. Connolly GP, Duley JA. Uridine and its nucleotides: biological actions, therapeutic potentials. Trends Pharmacol Sci. 1999;20(5):218-225.

12. Islam MR, Kim H, Kang SW, Kim JS, Jeong YM, et al. Functional characterization of a gene encoding a dual domain for uridine kinase and uracil phosphoribosyltransferase in *Arabidopsis thaliana*. Plant Mol Biol. 2007;63(4):465-477.

13. Schwartz EL, Baptiste N, Megati S, Wadler S, Otter BA. -Ethoxy-2'-deoxyuridine, a novel substrate for thymidine phosphorylase, potentiates the antitumor activity of 5-fluorouracil when used in combination with interferon, an inducer of thymidine phosphorylase expression. Cancer Res. 1995;55(16):3543-50.

14. Maring JG, Groen HJM, Wachters FM, Uges DRA, de Vries EGE. Genetics factors influencing pyrimidine-antagonist chemotherapy. Pharmacogenomics J. 2005;5(4):226-243.

15. Heidelberger C, Chaudhuri NK, Danneberg P, Mooren D, Griesbach L. Fluorinated pyrimidines, a new class of tumor-inhibitory compounds. Nature. 1957;179(4561):663-666.

16. Liu M, Cao D, Russell R, Handschumacher RE, Pizzorno G. Expression, characterization, and detection of human uridine phosphorylase and identification of variant uridine phosphorolytic activity in selected human tumors. Cancer Res. 1998;58(23):5418-24.

17. Cao D, Russell RL, Zhang D, Leffert JJ, Pizzorno G. Uridine phosphorylase (-/-) murine embryonic stem cells clarify the key role of this enzyme in the regulation of the pyrimidine salvage pathway and in the activation of fluoropyrimidines. Cancer Res. 2002;62(8):2313-7.

18. Longley DB, Harkin DP, Johnston PJ. 5-fluorouracil: mechanisms of action and clinicals strategies. Nat Rev Cancer. 2003;3(5):330-338.

19. Malet-Martino M, Martino R. Clinical studies of three oral prodrugs of 5-fluorouracil (capecitabine, UFT, S-1): a review. The Oncologist. 2002;7(4):288-323.

20. Rich TA, Shepard RC, Mosley ST. Four decades of continuing innovation with fluorouracil: current and future approaches to fluorouracil chemoradiation therapy. J Clin Oncol. 2004;22(11):2214-2232.

21. Iyer L, Ratain MJ. 5-fluorouracil pharmacokinetics: causes for variability and strategies for modulation in cancer chemotherapy. Cancer Invest. 1999;17(7):494-506.

22. Keefe DM, Schubert MM, Elting LS, Sonis ST, Epstein JB et al. Updated clinical practice guidelines for the prevention and treatment of mucositis. Nature Rev Cancer. 2007;109(5):820-831.

23. Sonis ST. The pathobiology of mucositis. Nature Ver Cancer. 2004;4(4):277-284.

24. Bowen JM, Gibson RJ, Keefe DM. Animal models of mucositis: implications for therapy. J Support Oncol. 2011;9(5):161-168.

25. Soares PMG, Mota JMSC, Gomes AS, Oliveira RB, Assreuy MAS et al. Gastrointestinal dysmotility in 5-fluorouracil-induced intestinal mucositis outlasts inflammatory process resolution. Cancer Chemother Pharmacol. 2008;63(1):91-98.

26. Houghton JA, Houghton PJ, Wooten RS. Mechanism of induction of gastrointestinal toxicity in the mouse by 5-fluorouracil, 5-fluorouridine, and 5-fluoro-2'-deoxyuridine. Cancer Res. 1979;39(7 Pt 1):2406-2413.

27. Al Safarjalani ON, Rais R, Shi J, Schinazi RF, Naguib FNM et al. Modulation of 5-fluorouracil host-toxicity and chemotherapeutic efficacy against human colon tumors by 5-(Phenylthio)acyclouridine, a uridine phosphorylase inhibitor. Cancer Chemother Pharmacol. 2006;58(5):692-698.

28. Matin DS, Stolfi RL, Sawyer RC, Spiegelman S, Young CW. High-dose 5-fluorouracil with delayed uridine "rescue" in mice. Cancer Res. 1982;42(10):3964-3970.

29. Leyva A, van Groeningen CJ, Kraal I, Gall H, Peters GJ et al. Phase I and pharmacokinetic studies of high-dose uridine intended for rescue from 5-fluorouracil toxicity. Cancer Res. 1984;44(12 Pt 1):5928-5933.

30. van Groeningen CJ, Peters GJ, Pinedo HM. Modulation of fluorouracil toxicity with uridine. Seminars in Oncology. 1992;19(2):148-154.

31. Al Safarjalani ON, Rais R, Naguib FNM, el Kouni MH. Potent combination therapy for human breast tumors with high doses of 5-fluorouracil: remission and lack of host toxicity. Cancer Chemother Pharmacol. 2012;69(6):1449-1455.

32. Ashour OM, Naguib FNM, Goudgaon NM, Schinazi RF, el Kouni MH. Effect of 5-(phenylselenenyl)acyclouridine, an inhibitor of uridine pshophorylase, on plasma concentration of uridine released from 2',3',5'-tri-*O*-acetyluridine, a prodrug of uridine: relevance to uridine rescue in chemotherapy. Cancer Chemother Pharmacol. 2000;46(3):235-240.

33. Niedzwicki JG, el Kouni MH, Chu SH, Cha S. Pyrimidine acyclonucleosides, inhibitors od uridine phosphorylase. Biochem Pharmacol. 1981;30(15):2097-2101.

34. Krenitsky TA, Mellors JW, Barclay RK. Pyrimidine nucleosidases. Their classification and relationship to uric acid ribonucleoside phosphorylase. J Biol Chem. 1965;240:1281-1286.

35. el Kouni MH, Goudgaon NM, Rafeeq M, Al Safarjalani ON, Schinazi RF, Naguib FN. 5-phenylthioacyclouridine: a potent and specific inhibitor of uridine phosphorylase. Biochem Pharmacol. 2000;60(6):851-856.

36. Caradoc-Davies TT, Cutfield SM, Lamont IL, Cutfield JF. Crystal structures of *Escherichia coli* uridine phosphorylase in two native and three complexed forms reveal basis of substrate specificity, induced conformation changes and influence of potassium. J Mol Biol. 2004;337:337-354.

37. Lashkov AA, Gabdoulkhakov AG, Shtil AA, Mikhailov AM. Crystallization and preliminary X-ray diffraction analysis of *Salmonella typhimurium* uridine phosphorylase complexed with 5-fluorouracil. Acta Crystallogr Sect F Struct Biol Cryst Commun. 2009;65(Pt 6):601-603.

38. Paul D, O'Leary SE, Rajashankar K, Bu W, Toms A, et al. Glycal formation in crystals of uridine phosphorylase. Biochemistry. 2010;49(16):3499-3509.

39. Roosild TP, Castronovo S, Fabbiani M, Pizzorno G. Implications of the structure of human uridine phosphorylase 1 on the development of novel inhibitors for improving the therapeutic window of fluoropyrimidine chemotherapy. BMC Struct Biol. 2009;9(14):1-9.

40. Johansson M. Identification of a novel human uridine phosphorylase. Biochem Biophys Res Commun. 2003;307(1):41-46.

41. Cao D, Leffert JJ, McCabe J, Kim B, Pizzorno G. Abnormalities in uridine homeostatic regulation and pyrimidine nucleotide metabolism as a consequence of the deletion of the uridine phosphorylase gene. J Biol Chem. 2005;280(22):21169-21175.

42. Renck D, Ducati RG, Palma MS, Santos DS, Basso LA. The kinetic mechanism of human uridine phosphorylase 1: Towards the development of enzyme inhibitors for cancer chemotherapy. Arch Biochem Biophys. 2010;497(1-2):35-42.

43. Bose R, Yamada EW. Uridine phosphorylase, molecular properties and mechanism of catalisys. Biochemistry. 1974;13(10):2051-2056.

44. Kraut A, Yamada EW. Cytoplasmic uridine phosphorylase of rat liver. Characterization and kinetics. J Biol Chem. 1971;246(7):2021–2030.

45. Krenitsky TA. Uridine phosphorylase from *Escherichia coli*. Kinetic properties and mechanism. Biochem Biophys Acta. 1976;429(2):352–358.

46. Vita A, Huang CY, Magni G. Uridine phosphorylase from *Escherichia coli* B.: kinetic studies on the mechanism of catalysis. Arch Biochem Biophys. 1983;226(2):687–692.

47. Avraham Y, Grossovicz N, Yashphe J. Purification and characterization of uridine and thymidine phosphorylase from *Lactobacillus casei*. Biochem Biophys Acta. 1990;1040(2):287–293.

48. Krenitsky TA. Pentosyl transfer mechanisms of the mammalian nucleoside phosphorylases. J Biol Chem. 1968;243(11):2871–2875.

49. Robertson JG. Enzymes as a special class of therapeutic target: clinical drugs and modes of action. Curr Opin Struct Biol. 2007;17(6):674-679.

50. Niedzwicki JG, el Kouni MH, Chu SH, Cha S. Pyrimidine acyclonucleosides, inhibitors of uridine phosphorylase. Biochem Pharmacol. 1981;30(15):2097-2101.

51. Cha S. Development of inhibitors of pyrimidine metabolism. Yonsei Medical Journal. 1989;30(4):315-326.

52. Niedzwicki JG, Chu SH, el Kouni MH, Rowe EC, Cha S. 5-benzylacyclouridine e 5-benzyloxybenzylacyclouridine, potent inhibitors of uridine phosphorylase. Biochem Pharmacol. 1982;31(10):1857-1861.

53. Naguib FN, el Kouni MH, Chu SH, Cha S. New analogues of benzylacyclouridines, specific and potent inhibitors of uridine phosphorylase from human and mouse livers. Biochem Pharmacol. 1987;36(13):2195-2201.

54. Darnowski JW, Handschumacher RE. Tissue-specific enhancement of uridine utilization and 5-fluorouracil therapy in mice by benzylacyclouridine. Cancer Res. 1985;45(11 Pt 1):5364-5368.

55. Pizzorno G, Yee L, Burtness BA, Marsh JC, Darnowski JW et al. Phase I clinical and pharmacological studies of benzylacyclouridine, a uridine phosphorylase inhibitor. Clin Cancer Res. 1998;4(5):1165-1175.

56. Goudgaon NM, Naguib FN, el Kouni MH, Schinazi RF. Phenylselenenyl- and phenylthio-substituted pyrimidines as inhibitors of dihydrouracil dehydrogenase and uridine phosphorylase. J Med Chem. 1993;36(26):4250-4254.

57. Al Safarjalani ON, Zhou XJ, Naguib FN, Goudgaon NM, Schinazi RF et al. Modulation of the pharmacokinetics of endogenous plasma uridine by 5-(phenylthio)acyclouridine, a uridine pshophorylase inhibitor: implications for chemetherapy. Cancer Chemother Pharmacol. 2001;48():145-150.

58. Al Safarjalani ON, Zhou XJ, Naguib FN, Goudgaon NM, Schinazi RF et al. Enhancement of the bioavailability of oral uridine by coadministration of 5-(phenylthio)acyclouridine, a uridine phosphorylase inhibitor: implications for uridine rescue regimens in chemotherapy. Cancer Pharmacol Chemother. 2001;48():389-397.

59. Al Safarjalani ON, Zhou XJ, Rais RH, Shi J, Schinazi RF et al. 5-(phenylthio)acyclouridine: a powerful enhancer of oral uridine bioavailability: relevance to chemotherapy with 5-fluorouracil and other uridine rescue regimens. Cancer Pharmacol Chemother. 2005;55():541-551.

60. Copeland RA. Evaluation of enzyme inhibitors in drug discovery: A guide for medicinal chemists and pharmacologists. 1ª edição. 2005.

61. Schramm VL. Enzymatic transition states and transition state analogues. Curr Opin Struct Biol. 2005;15(6):604-613.

62. Kline PC, Schramm VL. Purine nucleoside phosphorylase. Catalytic mechanism and transition-state analysis of the arsenolysis reaction. Biochemistry. 1993;32(48):13212-13219.

63. Lewandowicz A. Tight binding transition state analogues of purine nucleoside phosphorylase – meaning, design and properties. Postepy Biochem. 2004;50(3):218-227.

64. Werner RM, Stivers JT. Kinetic isotope effect studies of the reaction catalyzed by uracil DNA glycosylase: evidence for an oxacarbenium ion-uracil anion intermediate. Biochemistry. 2000;39(46):14054-14064.

65. Schwartz PA, Vetticatt MJ, Schramm VL. Transition state analysis of the arsenolytic depyrimidination of thymidine by human thymidine phosphorylase. Biochemistry. 2011;50(8):1412-1420.

66. Komissarov AA, Moltchan OK, Romanova DV, Debabov VG. Enzyme-catalyzed uridine phosphorylasis: SN2 mechanism with phosphate activation by desolvation. FEBS Lett. 1994;355(2):192-194.

67. Silva RG, Vetticatt MJ, Merino EF, Cassera MB, Schramm VL. Transition-state analysis of *Trypanosoma cruzi* uridine phosphorylase-catalyzed arsenolysis of uridine. J Am Chem Soc. 2011;133(25):9923-9931.

68. Semeraro T, Lossani A, Botta M, Ghiron C, Alvarez R et al. Simplified analogues of immicillin-G retain potente human purine nucleoside phosphorylase inhibitory activity. J Med Chem. 2006;49(20):6037-6045.

69. Clinch K, Evans GB, Fröhlich RFG, Furneaux RH, Kelly PM et al. Third-generation immucillins: syntheses and bioactivities of acyclic immucillin inhibitors of human purine nucleoside phosphorylase. J Med Chem. 2009;52(4):1126-1143.

70. Jain HV, Rasheed R, Kalman TI. The role of phosphate in the action of thymidine phosphorylase inhibitors: implications for the catalytic mechanism. Bioorg Med Chem Lett. 2010;20(5):1648-1651.

71. Robertson JG. Mechanistic basis of enzyme-targeted drugs. Biochemistry. 2005;44(15):5561-5571.

72. Rooseboom M, Commandeur JNM, Vermuelen NPE. Enzyme-catalyzed activation of anticancer prodrugs. Pharmacol Rev. 2004;56(1):53-102.

73. Huang PS, Oliff A. Drug-targeting strategies in cancer therapy. Curr Opin Genet Dev. 2001;11(1):104–110.

74. Stavrovskaya AA. Cellular mechanisms of multidrug resistance of tumor cells. Biochemistry (Mosc). 2000;65(1):95–106.

75. Chodera JD, Mobley DL. Entropy-enthalpy compensation: role and ramifications in biomolecular ligand recognition and design. Annu Rev Biophys. 2013;42():121-142.

ANEXOS

ANEXO A – Artigo publicado “The kinetic mechanism of human uridine phosphorylase 1: Towards the development of enzyme inhibitors for cancer chemotherapy”

ANEXO B – Carta de Aprovação do Comitê de Ética para o Uso de Animais

ANEXO C – Patente

ANEXO D – Carta de submissão do manuscrito do Capítulo 3

ANEXO E – Artigo publicado “Analysis of select members of the E26 (ETS) transcription factors family in colorectal cancer”

ANEXO A

The kinetic mechanism of human uridine phosphorylase 1: Towards the development of enzyme inhibitors for cancer chemotherapy

Daiana Renck, Rodrigo G. Ducati, Mario S. Palma, Diógenes S. Santos, Luiz A. Basso.

Artigo publicado
Archives of Biochestry and Biophysics, 2010, 497: 35-42

Archives of Biochemistry and Biophysics 497 (2010) 35–42

Contents lists available at ScienceDirect

Archives of Biochemistry and Biophysics

journal homepage: www.elsevier.com/locate/yabbi

The kinetic mechanism of human uridine phosphorylase 1: Towards the development of enzyme inhibitors for cancer chemotherapy ☆

Daiana Renck [a,b], Rodrigo G. Ducati [a], Mario S. Palma [c], Diógenes S. Santos [a,b,*], Luiz A. Basso [a,b,**]

[a] Centro de Pesquisas em Biologia Molecular e Funcional (CPBMF), Instituto Nacional de Ciência e Tecnologia em Tuberculose (INCT-TB), Pontifícia Universidade Católica do Rio Grande do Sul (PUCRS), 6681/92-A Av. Ipiranga, 90619-900 Porto Alegre, RS, Brazil
[b] Programa de Pós-Graduação em Biologia Celular e Molecular, Pontifícia Universidade Católica do Rio Grande do Sul (PUCRS), Porto Alegre, RS, Brazil
[c] Laboratório de Biologia Estrutural e Zooquímica, Centro de Estudos de Insetos Sociais, Departamento de Biologia, Instituto de Biociências de Rio Claro, Universidade Estadual Paulista (UNESP), Rio Claro, SP, Brazil

ARTICLE INFO

Article history:
Received 18 January 2010
and in revised form 5 March 2010
Available online 11 March 2010

Keywords:
Cancer chemotherapy
Initial velocity
Product inhibition
Fluorescence spectroscopy
pH-rate profiles
Uridine phosphorylase kinetic mechanism

ABSTRACT

Uridine phosphorylase (UP) is a key enzyme in the pyrimidine salvage pathway, catalyzing the reversible phosphorolysis of uridine to uracil and ribose-1-phosphate (R1P). The human UP type 1 (hUP1) is a molecular target for the design of inhibitors intended to boost endogenous uridine levels to rescue normal tissues from the toxicity of fluoropyrimidine nucleoside chemotherapeutic agents, such as capecitabine and 5-fluorouracil. Here, we describe a method to obtain homogeneous recombinant hUP1, and present initial velocity, product inhibition, and equilibrium binding data. These results suggest that hUP1 catalyzes uridine phosphorolysis by a steady-state ordered bi bi kinetic mechanism, in which inorganic phosphate binds first followed by the binding of uridine, and uracil dissociates first, followed by R1P release. Fluorescence titration at equilibrium showed cooperative binding of either P_i or R1P binding to hUP1. Amino acid residues involved in either catalysis or substrate binding were proposed based on pH-rate profiles.

Pyrimidine nucleoside phosphorylases are key enzymes in the pyrimidine salvage pathway. Two types of enzymes have been identified in human cells: uridine phosphorylase (UP[1]; EC 2.4.2.3) and thymidine phosphorylase (EC 2.4.2.4) [1–3]. UP belongs to the nucleoside phosphorylase (NP) super-family of proteins, in the NP-1 subset [4], and plays an important role in nucleoside metabolism, catalyzing the phosphorolysis of uridine (Urd) to uracil and ribose-1-phosphate (R1P) (Fig. 1). These products can be further utilized for nucleoside synthesis [5,6]. In humans, there are two isoforms of UP, hUP1 [3] and hUP2 [2], which are encoded by two different genes in distinct chromosomes. The alignment of the isoforms showed that they share approximately 60% amino acid sequence identity [2]. The hUP1 cDNA contains an open reading frame coding for a sequence of 310 amino acid residues corresponding to a protein with a subunit molecular mass of 33.9 kDa that is dimeric in solution [3,7], which is in contrast to the hexameric *Escherichia coli* enzyme [8,9].

Although UP is present in most normal and tumoral tissues, its activity as well as its expression is elevated in certain tumors, a feature that may contribute to selectivity of chemotherapeutic agents [3,10–12]. Studies have shown that this expression can be up-regulated by treating tumor cells with cytokines such as interferon-α, interferon-γ, tumor necrosis factor-α, and interleukin-1α [3,13]. RT-PCR analysis demonstrated that basic fibroblast growth factor (bFGF) increases the expression level of mouse UP1 in osteolineage cell lines; the induction by bFGF is dependent of NFκB activity [14]. In addition, it has been shown that tumor-associated chromosomal translocation in Ewing's family tumors, where the N-terminus of Ewing's sarcoma (EWS) gene fuses with the C-terminus of some ETS transcription factors, up-regulates UP promoter

☆ This work was supported by the National Institute of Science and Technology on Tuberculosis (DECIT/SCTIE/MS-MCT-CNPq-FNDCT-CAPES) and the Millennium Initiative Program (CNPq) to D.S.S. and L.A.B. D.S.S. (CNPq, 304051/1975-06), L.A.B. (CNPq, 520182/99-5), and M.S.P. (CNPq, 500079/90-0) are Research Career Awardees of the National Research Council of Brazil (CNPq). R.G.D. is a post-doctoral fellow of CNPq. D.R. is recipient of an MSc scholarship awarded by BNDES.

* Corresponding author. Fax: +55 51 33203629.
** Corresponding author at: Centro de Pesquisas em Biologia Molecular e Funcional (CPBMF), Instituto Nacional de Ciência e Tecnologia em Tuberculose (INCT-TB), Pontifícia Universidade Católica do Rio Grande do Sul (PUCRS), 6681/92-A Av. Ipiranga, 90619-900 Porto Alegre, RS, Brazil. Fax: +55 51 33203629.
E-mail addresses: diogenes@pucrs.br (D.S. Santos), luiz.basso@pucrs.br (L.A. Basso).

[1] *Abbreviations used*: Arg, arginine; BAU, 5-benzylacyclouridine; CV, column volume; bFGF, basic fibroblast growth factor; ESI-MS, electrospray ionization mass spectrometry; EWS, Ewing's sarcomas; 5-FU, 5-fluorouracil; FUrd, fluorouridine; FUMP, fluorouridine monophosphate; FUDP, fluorouridine diphosphate; FUTP, fluorouridine triphosphate; FdUrd, fluorodeoxyuridine; FdUMP, fluorodeoxyuridine monophosphate; FdUDP, fluorodeoxyuridine diphosphate; FdUTP, fluorodeoxyuridine triphosphate; Hepes, *N*-2-hydroxyethylpiperazyne-*N*′-2-ethanesulfonic acid; His, histidine; hUP1, human uridine phosphorylase 1; IPTG, isopropyl-β-D-thiogalactopyranoside; LB, Luria–Bertani; NP, nucleoside phosphorylase; OPRT, orotate phosphoribosyltransferase; P_i, inorganic phosphate; PNP, purine nucleoside phosphorylase; R1P, ribose-1-phosphate; SDS-PAGE, sodium dodecyl sulfate-polyacrylamide gel eletrophoresis; TB, terrific broth; TK, thymidine kinase; TP, thymidine phosphorylase; Tris, tris(hydroxymethyl)aminomethane; Urd, uridine; UK, uridine kinase; UP, uridine phosphorylase.

0003-9861/$ - see front matter © 2010 Elsevier Inc. All rights reserved.
doi:10.1016/j.abb.2010.03.004

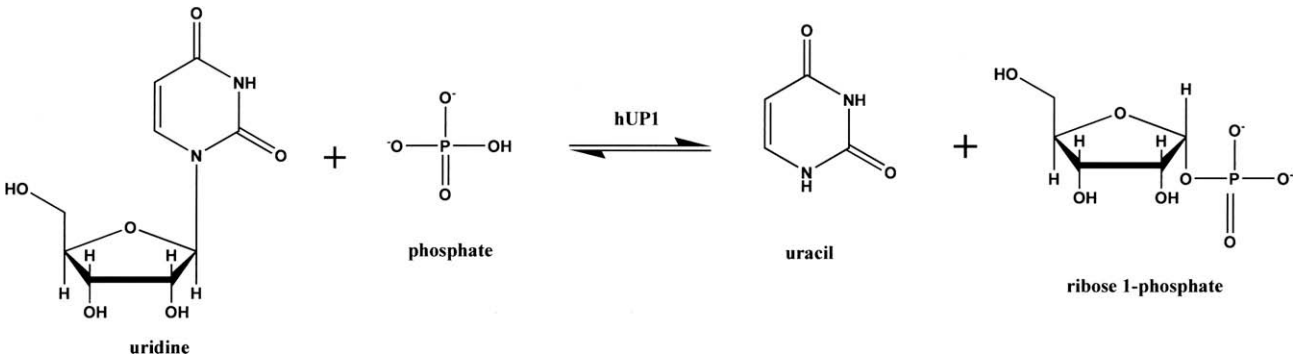

Fig. 1. Chemical reaction catalyzed by hUP1.

in vivo, suggesting that UP could be a direct target of EWS/ETS fusion proteins [15,16]. In contrast, the activity and gene promoter levels of UP have been shown to be down-regulated by wild-type p53, a tumor suppressor gene that plays a key role in cell growth control, DNA damage repair, and apoptosis [1,17].

UP plays an important role in the homeostatic regulation of Urd concentration in plasma (1–5 μM) and tissues, and affects activation and catabolism of several nucleoside analogues used in cancer chemotherapy [2]. These analogues include fluoropyrimidines, such as 5-fluorouracil (5-FU) [1,8], which is a uracil analogue with a fluorine atom at the C-5 position. This compound was developed in 1957 [18] after the observation that rat tumoral tissues use uracil more rapidly than normal tissues, which indicated that uracil metabolism is a potential target for chemotherapy [8]. Since then, 5-FU has been used in clinical practice against many types of solid tumors; yet, most of its use is related to colorectal cancer [8,19]. 5-FU is converted to fluorodeoxyuridine monophosphate (FdUMP), fluorodeoxyuridine triphosphate (FdUTP), and fluorouridine triphosphate (FUTP), the three main active metabolites. The main mechanism of 5-FU activation is either directly by orotate phosphoribosyltransferase (OPRT), or indirectly by the sequential action of UP converting 5-FU to fluorouridine (FUrd) which, in turn, is converted to fluorouridine monophosphate (FUMP) by uridine kinase (UK) [8,14]. FUMP is phosphorylated to fluorouridine diphosphate (FUDP), which can be either phosphorylated to FUTP or converted by ribonucleotide reductase into fluorodeoxyuridine diphosphate (FdUDP) [8]. The latter, in turn, can either be phosphorylated to FdUTP or dephosphorylated to FdUMP, both of which are active metabolites. There is also an alternative pathway that involves conversion of 5-FU to fluorodeoxyuridine (FdUrd) by thymidine phosphorylase (TP), and conversion of FdUrd to FdUMP by thymidine kinase (TK). The main metabolites of 5-FU exert their anti-cancer activity either by disrupting RNA synthesis (FUTP), or inhibiting thymidylate synthase (TS) enzyme activity (FdUMP) that converts dUMP to deoxythymidine monophosphate (dTMP), which is needed for DNA synthesis and repair. In addition, inhibition of TS by FdUMP results in accumulation of dUMP leading to increased levels of dUTP. The latter and the 5-FU metabolite FdUMP can be misincorporated into DNA. Clinical evidences have demonstrated the ability of Urd to reduce bone marrow and gastrointestinal toxicity induced by 5-FU, called "*rescue of* 5-*FU* toxicity" [2,6,10,20]. High doses of uridine are required to produce the "rescue" effect due to the short half-life of plasma uridine of only 2 min and the regulation of plasma uridine homeostasis at the 2–4 μM level by the activity of hepatic UP [6,10]. However, these high doses needed to produce this effect are not well tolerated and produce dose-limiting effect in humans. It is thus necessary to develop a drug capable of maintaining elevated endogenous levels of Urd [6,7,10] to protect the normal tissues through Urd rescue effect. Accordingly, inhibition of UP activity appears an attractive therapeutic strategy to rescue 5-FU toxicity. Acyclouridine analogues, including 5-benzylacyclouridine (BAU), have been designed as hUP1 inhibitors, and BAU has been shown in clinical trials to be capable of increasing plasma Urd concentration, thereby increasing the therapeutic index of 5-FU [7].

Enzyme inhibitors make up roughly 25% of the drugs marketed in United States [21]. Enzymes catalyze multistep chemical reactions to achieve rate accelerations by stabilization of the transition-state structure [22]. Accordingly, mechanistic analysis (kinetic, chemical, and catalytic mechanisms) should always be a top priority for enzyme-targeted drug programs aiming at the rational design of potent enzyme inhibitors. Here we describe amplification, cloning, and sequencing of the recombinant hUP1 coding gene. We also present heterologous protein expression in *E. coli*, purification to homogeneity, N-terminal amino acid sequencing, electrospray ionization mass spectrometry analysis, determination of true steady-state kinetic parameters, product inhibition, equilibrium fluorescence of substrate/product binding, and pH-rate profiles of functional recombinant hUP1 enzyme. These results provide a solid foundation on which to base function-guided hUP1 enzyme inhibitors with potential anti-cancer activity.

Materials and methods

Amplification and cloning of the human UPP1 gene

The human *UPP*1 coding sequence was searched on the GeneBank (BC007348) of the National Institute for Biotechnology Information (http://www.ncbi.nlm.nhi.gov).

The cDNA of *UPP*1 was obtained by RT-PCR amplification of colorectal RNA (from Ambion; Austin, TX, USA). The oligonucleotide primers used (forward primer, 5′-CAGTTGGCCATATGGCGGC CACGGGAGC-3′; and reverse primer, 5′-GCGGAGAAGCTTGGCAGC GCTCAGGCC-3′) contained, respectively, *Nde*I and *Hin*dIII (New England Biolabs) restriction sites (underlined). The PCR product was analyzed on 1% agarose gel, and a 930-bp band was detected and purified. The DNA fragment was cloned into pCR-Blunt cloning vector (Invitrogen), cleaved with *Nde*I and *Hin*dIII restriction enzymes, and subcloned into the pET-23a(+) expression vector (Novagen). The complete *UPP*1 gene sequence was determined by automated DNA sequencing to confirm sequence integrity and the absence of mutations in the cloned fragment.

Expression and purification of recombinant hUP1

The pET-23a(+)::*UPP*1 recombinant plasmid was transformed into *E. coli* Rosetta (DE3) competent cells (Novagen) and selected on Luria–Bertani (LB) agar plates containing 50 μg mL^{-1} ampicillin and 34 μg mL^{-1} cloranfenicol. A single colony was grown overnight

in LB medium pH 7.2 (60 mL) containing the same antibiotics, at 37 °C. An aliquot of this culture (10 mL) was used to inoculate terrific broth (TB) medium (2.5 L, with the same antibiotics) and grown for 36 h at 30 °C after reaching an $OD_{600\ nm}$ of 0.4–0.6, without isopropyl-β-D-thiogalactopyranoside (IPTG) induction. The same procedure was employed for *E. coli* Rosetta (DE3) cells transformed with pET-23a(+) (control). The cells (40 g) were harvested by centrifugation at 11,800*g* for 30 min at 4 °C and stored at −20 °C. Soluble protein expression was analyzed by 12% sodium dodecyl sulfate–polyacrylamide gel eletrophoresis (SDS–PAGE) stained with Coomassie Brilliant Blue [23].

All purification steps were performed at 4 °C and sample elution was monitored by UV detection. Frozen cells (5 g) were suspended in 25 mL of 50 mM *N*-2-hydroxyethylpiperazyne-*N*′-2-ethanesulfonic acid (Hepes) pH 7.0 (buffer A) and incubated with 0.2 mg mL^{-1} lysozyme (Sigma) for 30 min. The cells were disrupted by sonication (five pulses of 10 s) and the solution was cleared by centrifugation at 48,000*g* for 30 min. The supernatant was treated with 1% (wt/vol) streptomycin sulfate (Sigma; final concentration) for 30 min to precipitate the nucleic acids, and centrifuged (48,000*g* for 30 min). The supernatant was dialyzed against buffer A (2 × 2 L, 3 h each). Residual precipitate was removed by centrifugation (48,000*g* for 30 min) and the supernatant was loaded onto an SP Sepharose Fast Flow cation exchange column (GE Healthcare) pre-equilibrated with buffer A. The column was washed with five column volumes (CV) of buffer A and the adsorbed material was eluted with 15 CV linear gradient (0–100%) of 50 mM Hepes 200 mM NaCl pH 7.0 (buffer B) at a 1 mL min^{-1} flow rate. The target recombinant protein was eluted at approximately half of the gradient, where a single SDS–PAGE band could be observed. The homogenous recombinant protein was dialyzed against 100 mM tris(Hydroxymethyl)aminomethane (Tris) pH 7.4 (3 × 2 L, 3 h each), concentrated, and stored at −80 °C. Protein concentration was determined with Bradford Protein Assay Kit (Bio-Rad Laboratories) and bovine serum albumin was used as standard [24]. All subsequent activity and binding assays were performed in 100 Tris pH 7.4, unless stated otherwise.

Amino acid sequence and mass spectrometry analysis

The N-terminal amino acid sequence of homogeneous recombinant hUP1 protein was analyzed by automated Edman degradation sequencing using a gas-phase sequencer PPSQ-21 A (Shimadzu) [25].

hUP1 was assessed by electrospray ionization mass spectrometry (ESI-MS) according to Chassaigne and Lobinski, with some adaptations [26]. The sample was analyzed on Quattro-II triple-quadrupole mass spectrometer (Micromass; Altrincham, UK). During all experiments, the source temperature was maintained at −80 °C and the capillary voltage at 3.6 kV; a drying nitrogen gas flow (200 L h^{-1}) and a nebulizer gas flow (20 L h^{-1}) were used. Intact horse heart myoglobin was used to calibrate the mass spectrometer and its typical cone voltage-induced fragments. hUP1 subunit molecular mass was determined by adjusting the mass spectrometer to yield a peak with a half-height of one mass unit, and the sampling cone-to-skimmer lens voltage controlling the transfer of ions to the mass analyzer was set to 38 V. Approximately 50 pmol of each sample were injected into the electrospray transport solvent. The ESI spectrum was obtained in the multichannel acquisition mode, with scanning from 500 to 1,800 *m*/*z* at a scan time of 7 s. The mass spectrometer is equipped with MassLynx and Transform softwares for data acquisition and spectrum handling.

hUP1 enzymatic assay

Recombinant hUP1 enzyme activity was monitored in an UV-2550 UV/Visible spectrophotometer (Shimadzu). All assays were performed under initial rate conditions at 37 °C and 100 mM Tris pH 7.4, in 500 μL total reaction volumes for 60 s. This assay was based on the maximum difference in absorbance at 280 nm between Urd and uracil (ΔA = 2100 M^{-1} cm^{-1}), in which a decrease in absorbance is observed upon conversion of Urd to uracil [27]. One unit (U) of enzyme activity was defined as the amount of enzyme that catalyses the formation of 1 μmol of product per min.

Initial velocity measurements

Initial velocity studies were carried out to determine the true steady-state kinetic parameters, in the forward direction. Saturation curves were performed varying concentrations of Urd (20–500 μM) against several fixed-varying concentrations of inorganic phosphate (P_i) (1–10 mM).

Product inhibition patterns

To provide an additional experimental approach to distinguish between the possible kinetic mechanisms, product inhibition studies were carried out at varying concentrations of one substrate, fixed concentrations of the co-substrate (in nonsaturating levels), and fixed-varying concentrations of products (either R1P or uracil). The experimental conditions were as follows: varying Urd concentrations (20–500 μM), fixed P_i concentration (2 mM), and fixed-varying concentrations of either uracil (50–600 μM) or R1P (24–160 μM); varying P_i concentrations (1–10 mM), fixed Urd concentration (50 μM), and fixed-varying concentrations of either uracil (50–300 μM) or R1P (80–320 μM).

Equilibrium binding by fluorescence spectroscopy

Fluorescence measurements were carried out in an RF-5301 PC Spectrofluorophotometer (Shimadzu) at 25 °C. Measurements of intrinsic hUP1 protein fluorescence employed excitation wavelength at 280 nm in each binding experiment, and the emission wavelength ranged from 285 to 350 nm. The slits for excitation and emission were both 3 nm. Fluorescence titrations of binary complex formation were carried out by making microliter additions of the following compounds to 2 mL containing 10 μM hUP1: 40 mM P_i stock solution (19.99–434.2 μM final concentration); 5 mM Urd stock solution (2.498–97.92 μM final concentration); 10 mM uracil stock solution (4.997–123.3 μM final concentration); 4 mM R1P stock solution (1.99–41.53 μM final concentration). Control experiments were employed to both determine the maximum ligand concentrations to be used with no inner filter effect and to account for any dilution effect on protein fluorescence.

pH-rate profiles

To determine the dependence of the kinetic parameters on pH, initial velocities were measured in the presence of varying concentrations of one substrate and a saturating level of the other in a buffer mixture of 2-(*N*-morpholino)ethanesulfonic acid /Hepes/2-(*N*-cyclohexylamino)ethanesulfonic acid over the following pH values: 5.0, 5.5, 6.0, 6.5, 7.0, 7.5, 8.0, 8.5, and 9.0 [28]. The data were plotted as pH values versus either log k_{cat} or log k_{cat}/K_M. As the K_M values changed as a function of pH, different concentration ranges of the variable substrate as well as the fixed substrate had to be employed. For varying Urd concentrations the experimental conditions were: at pH 5.0: P_i = 20 mM, 200 μM ⩽ Urd ⩽ 900 μM; at pH 5.5: P_i = 20 mM, 100 μM ⩽ Urd ⩽ 800 μM; at pH 6.0: P_i = 12 mM, 20 μM ⩽ Urd ⩽ 800 μM; at pH 6.5: P_i = 10 mM, 20 μM ⩽ Urd ⩽ 700 μM; at pH 7.0 and 7.5: P_i = 10 mM, 20 μM ⩽ Urd ⩽ 500 μM; at pH 8.0: P_i = 10 mM, 20 μM ⩽ Urd ⩽ 700 μM; at pH 8.5: P_i = 10 mM, 20 μM ⩽ Urd ⩽ 600 μM; and at pH 9.0: P_i = 10 mM, 20 μM ⩽ Urd ⩽ 800 μM. For

varying P_i concentrations the experimental ranges employed were as follows: at pH 5.0: Urd = 800 μM, 2 mM ⩽ P_i ⩽ 20 mM; at pH 5.5: Urd = 700 μM, 2 mM ⩽ P_i ⩽ 16 mM; at pH 6.0: Urd = 700 μM, 0.5 mM ⩽ P_i ⩽ 8 mM; at pH 6.5: Urd = 600 μM, 0.05 mM ⩽ P_i ⩽ 8 mM; at pH 7.0 and 7.5: Urd = 500 μM, 0.1 mM ⩽ P_i ⩽ 8 mM; at pH 8.0: Urd = 600 μM, 0.1 mM ⩽ P_i ⩽ 8 mM; at pH 8.5: Urd = 500 μM, 0.05 mM ⩽ P_i ⩽ 5 mM; and at pH 9.0: Urd = 700 μM, 0.05 mM ⩽ P_i ⩽ 5 mM.

Results and discussion

Amplification, cloning, and DNA sequencing

The PCR amplification protocol yielded a product with an expected size corresponding to the human *UPP*1 (930-bp) DNA coding sequence (data not shown). The fragment was purified from the agarose gel and ligated into the pET-23a(+) expression vector. Nucleotide sequence analysis confirmed both identity and integrity of human *UPP*1 DNA coding sequence.

Expression of recombinant hUP1 protein

The pET-23a(+)::*UPP*1 recombinant plasmid was transformed into *E. coli* Rosetta (DE3) host cells by electroporation. Analysis by SDS–PAGE (Fig. 2) showed that the cell extracts contained the recombinant protein, in the insoluble and soluble fraction, with an apparent molecular mass of 33 kDa, in agreement with the expected size of 33.934 kDa for hUP1. Among a number of protocols tested, the best experimental condition for expression of recombinant hUP1 occurred with *E. coli* Rosetta (DE3) cells grown for 36 h (after reaching an $OD_{600\ nm}$ of 0.4–0.6, without IPTG induction) at 30 °C in TB medium. The pET expression vector system (Novagen) has a strong IPTG-inducible bacteriophage T7 *lacUV5* late promoter that controls the T7 RNA polymerase to transcribe cloned target genes [29]. It has been shown that *lac*-controlled systems could have high-levels of protein expression in the absence of inducer [30,31]. It has been proposed that leaky protein expression is due to derepression of the *lac*-controlled system when cells approach stationary phase in complex medium and that cyclic AMP, acetate, and low pH are required to achieve high-level expression in the absence of IPTG induction, which may be part of a general cellular response to nutrition limitation [32]. However, more recently, it has been shown that unintended induction in the pET system is due to the presence of as little as 0.0001% of lactose in the medium [33]. It is noteworthy that a large amount of recombinant hUP1 protein remained in the insoluble fraction (Fig. 2, lane 3). Although inclusion body formation can greatly simplify protein purification, there is no guarantee that the *in vitro* refolding will yield large amounts of biologically active protein. Moreover, inclusion body purification schemes present a number of problems such as: use of denaturants that are expensive and can cause irreversible modifications of protein structure that will elude all of the most sophisticated analytical tests, refolding usually must be done in very dilute solution and the protein reconcentrated, and refolding encourages protein isomerization leading to precipitation during storage [34]. Since we aimed at determining the mode of action of recombinant hUP1 enzyme, we deemed more appropriate to avoid solubilizing agents.

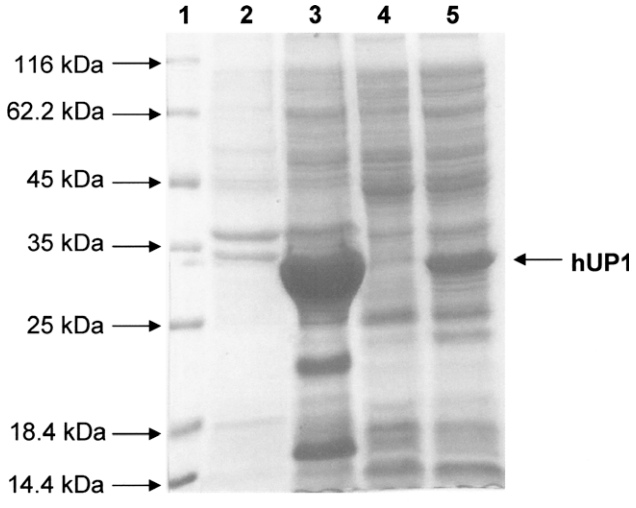

Fig. 2. The 12% SDS–PAGE analysis of total insoluble and soluble proteins. Expression of hUP1 after 36 h of cell growth after reaching an $OD_{600\ nm}$ of 0.4–0.6 in TB medium without addition of IPTG. Lane 1, Protein Molecular Weight Marker (Fermentas); lane 2, insoluble *E. coli* Rosetta (DE3) [pET-23a(+) (control)] extract; lane 3, insoluble *E. coli* Rosetta (DE3) [pET-23a(+)::*UPP*1] extract; lane 4, soluble *E. coli* Rosetta (DE3) [pET-23a(+) (control)] extract; lane 5, soluble *E. coli* Rosetta (DE3) [pET-23a(+)::*UPP*1] extract.

Purification of recombinant hUP1 protein

Recombinant hUP1 protein was efficiently purified to homogeneity (Fig. 3) by a single-step purification protocol, using a cation exchange column. The target protein eluted at approximately 50% of buffer B. The 3.8-fold purification protocol resulted in a protein yield of 43% and 20.8 mg of active recombinant hUP1 protein from 5 g of cells (Table 1). In contrast to Roosild et al. [7], we found no need to add potassium salt in the purification buffers to prevent protein aggregation and precipitation. The homogeneous protein was stored at −80 °C, with no loss of activity.

Mass spectrometry and N-terminal amino acid sequencing

The subunit molecular mass value for hUP1 was determined to be 33,934.00 Da by electrospray ionization mass spectrometry (ESI-MS). Since the predicted molecular mass is 33,934.00 Da, this result indicates removal of the N-terminal methionine (predicted methionine molecular mass = 131.20 Da). These results provide evidence that confirm the identity of recombinant hUP1.

The Edman degradation method identified the first 21 N-terminal amino acid residues of the recombinant hUP1 as: AATGANAEKAESHNDCPVRLL. This result unambiguously demonstrates that the purified protein is hUP1, and confirms the removal of the N-terminal methionine. Protein N-terminal methionine excision is a common type of post-translational modification process that occurs in the cytoplasm of many organisms displaying protein synthesis. The cleavage of the initiator methionine is usually directed by the penultimate amino acid residues with the smallest side chain radii of gyration (Gly, Ala, Ser, Thr, Pro, Val, and Cys) [35], which is in agreement with removal of the N-terminal methionine

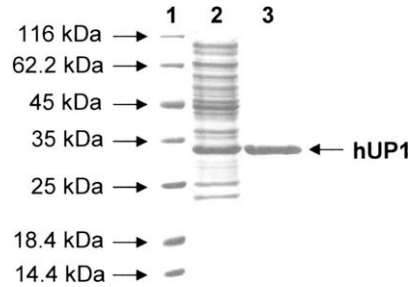

Fig. 3. The 12% SDS–PAGE analysis of pooled fractions from hUP1 purification steps. Lane 1, Protein Molecular Weight Marker (Fermentas); lane 2, crude extract; lane 3, SP Sepharose Fast Flow cation exchange elution.

Table 1
Purification of hUP1 from *E. coli* Rosetta (DE3). Typical purification protocol from 5 g wet cell paste (300 mL of culture).

Purification step	Total protein (mg)	Total enzyme activity (U)	Specific activity (U mg^{-1})	Purification fold	Yield (%)
Crude extract	180.3	367.5	2.04	1.0	100
SP Sepharose Fast Flow	20.8	159.9	7.70	3.8	43

from hUP1 since alanine is the penultimate N-terminal amino acid residue.

Initial velocity and steady-state kinetic parameters

The double-reciprocal plots for the forward reaction (phosphorolysis) showed a family of lines intersecting to the left of the *y*-axis (Fig. 4A and B), which is consistent with ternary complex formation and a sequential mechanism [36]. Ping-pong and rapid equilibrium ordered mechanisms could be ruled out, since these mechanisms display parallel lines and intersecting lines at the *y*-axis, respectively. The data were fitted to the following equation: $v = VAB/(K_{ia}K_b + K_aB + K_bA + AB)$, yielding the following true steady-state kinetic parameters: $k_{cat} = 7.5\ (\pm 0.2)\ s^{-1}$, $K_{Urd} = 51\ (\pm 4)\ \mu M$, $K_{P_i} = 2462(\pm 228)\ \mu M$, $k_{cat}/K_{Urd} = 14.7\ (\pm 1.2) \times 10^4\ M^{-1}\ s^{-1}$, and $k_{cat}/K_{P_i} = 3.05(\pm 0.28) \times 10^3\ M^{-1}\ s^{-1}$. These values are different from the apparent steady-state kinetic constants reported for human liver UP1 [10]. Although it is not possible to offer a clear explanation for these differences, here we present the true steady-state kinetic parameters whereas Liu et al. [10] presented apparent steady-state kinetic parameters.

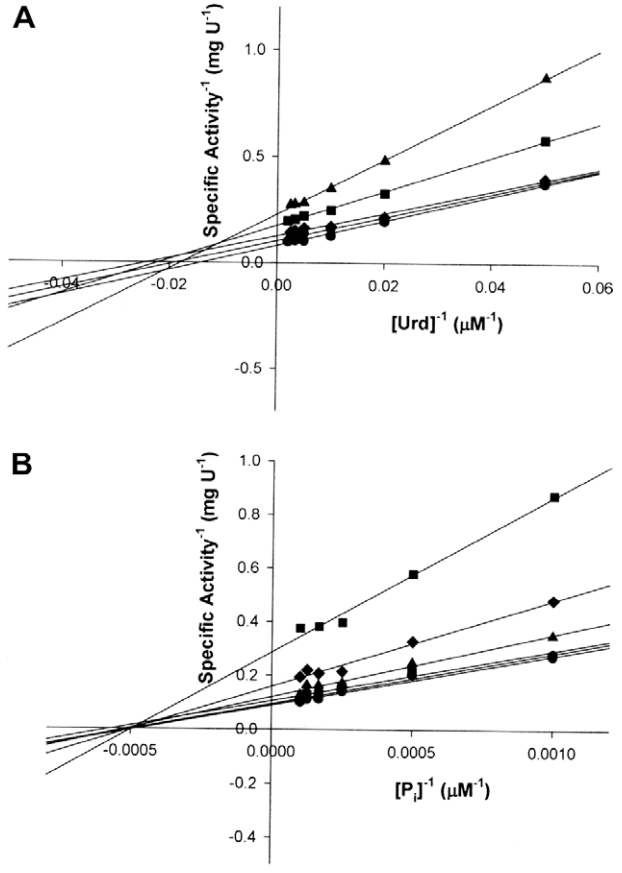

Fig. 4. Intersecting initial velocity patterns for hUP1 with either Urd (A) or P_i (B) as the variable substrate. Each curve represents fixed-varying levels of the co-substrate.

Product inhibition

The initial velocity results described above cannot distinguish between a steady-state ordered bi bi mechanism and rapid equilibrium random bi bi system. Accordingly, product (either R1P or uracil) inhibition measurements were carried out to determine the order of substrate addition to the enzyme. The data were fitted to an equation for either competitive or noncompetitive inhibition: $v = VA/[K_a(1 + I/K_{is}) + A]$ or $v = VA/[K_a(1 + I/K_{is}) + A(1 + K_{ii})]$, respectively. The double-reciprocal plots revealed a pattern of three noncompetitive and one competitive inhibition (Table 2). This pattern is in agreement with a steady-state ordered bi bi kinetic mechanism [36], in which P_i binds first to free hUP1 enzyme followed by Urd binding to form the catalytically competent ternary complex. This pattern also suggests that uracil is released first followed by R1P dissociation from the R1P–hUP1 binary complex. In addition, a steady-state random bi bi mechanism could be discarded because double-reciprocal plots were linear in initial velocity studies and the pattern of product inhibition would be noncompetitive for all substrate–product pairs. The steady-state ordered bi bi kinetic mechanism for hUP1 is in agreement with the cytoplasmic rat liver UP [19,37]. However, this mechanism is in disagreement with the random order of substrate addition for UP from both *E. coli* [38,39] and *Lactobacillus casei* [40], and in disagreement with the ordered mechanism for UP from guinea pig, in which binding of uracil precedes that of P_i [41].

Equilibrium binding of ligands to hUP1

Binding experiments were employed to confirm the order of substrate addition proposed by product inhibition for hUP1, and to reinforce the proposal of the order of product dissociation from the catalytically competent ternary complex. Intrinsic hUP1 fluorescence enhanced upon either P_i or R1P binding to free hUP1. Plots of either P_i or R1P concentration versus relative protein fluorescence variation upon binary complex formation (Fig. 5A and B) were sigmoidal, and the data were fitted to the Hill equation [42]: $F/F_{max} = A^n/(K' + A^n)$, yielding values of $K' = 106\ (\pm 56)$ mM and $n = 2.0\ (\pm 0.1)$ for P_i, and $K' = 297\ (\pm 102)\ \mu M$ and $n = 2.0\ (\pm 0.1)$ for R1P. K' represents the mean dissociation constant for hUP1:ligand binary complex formation, which is composed of interaction factors and the intrinsic dissociation constant, and n represents the total number of binding sites [36]. The value of 2 for n is in agreement with the dimeric form of hUP1 in solution demonstrated by size-exclusion chromatography and multi-angle static light scattering [7]. Positive cooperativity in the binding of P_i or R1P to hUP1 was supported by upward-curved double-reciprocal plots (insets in Fig 5A and B, respectively). No enhancement in intrinsic protein fluorescence could be detected upon binding of either uridine or uracil to free hUP1, thereby lending support to the proposed kinetic mechanism for hUP1. Interestingly, based on crystal structures of ternary complexes of *E. coli* UP either with

Table 2
Product inhibition patterns for hUP1.[a]

Variable substrate	Product inhibitor	Inhibition type[b]	K_{is} (μM)[c]	K_{ii} (μM)[d]
Uridine	Uracil	NC	50 ± 7	618 ± 119
Uridine	R1P	NC	34 ± 7	2.16 × 10^{6}[e]
P_i	Uracil	NC	137 ± 27	251 ± 20
P_i	R1P	C	494 ± 61	–

[a] At 37 °C and 100 mM Tris pH 7.4.
[b] NC = noncompetitive, C = competitive.
[c] K_{is} is the slope inhibition constant.
[d] K_{ii} is the intercept inhibition constant.
[e] This value was poorly defined due to a large SE value.

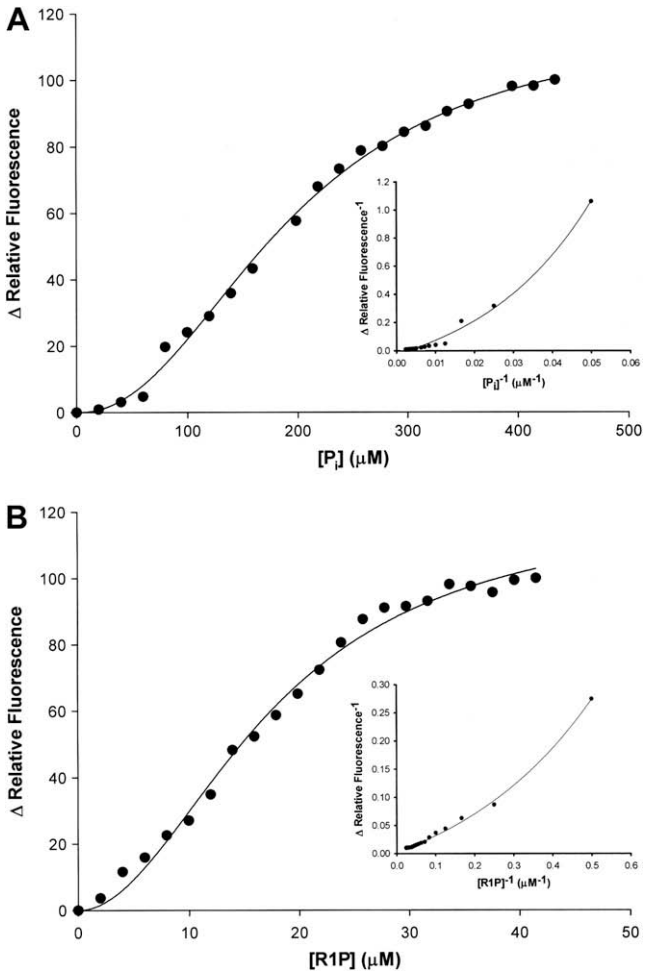

Fig. 5. Dissociation constant for hUP1 with P_i (A) and with R1P (B) binary complex formation monitoring changes in intrinsic protein fluorescence. Insets represent the fit of double-reciprocal plots of the fluorescence data to an exponential growth equation.

5-FU and R1P or FUrd and P_i, it has been proposed that there appears to be a cooperative pattern of substrate binding [18]. Our results demonstrate that there is indeed cooperativity that is brought about by P_i or R1P binding to hUP1.

The initial velocity, product inhibition, and equilibrium binding results are consistent with a steady-state ordered bi bi kinetic mechanism, in which P_i binds first to the free enzyme, followed by the binding of Urd to form the catalytically competent ternary complex, and uracil is the first product to dissociate from the complex, followed by the release of R1P (Fig. 6).

pH-rate profiles

pH dependence of the kinetic parameters was evaluated to probe acid–base catalysis in hUP1 mode of action. The bell-shaped pH-rate profiles were fitted to the following equation: $\log y = \log[C/(1 + H/K_a + K_b/H)]$, yielding K_a and K_b, respectively, the apparent acid and base dissociation constants for ionizing groups. In this equation, y represents the apparent kinetic parameter (k_{cat} or k_{cat}/K_M), C is the pH-independent plateau value of y, and H is the proton concentration. The bell-shaped pH-rate profiles showed values of 1 for the acidic limb and −1 for the basic limb, indicating participation of a single ionizable group in each limb. The data from pH 5.0–6.0 for k_{cat}/K_{P_i}, and pH 5.0 for k_{cat}/K_{Urd} were not included in the analysis, since these saturation curves were sigmoidal. It is interesting to note that, as has been pointed out in a recent review showing a timeline of evolution of allostery as a concept [43], pH is now considered an allosteric effector. At any rate, as the intracellular pH is near neutral, we deemed more appropriate to consider only the pH values that yielded hyperbolic curves to allow a more straightforward data analysis.

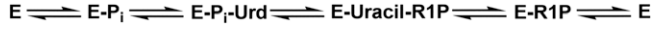

Fig. 6. Proposed kinetic mechanism for hUP1.

The pH-rate profile for k_{cat} indicates that protonation of a group with pK_a value of 5.5 (±0.6) and deprotonation of another group with pK_a value of 8.2 (±0.9) play a critical role in hUP1 enzyme catalysis (Fig. 7A). The amino acid side chain having a pK_a value of 5.5 that has to be deprotonated for efficient catalysis may tentatively be ascribed to the conserved His36 residue showed by crystallography to interact with the acyclic moiety of 5-benzylacyclouridine (BAU, an inhibitor of hUP1) [7]. In the usually predominant nonionized tautomeric form of His36, the N-3 nitrogen (ε2) with the hydrogen atom may act as an electrophile and H-bond donor, whereas N-1 nitrogen (δ1) atom may act as a nucleophile and acceptor for H-bonding. However, the position of the hydrogen atom can vary with conditions in the local environment of hUP1 active site. The conserved Tyr35 is a candidate for the residue having a pK_a value of 8.2 that has to be protonated for efficient hUP1 catalysis to occur.

The pH dependence of k_{cat}/K_{P_i} (Fig. 7B) indicates that protonation of a group and deprotonation of another group with an average pK_a value of 7.7 (± 0.8) abolish P_i binding. These data suggest that there is no pH plateau in which hUP1 would be fully in its active form as regards P_i binding. In other words, with increasing pH, before one group has been fully deprotonated to give its active form, another group required in the protonated form has started to lose its proton. Amino acid sequence comparison demonstrates conservation of three arginine residues (Arg64, Arg94, and Arg138) in hUP1. Although these residues are involved in P_i binding, the crystal structure of hUP1 has shown that Arg64 is bent away from the P_i anion in the active site, leaving two guanidinium groups (Arg94 and Arg138), one from each subunit of the dimer, to bind the substrate [7]. Based on this finding, the Arg64 residue has been suggested not to participate in P_i binding [7]. The pK_a value of the δ-guanido group of arginine in solution is usually about 12. How can one reconcile the pK_a values of 7.7 for amino acid side chains involved in P_i binding? It has been pointed out by Copeland [44] that in some cases the pK_a values that are measured cannot be correctly ascribed to a particular amino acid, but rather reflect a specific set of residue interactions within an enzyme molecule that create *in situ* a unique acid–base center. Moreover, the hydrophobic interior of enzyme active sites that undergo domain closure can greatly perturb the pK_a values of amino acid side chains relative to their typical pK_a values in aqueous solution. At any rate, site-directed mutagenesis of Arg64, Arg94, and Arg138 residues of hUP1 and crystal structure determination of these mutants will have to be carried out to ascertain the role, if any, of these residues in P_i binding.

The pH dependence of k_{cat}/K_{Urd} (Fig. 7C) indicates that protonation of group with pK_a of 6.5 (±0.6) and deprotonation of another group with pK_a of 8.4 (±0.9) abolish uridine binding. The side chains of His8 and Glu198 have been shown to be involved in *E. coli* UP ribose binding site [18], corresponding to His36 and Glu250 in hUP1. The side chain of His36 is a more likely candidate for the group with pK_a value of 6.5 that has to be deprotonated to interact with the 5′-OH group of the ribose moiety of Urd in hUP1. There are also H-bonds formed between the 2′-OH group of ribose and the main-chain nitrogen of Met197 (Met249 in hUP1) and the side chain of Arg91 (Arg138 in hUP1) [18]. As Arg138 has been shown to be involved in P_i binding in hUP1 [7], it is not likely that

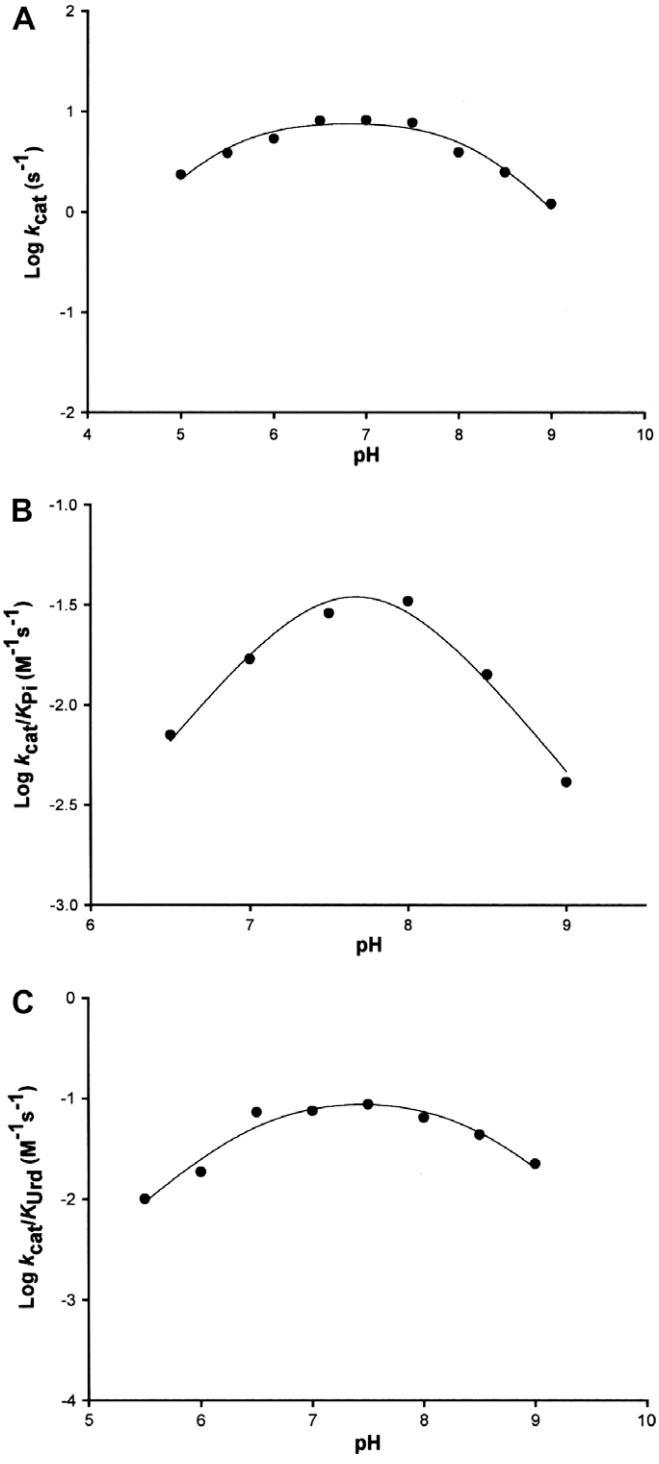

Fig. 7. pH dependence of hUP1 kinetic parameters. Plots: (A) log k_{cat}, (B) log k_{cat}/K_{P_i}, and (C) log k_{cat}/K_{Urd}.

Arg138 represents the group with pK_a of 8.4 whose deprotonation abolishes Urd binding. The crystal structure of *E. coli* UP has also shown that Gln166 and Arg168 are key residues in the uracil binding pocket and together with a tightly bound water molecule are seen to be involved in the substrate specificity of UP [18]. These residues correspond to Gln217 and Arg219 in human UP1 [7]. It is unlikely that this role is played by Gln217 because its amine side chain does not ionize. On the other hand, the δ-guanidinium group of the side chain of the conserved Arg168 amino acid in *E. coli* UP (Arg219 in hUP1) interacts with the O4 of the carbonyl group of uracil, and it has been proposed to play a role in substrate selectivity *via* an electrostatic effect [18]. It is thus tempting to assign to the guanidinium side chain of Arg219 residue the pK_a value of 8.4 that has to be protonated for Urd binding to occur. Notwithstanding, site-directed mutagenesis will have to be carried out to assign any role in substrate binding and catalysis to a particular amino acid residue in hUP1.

Summary

Here we describe an efficient method to obtain homogeneous recombinant hUP1. We also present initial velocity, product inhibition, and equilibrium binding data which show that hUP1 catalyzes the phosphorolysis of Urd by a steady-state ordered bi bi kinetic mechanism, in which P_i binds first to free enzyme, followed by the binding of Urd to form the catalytically competent ternary complex, and uracil is the first product to dissociate from the complex, followed by R1P release. Amino acid residues involved in either catalysis or substrate binding were proposed based on pH-rate profiles. A comparison between the crystal structure of free hUP1 and BAU-hUP1 binary complex showed that there is a large inter-domain motion between monomers of dimeric hUP1 [7]. These findings prompted the authors to propose that the "open" conformation of hUP1 provides an opportunity to develop a novel class of allosteric inhibitors of this enzyme that lock the protein in a functionally disabled form [7]. However, there was no experimental evidence showing that hUP1 exhibits allostery. Thermodynamic dissociation constants were assessed by the enhancement of intrinsic protein fluorescence upon P_i or R1P binding to hUP1, and the results demonstrated that these substrates exhibit cooperative binding to the enzyme. These results lend support to the proposal of designing allosteric inhibitors of hUP1 enzyme activity. It has been proposed that the conservation of key residues and interactions with substrate in the phosphate and ribose binding pockets would indicate that ribooxocarbenium ion formation during catalysis of UP may be similar to that proposed for *E. coli* purine nucleoside phosphorylase (PNP) [18]. Human PNP catalyzes the phosphorolysis of *N*-ribosidic bonds of 6-oxy-purine nucleosides and deoxynucleosides to the corresponding purine base and α-D-ribose 1-phosphate. Transition-state analogues that have picomolar inhibition constants have been developed for human PNP based on the transition-state structure for calf spleen PNP [45]. For instance, Immucillin-H possesses features of the transition state which include an elevated pK_a at the N7 position of the 9-deazahypoxanthine ring, a positive charge in the protonated iminoribitol moiety to mimic the ribooxocarbenium ion, and an enzymatically stable carbon–carbon ribosidic bond [45]. Human PNP has a later transition state and DADMe-Immucillin-H has been synthesized to be a mimicry of the proposed transition state. On the other hand, bovine PNP has an earlier transition state and Immucillin-H has been synthesized to be a mimicry of this transition state. It has been shown that DADMe-Immucillin-H binds more tightly to human PNP than Immucillin-H, thereby showing that even though bovine and human PNPs share 87% sequence identity and have totally conserved active site residues, inhibitors with differential specificity can be designed [46]. The crystal structure of human PNP in complex with Immucillin-H showing the amino acid residues that interact with this transition-state analogue has been reported [47]. Accordingly, the transition-state analogues of human PNP could serve as blueprints for the design of inhibitors of hUP1 enzyme activity. As hUP1 is a molecular target for the design of specific inhibitors intended to boost endogenous uridine levels for the purpose of rescuing normal tissues from the toxicity of fluoropyrimidine nucleoside chemotherapeutic agents, the data here

presented provide pivotal data for the design of function-based inhibitors. Understanding the mode of action of hUP1 will inform us on how to better design inhibitors targeting hUP1 with potential therapeutic application in cancer chemotherapy.

References

[1] G. Pizzorno, D. Cao, J.J. Leffert, R.L. Russel, D. Zhang, R.E. Handschumacher, Biochim. Biophys. Acta 1587 (2002) 133–144.
[2] M. Johansson, Biochem. Biophys. Res. Commun. 307 (2003) 41–46.
[3] S.I. Watanabe, T. Uchida, Biochem. Biophys. Res. Commun. 216 (1995) 265–272.
[4] M.J. Pugmire, S.E. Ealick, Biochem. J. 361 (2002) 1–25.
[5] D. Cao, J.J. Leffert, J. McCabe, B. Kim, G. Pizzorno, J. Biol. Chem. 280 (2005) 21169–21175.
[6] D. Cao, R.L. Russell, D. Zhang, J.J. Leffert, G. Pizzorno, Cancer Res. 62 (2002) 2313–2317.
[7] T.P. Roosild, S. Castronovo, M. Fabbiani, G. Pizzorno, BMC Struct. Biol. 16 (2009) 9–14.
[8] D.B. Longley, D.P. Harkin, P.G. Johnston, Nat. Rev. Cancer 3 (2003) 330–338.
[9] E.Y. Morgunova, A.M. Mikhailov, A.N. Popov, E.V. Blagova, E.A. Smirnova, B.K. Vainshtein, C. Mao, S.R. Armstrong, S.E. Ealick, A.A. Komissarov, E.V. Linkova, A.A. Burlakova, A.S. Mironov, V.G. Debabov, FEBS Lett. 367 (1995) 183–187.
[10] M. Liu, D. Cao, R. Russell, R.E. Handschumacher, G. Pizzorno, Cancer Res. 58 (1998) 5418–5424.
[11] H. Miyashita, Y. Takebayashi, J.F. Eliason, F. Fujimori, Y. Nitta, A. Sato, H. Morikawa, A. Ohashi, K. Motegi, M. Fukumoto, S. Mori, T. Uchida, Cancer 94 (2002) 2959–2966.
[12] T.A. Krenitsky, M. Barclay, J.A. Jacquez, J. Biol. Chem. 239 (1964) 805–812.
[13] D. Cao, M.A. Nimmakayalu, F. Wang, D. Zhang, R.E. Handschumacher, P. Bray-Ward, G. Pizzorno, Cancer Res. 59 (1999) 4997–5001.
[14] Y. Im, H.K. Shin, H. Kim, S. Jeong, S. Kim, Y. Kim, D.H. Lee, S. Jeon, H. Lee, J. Choi, Mol. Cells 28 (2009) 119–124.
[15] B. Deneen, H. Hamidi, C.T. Denny, Cancer Res. 63 (2003) 4268–4274.
[16] A. Arvand, C.T. Denny, Oncogene 20 (2001) 5747–5754.
[17] D. Zhang, D. Cao, R. Russell, G. Pizzorno, Cancer Res. 61 (2001) 6899–6905.
[18] T.T. Caradoc-Davies, S.M. Cutfield, I.L. Lamont, J.F. Cutfield, J. Mol. Biol. 337 (2004) 337–354.
[19] R. Bose, E.W. Yamada, Biochemistry 13 (1974) 2051–2056.
[20] G.P. Connolly, J.A. Duley, Trends Pharmacol. Sci. 20 (1999) 218–225.
[21] J.G. Robertson, Biochemistry 44 (2005) 5561–5571.
[22] J.G. Robertson, Curr. Opin. Struct. Biol. 17 (2007) 674–679.
[23] U.K. Laemmli, Nature 227 (1970) 680–685.
[24] M.M. Bradford, Anal. Biochem. 72 (1976) 248–254.
[25] B.M. de Souza, M.S. Palma, Biochim. Biophys. Acta 1778 (2008) 2797–2805.
[26] H. Chassaigne, R. Lobinski, Analyst 123 (1998) 2125–2130.
[27] G. Magni, Methods Enzymol. 51 (1978) 290–296.
[28] P.F. Cook, W.W. Cleland, Enzyme Kinetics and Mechanisms, Garland Science, London, New York, 2007.
[29] K.C. Kelley, K.J. Huestis, D.A. Austen, C.T. Sanderson, M.A. Donohue, S.K. Stickel, E.S. Kawasaki, M.S. Osburne, Gene 156 (1995) 33–36.
[30] C. Rizzi, J. Frazzon, F. Ely, P.G. Weber, I.O. Fonseca, M. Gallas, J.S. Oliveira, M.A. Mendes, B.M. Souza, M.S. Palma, D.S. Santos, L.A. Basso, Protein Expr. Purif. 40 (2005) 23–30.
[31] R.G. Silva, L.P. Carvalho, J.S. Oliveira, C.A. Pinto, M.A. Mendes, M.S. Palma, L.A. Basso, D.S. Santos, Protein Exp. Purif. 27 (2003) 158–164.
[32] T.H. Grossman, E.S. Kawasaki, S.R. Punreddy, M.S. Osburne, Gene 209 (1998) 95–103.
[33] F.W. Studier, Protein Expr. Purif. 41 (2005) 207–234.
[34] C.H. Schein, Biotechnology 7 (1989) 1141–1149.
[35] P.H. Hirel, M.J. Schmitter, P. Dessen, G. Fayat, S. Blanquet, Proc. Natl. Acad. Sci. 86 (1989) 8247–8251.
[36] I.H. Segel, Enzyme Kinetics, Behavior and Analysis of Rapid Equilibrium and Steady-state Enzyme Systems, John Wiley and Sons, Inc., New York, 1975.
[37] A. Kraut, E.W. Yamada, J. Biol. Chem. 246 (1971) 2021–2030.
[38] T.A. Krenitsky, Biochim. Biophys. Acta 429 (1976) 352–358.
[39] A. Vita, C.Y. Huang, G. Magni, Arch. Biochem. Biophys. 226 (1983) 687–692.
[40] Y. Avraham, N. Grossovicz, J. Yashphe, Biochem. Biophys. Acta 1040 (1990) 287–293.
[41] T.A. Krenitsky, J. Biol. Chem. 243 (1968) 2871–2875.
[42] A.V. Hill, Biochem. J. 7 (1913) 471–480.
[43] N.M. Goodey, S.J. Benkovic, Nat. Chem. Biol. 4 (2008) 474–482.
[44] R.A. Copeland, Enzymes: A Practical Introduction to Structure, Mechanism, and Data Analysis, Wiley-VCH, New York, 2000.
[45] V.L. Schramm, Arch. Biochem. Biophys. 433 (2005) 13–26.
[46] E.A. Taylor Ringia, P.C. Tyler, G.B. Evans, R.H. Furneaux, A.S. Murkin, V.L. Schramm, J. Am. Chem. Soc. 128 (2006) 7126–7127.
[47] W.F. Azevedo Jr., F. Canduri, D.M. Santos, J.H. Pereira, M.V. Dias, R.G. Silva, M.A. Mendes, L.A. Basso, M.S. Palma, D.S. Santos, Biochem. Biophys. Res. Commun. 309 (2003) 917–922.

ANEXO B

Carta de Aprovação da Comissão de Ética para o Uso de Animais

Pontifícia Universidade Católica do Rio Grande do Sul
PRÓ-REITORIA DE PESQUISA E PÓS-GRADUAÇÃO
COMITÊ DE ÉTICA PARA O USO DE ANIMAIS

Ofício 180/10 – CEUA Porto Alegre, 04 de novembro de 2010.

Senhor Pesquisador:

O Comitê de Ética para o Uso de Animais apreciou e aprovou seu protocolo de pesquisa, registro CEUA 10/00199, intitulado: "Avaliação dos efeitos de inibidores da enzima uridina fosforilase humana sobre a toxidade do quimioterápico 5-Fluorouracil em ratos".

Sua investigação está autorizada a partir da presente data.

Atenciosamente,

Profa. Dra. Anamaria Gonçalves Feijó
Coordenadora do CEUA – PUCRS

Ilmo. Sr.
Prof. Dr. Luiz Augusto Basso
Fabio
N/Universidade

PUCRS
Campus Central
Av. Ipiranga, 6690 – Prédio 60, sala 314
CEP: 90610-000
Fone/Fax: (51) 3320-3345
E-mail: ceua@pucrs.br

ANEXO C

Patente

CONFIDENCIAL

03/09/2013 860130002120 18:09 NPWB

0000221305770760

BR 10 2013 022567 3

Protocolo | Número | Código QR

INSTITUTO NACIONAL DA PROPRIEDADE INDUSTRIAL
Diretoria de Patentes
Sistema e-Patentes/Depósito

DIRPA e-PATENTES

Tipo de Documento:	DIRPA	Página:
Recibo de Peticionamento Eletrônico		1 / 2

Título do Documento:

Recibo

DIRPA-FQ001 - Depósito de Pedido de Patente ou de Certificado de Adição

Código:	Versão:
RECIBO	01

Modo: **Produção**

O Instituto Nacional da Propriedade Industrial informa:

Este é um documento acusando o recebimento de sua petição conforme especificado abaixo:

Dados do INPI:

Número de processo:	BR 10 2013 022567 3
Número da GRU principal:	00.000.2.2.13.0577076.0 (serviço 200)
Número do protocolo:	860130002120
Data do protocolo:	03 de Setembro de 2013, 18:09 (BRT)
Número de referência do envio:	3042

Dados do requerente ou interessado:

Tipo de formulário enviado:	DIRPA-FQ001 v.003
Referência interna:	Inibidores Uridina
Primeiro requerente ou interessado:	União Brasileira de Educação e Assistência
CNPJ do primeiro requerente ou interessado:	88.630.413/0001-09
Número de requerentes ou interessados:	1
Título do pedido:	USO DE 6-HIDROXI-2-PIRIDONAS E SEUS DERIVADOS NA PREPARAÇÃO DE UMA COMPOSIÇÃO FARMACÊUTICA QUE ATUE PELA INIBIÇÃO DA ENZIMA URIDINA FOSFORILASE HUMANA

Arquivos enviados:

Arquivo enviado	Documento representado pelo arquivo	Número de páginas
[package-data.xml]	Arquivo com informações do pacote em XML	---
[brf101-request.xml]	Formulário de depósito de pedido de patente ou de certificado de adição em XML	---
[application-body.xml]	Arquivo com dados do corpo do conteúdo patentário em XML	---
[brf101-request.pdf]	Formulário de depósito de pedido de patente ou de certificado de adição em PDF	
PUCRS-InibidoresUridinaFosforilase.pdf *[DOCUMENTO.pdf]*	Arquivo com conteúdo técnico-patentário da petição *- Relatório descritivo em formato eletrônico PDF páginas 1 a 22* *- Reivindicações em formato eletrônico PDF páginas 23 a 25* *- Resumo em formato eletrônico PDF página 26* *- Desenhos em formato eletrônico PDF páginas 27 a 31* *[Número de desenhos: 10, Desenho para resumo: 1, Cor dos desenhos: Preto e Branco]*	31
Relatório Inibidores Uridina Fosforilase.txt *[RELATDESCTXT.txt]*	Relatório descritivo em formato eletrônico texto	---
Revindicações Inibidores Uridina Fosforilase.txt *[REIVINDTXT.txt]*	Reivindicações em formato eletrônico texto	---
Resumo Inibidores Uridina Fosfolirase.txt *[RESUMOTXT.txt]*	Resumo em formato eletrônico texto	---
02-PUCRS-A0076-12 - Inibidores de uridina fosforilase.pdf *[GRU-1.pdf]*	Guia de Recolhimento da União (GRU) paga com comprovante de pagamento em formato eletrônico PDF *[Código de serviço: 200, Número: 00.000.2.2.13.0577076.0, Nome do sacado: União Brasileira de Educação e Assistência]*	1
Procuração PUCRS.pdf *[INDEXADO-1.pdf]*	Procuração em formato eletrônico PDF	1

ANEXO D

Carta de submissão do manuscrito do Capítulo 3

----- Forwarded Message -----
From: "hspik001@umaryland.edu" <hspik001@umaryland.edu>
To: camposmmartha@yahoo.com; luiz.basso@pucrs.br
Sent: Thursday, September 19, 2013 9:49 AM
Subject: Manuscript submitted - CCP-13-0533

Date: 19-Sep-2013

Manuscript No. CCP-13-0533
Title: Human uridine phosphorylase-1 inhibitors: a new approach to ameliorate 5-fluorouracil-induced intestinal mucositis
Authors: Renck, Daiana; Santos Jr, Andre; Machado, Pablo; Petersen, Guilherme; Lopes, Tiago; Santos, Diogenes; Campos, Maria; Basso, Luiz

Dear Dr. Campos

Thank you for the submission of your above mentioned manuscript.
Your paper has been received in the Cancer Chemotherapy and Pharmacology
Editorial Office and will be given full consideration
for publication.

Please be sure to mention the manuscript number in all
future correspondence. If there are any corrections to your street address or e-mail address, please log into ManuscriptCentral at
http://mc.manuscriptcentral.com/ccp and edit your information as appropriate.

Authors submitting manuscripts to our European Office PLEASE NOTE - both Professor Herbie Newell, Editor-in-Chief and Sandra Cartwright, Managing Editor are on holiday until July 26, 2013. This may cause a slight delay in manuscript processing. They will respond to all inquiries upon their return.

Yours sincerely,

Editorial Office
Cancer Chemotherapy and Pharmacology

ANEXO E

Analysis of select members of the E26 (ETS) transcription factors family in colorectal cancer

Candida Deves, Daiana Renck, Bernardo Garicochea, Vinícius D. da Silva, Tiago G. Lopes, Henrique Fillman, Lucio Fillman, Silvana Lunardini, Luiz A. Basso, Diógenes S. Santos, Eraldo L. Batista Jr.

Artigo publicado
Virchows Archives, 2011, 458: 421-430

Virchows Arch (2011) 458:421–430
DOI 10.1007/s00428-011-1053-6

ORIGINAL ARTICLE

Analysis of select members of the E26 (ETS) transcription factors family in colorectal cancer

Candida Deves · Daiana Renck · Bernardo Garicochea · Vinicius Duval da Silva · Tiago Giulianni Lopes · Henrique Fillman · Lucio Fillman · Silvana Lunardini · Luis Augusto Basso · Diogenes Santiago Santos · Eraldo L. Batista Jr.

Received: 29 June 2010 / Revised: 25 January 2011 / Accepted: 28 January 2011 / Published online: 12 February 2011

Abstract The E-twenty-six (ETS) family of transcription factors is known to act as positive or negative regulators of the expression of genes that are involved in diverse biological processes, including those that control cellular proliferation, differentiation, hematopoiesis, apoptosis, metastasis, tissue remodeling, and angiogenesis. Identification of target gene promoters of normal and oncogenic transcription factors provides new insights into the regulation of genes that are involved in the control of normal cell growth and differentiation. The aim of the present investigation was to analyze the differential expression of 11 ETS (ELF-3, ESE3, ETS1, ETV3, ETV4, ETV6, NERF, PDEF, PU1, Spi-B, and Spi-C) as potential markers for prognostic of colorectal cancer. A series of paired tissue biopsies consisting of a tumor and a non-affected control sample were harvested from 28 individuals suffering from diagnosed colorectal lesions. Total RNA was isolated from the samples, and after reverse transcription, differential expression of the select ETS was carried out through real-time polymerase chain reaction. Tumor staging as determined by histopathology was carried out to correlate the degree of tumor invasiveness with the expression of the ETS genes. The results demonstrated a different quantitative profile of expression in tumors and normal tissues. ETV4 was significantly upregulated with further increase in the event of lymph node involvement. PDEF and Spi-B presented down-regulation, which was more significant when lymph node involvement was present. These findings were supported by immunohistochemistry of tumoral tissues. The results suggest that select ETS may serve as potential markers of colorectal cancer invasiveness and metastasis.

C. Deves · D. Renck · L. A. Basso · D. S. Santos · E. L. Batista Jr.
Center for Research on Molecular
and Functional Biology (CP-BMF),
Pontificia Universidade Catolica do Rio Grande do Sul (PUCRS),
Av. Ipiranga 6681 Bld. 92A,
Porto Alegre, RS, Brazil

B. Garicochea · H. Fillman · L. Fillman · S. Lunardini
Department of Internal Medicine,
School of Medicine, Hospital São Lucas,
Pontificia Universidade Catolica do Rio Grande do Sul (PUCRS),
Av. Ipiranga, 6690,
90610-000, Porto Alegre, RS, Brazil

V. D. da Silva · T. Giulianni Lopes
Department of Pathology, School of Medicine,
Hospital São Lucas,
Pontificia Universidade Catolica do Rio Grande do Sul (PUCRS),
Av. Ipiranga, 6690,
90610-000, Porto Alegre RS, Brazil

C. Deves · D. Renck · L. A. Basso · D. S. Santos · E. L. Batista Jr.
Graduate Program in Cellular and Molecular Biology,
Faculdade de Biociencias,
Pontificia Universidade Catolica do Rio Grande do Sul (PUCRS),
Av. Ipiranga 6681 Bld. 12,
Porto Alegre, RS, Brazil

E. L. Batista Jr.
School of Dental Medicine,
Pontificia Universidade Catolica do Rio Grande do Sul (PUCRS),
Av. Ipiranga 6681 Bld. 06,
Porto Alegre, RS, Brazil

D. S. Santos (✉) · E. L. Batista Jr. (✉)
Centro de Pesquisas em Biologia
Molecular e Funcional—CPBMF/Tecnopuc,
Pontificia Universidade Católica do Rio Grande do Sul - PUCRS,
Av. Ipiranga 6681 Bld. 92A,
90619-900, Porto Alegre, RS, Brazil
e-mail: diogenes@pucrs.br
e-mail: eraldo.junior@pucrs.br